UNIVERSITÀ DEGLI STUDI DI PADOVA

TESI DI LAUREA MAGISTRALE IN INGEGNERIA CIVILE

CORRELAZIONE DI IMMAGINI DIGITALI PER LA VALUTAZIONE DI DEFORMAZIONI DI PROFILI IN ACCIAIO

USE OF DIGITAL IMAGE CORRELATION FOR STEEL SECTION STRAIN EVALUATION

Relatore:

Prof. CLAUDIO MODENA

Prof. CHRISTOS GEORGAKIS

Studente:

MATTEO FURLAN

a.a. 2013-2014

INDEX

Acknowledgments

A special acknowledgment goes to Associated Professor Christos Georgakis for the help, support and assistance he gave me throughout my stay in Denmark.
I give thanks to my supervisor, Associate Professor Claudio Modena who permit me to carry on the Master Thesis in DTU.
Special thanks are also for Ph.D Jan Winkler and Ieva Paegle for their helpful advices and support about Aramis, for Silvia Finazzi for the support and for her helpful tips about the spray pattern and for the lab technician for their assistance during testing.
I would like to thank my friends, especially my flatmates, with whom I shared a great period of time during our stay in Copenhagen and who made these months really special.
Last but not least a great thanks to my family who made this possible for me and supported me in these years of study and to my best friends, whose friendship has never failed, even thought my last two years abroad.

Abstract

Bridge structures are exposed to several external loads as traffic, earthquake and wind. Structures may get ruined during their lifetime in unpredicted ways which could be reasons of structural damage and consequently costly repair and of loss of human lives. To prevent this possibility health monitoring has become an important way to evaluate the structural integrity.

In this thesis were carried out real time displacements measurement on bridges evaluating steel section strain. The main objective of the work was to discover if it is possible to realize the presence of a hidden crack just studying and analyzing local strain of the structure.

The technique used in this work is Digital Image Correlation (DIC), because it is innovative, highly cost-effective and easy to implement, but still maintain the advantages of high resolution. Fields tests were carried out building a steel plate structure, where the behavior of a bolted joint increasing loads in the terminal side of the plate was checked.

Key words: Digital Image Correlation, Local strain, global displacements, ideal conditions.

Introduction

Bridge health monitoring has become an important topic in the current engineering research. This has been motivated by the possibility for a structure to get deteriorated during its lifetime in unexpected ways and to get an inadequate structural behavior can lead to a possible loss of safety. So become really important to be able to obtain displacement of the structure, especially when they start to overcome a certain loading condition. Installation of these sensors in a flexible bridge is costly but possible because during last decades new technologies helped to improve this monitoring process also if bridges span over rivers, highways and mountainous terrain. So nowadays the range of applications covered by sensors is really wide and is possible to perform measurement of a specific point of the bridge, but still with problems due to the need of a stationary platform to fasten wireless sensors close to the structure. These difficulties can be deleted using the most recent no-contact technologies, as photogrammetry and laser technologies, but the last one is costly so in thesis we will use the first one, known as Digital Image Correlation.

The aim of the project was to analyze and reproduce the behavior of a steel bolted joint in damaged conditions in order to understand if the Digital Image Correlation(DIC) can be used to catch the presence of a crack in a beam also if it is hidden from a plate or another structural element, just using local strain of the bolts of the joint and comparing the results with the ones in undamaged conditions. The phenomenon was studied via tests in the laboratory (ideal conditions) and pictures were taken from different distances trying to understand the limits of the method.

The work was divided in the following sections:

***Review of structural health monitoring*:**
This chapter of the thesis is a complete overview of the topic. Starting from a general introduction about the Structural Health Monitoring, explains the evolution of the monitoring technique during last decades, focusing in the last part on the one used in this thesis, Digital Image Correlation.

Conceptual framework:
This chapter presents a detailed description of the work carried out in the thesis, specifying point by point the instrumentation set up, the applied load and the different structure conditions during the various tests. All the technologies used during test are here explained.

Undamaged condition:
In this section the undamaged condition of the structure is presented. After an overview of the test, results comparison between digital image correlation and strain gauges methods are presented. Brief comments about the results are reported.

Damaged condition:
In this chapter the damaged condition of the structure is presented. After an overview of the test, results comparison between digital image correlation and strain gauges methods are presented. Brief comments about the results are reported.

Results comparison:

This section contains a comparison between the undamaged and damaged condition of the structure, in order to obtain results related to the main objective of the thesis.

Conclusions:

Final comments about the comparison of the health monitoring structures methods are presented. Final conclusion regarding Aramis reliability are reported.

Chapter 1

Structural Health Monitoring

1.1 Background

Structural Health monitoring(SMH) represent the process of implementing a damage identification strategy for civil engineering buildings, where damage means changes to the material and/or geometric properties might lead to compromise the integrity of the structure. The same holds true for bridges, structures in which this thesis will focused on.

Bridges are subjected to several types of external loads during their lifetime. These actions can be environmental like an earthquake or the wind, or can be due to human interaction. All external load leads some changes into the bridge and this induces new stresses on it. Since it is not possible to calculate the exact effect on the structure, the new state has to be continuously compare with the initial and undamaged one, so as to be able to estimate the residual life. This process is called monitoring. The most important steps are to identify, locate and classify type and severity of damages and estimated the effects on the structural performance. Even if the found damage does not imply a total loss of system functionality, the part of the structure close to it is not working in the optimal way, so the damage could grow and it could reach a point no more acceptable for a safety use of the bridge. To avoid this possibility, once the damage is identified and valuated is necessary to intervene as quickly as possible.

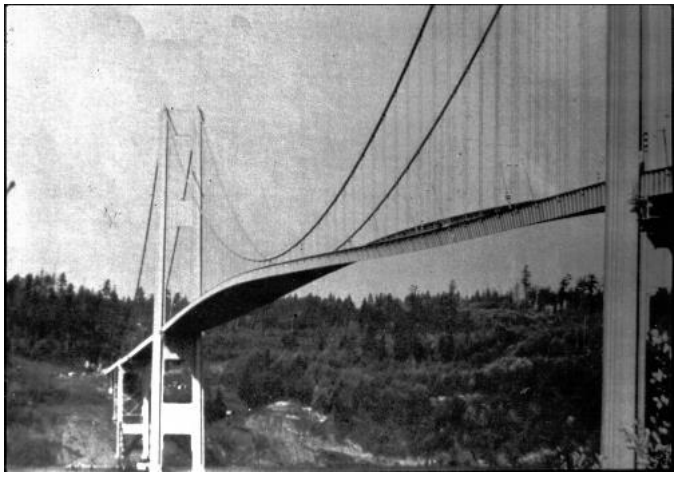

Fig. 1.1: Tacoma Narrows Bridge, some instants before the collapse in 1940.

Nowadays many SHM systems use a network of sensors connected to an external data acquisition unit. Since the presence of cable presence between them was cause of limitation, most modern systems use wireless transmitters and receivers. But health monitoring technique born in a simple way, based on visual monitoring and mere tests. some of were also done destroying part of the structure to check its condition. First and traditional methods met several problems, from the limitation of the access to some building areas to the impossibility to have a continuously inspection of the structure, passing through the subjectivity of the inspectors judgments.

These monitoring methods have been developed during last years and many if most recent ones use automatic sensor stably associated to the bridge. They have some high initial costs but make able to get cadenced data(with established time interval), giving real time information about the structure and above all in the moment of a particular event like an earthquake, to check immediately the bridge state: have sensors already fixed to the bridge means a save of time, no need for new investments and being able to decide if the structure have to be closed to be repaired or not after the event. So in a long-term view the benefits are higher than the cost, also because this technique avoids the possibility to waste money making periodical maintenance also if not necessary, but rather just when they are required.

Others still more recent techniques called no-contact technologies not even provide any sensor into the structure. They use modern technologies like photogrammetry and GPS System, where thanks to particular software it is possible to process and analyze data and keep the bridge continuously under control, checking local strain and global displacement and without problems about any breakdown of sensors into the bridge, besides an important save of money.

Whatever type of health monitoring need first of all to define the most important areas and parameters to monitor, namely those where (based on accurate analyses on the structural geometry of the structure) the structure might be more sensitive to damages.

In this context SHM represent an important and increasingly widespread checking method.

1.2 Historical review

Discounting as structural monitoring just a simple periodic visual observation, the formal structural monitoring and interpretation using recording instruments started in the second half of the last century and the great development came hand in hand with the electronic growth. Structural Health Monitoring growth involved mechanical and aerospace engineering, but after that moved also to engineering structures and infrastructures during last decades. Installation of large dams and long-span cable-bridges allows to receive the greatest attention and research effort, meanwhile was not given the same interest to residential and commercial structures, underestimating the benefits of a structural monitoring. Every single structure requires a prior

particular study to apply the monitoring technique, because building is unique and therefore every single case has to be studied like new.

Ross & Matthews (1995) and Mita(1999) identified the case where structural monitoring may be required:

- Modification of an existing structure;
- Monitoring of structures affected by external works;
- Monitoring during demolition;
- Structures subjected to long term movement or degradation of materials;
- Feedback loop to improve future design based on experience;
- Fatigue assessment;
- Novel system of construction;
- Assessment of post-earthquake structural integrity;
- Decline in construction and growth in maintenance needs;
- Move towards performance-based design philosophy.

As presented by Brown John in 2007 on the article "Structural health monitoring of civil infrastructure" are presented the main case of monitoring applications on civil structures and infrastructures.

Fig. 1.2: Main fields of application of the Structural Health Monitoring

1.2.1 Dams

During the year 1864, close to Sheffield(UK), 254 people lost their lives due to the failure of a 30 meters embankment dam. Due to that event a legislation was induced in order to have a regular inspection on dams. At present, the law governs dams in UK is the Reservoir Act of 1975: it requires the presence of a supervising engineer who is responsible to oversee the dam, it means also keeping and interpreting data. In this way dams are historically present as the first structure for the mandated application of SHM.

The main points of the SHM were fixed in the International Commission on Large Dams (ICOLD 2000).

- Range of tools and instrumentations to provide response data, supplemented by visual inspections;
- Need for automatic data collection;
- Intelligent interpretation of data against established behavior patterns and identification of anomalies.

The Italian company ENEL introduced for its dams a monitoring program reported by Fanelli(1992). All the principles dams of the company provide sensors to keep data about the structure with a regular time interval, such as:

- Relative or absolute displacements: horizontal crest displacement are the most important for concrete dams;
- Strains(for concrete dams);
- Uplift pressure quantifying loads, which, for example, contributed to the failure of Malpasset Dam in 1959;
- Seepage rates;
- Water level;
- Structural temperature;
- Meteorological conditions.

Dam case permitted to learn much about the monitoring technique and it was helpful also to be applied to many others type structures.

1.2.2 Bridges

One of the firsts cases of Bridge Health monitoring programs was held by Carder(1937) in two bridges in San Francisco: the Golden Gate and Bay Bridges. A sophisticated program concerned measuring periods of many components during their construction was made, in order to obtain information about the dynamic behavior and possible consequences of an earthquake to the structure.

Fig. 1.3: Golden Gate Bridge, San Francisco

The collapse of the Tacoma Narrow Bridge (1940), due to a wind-induced instability, was described by the University of Washington in 1954. The Tacoma Narrow collapse was helpful for understand more about the wind effect to the structure and the possible instability, reason why new section shapes were used in the new long-span suspended bridge. Nowadays the aerodynamics of these types of bridge is still an important topic whole knowledge have to be improve and this is the reason why high costly and

elaborate structural health monitoring systems to civil infrastructure are justified.

Several bridges were monitoring during last decades and this permitted to develop new SHM systems, implemented in Japan, Hong Kong, and later in North America.

Modern long-span suspension bridges programs provide inspection and maintenance in order to pick up visually if some important damage and/or deterioration come out. In this way is possible to reduce the density of sensorscounting just in a minimum but well located number, so as sensors are used to detect global changes such as foundation settlement, bearing failure, loss of main cable tension, rupture of deck element.

Conventional short-span bridges are monitored as well and SHM systems were developed during last decades. There is a history of research in full-scale testing for short-span highway bridge assessment(Salane et al. 1981; Bakht & Jaeger 1990) and the possibility to envelop it for automated monitoring exercises. In these type of bridges the visual inspection is less frequent as less important: SHM systems can give almost all the information about the structure. European research focused on short-span bridges and led to develop the BRIMOS system (Geier & Wenzel 2002) that permit to track dynamic characteristics. Australian studies permitted to analyze and get information about the strains in very short-span highways and railway bridges due to the presence of the vehicle.

1.2.3 Offshore installations

In 1970s, the energy crisis and discovery of large oil reserve in the North Sea permitted a quick growth in offshore infrastructure, especially for the part of the installation of steel and concrete products operating to depth up to 150m and subjected to important environmental loads. In 1977 inspections became

mandatory (Det Norske Veritas) and diver inspection were as expensive as danger, so vibration-based diagnostic systems were developed (Coppolino& Rubin 1980; Kenley &Dodds 1980; Shahrivar&Boukamp 1980; Brederode et al. 1986). As required from the Norwegian Petroleum Directorate, data about structure performance were taken and managed from an operator of the platform, in order to monitoring the shelf and its foundation, identifying dynamics properties and load-response mechanisms.

Fig. 1.4: Example of an offshore platform

Around 1980s increased the number of system identification techniques whole led to the modern discipline of 'operational modal analysis' (Peeters& De Roeck 2001). The increasing of reliability and accuracy of dynamic parameter estimates for the vibration-based diagnostics permitted to say detection was possible but just under controlled conditions or where were structural damage.
The most important problem of offshore installation and in which the research is still working on is about the non-stationary nature of the structure, subjected to many changes in mass properties due to fluid movements and drilling operations.

1.2.4 Buildings and Towers

Health monitoring on buildings started due to the necessity to study the structural behavior during earthquakes and storms. At the beginning, the low-amplitude dynamics response was based on vibration testing (Hudson 1977; Jeary & Ellis 1981) but knowing the building response during a typical but not ultimate large amplitude loading eventwas more important, and this has required long term monitoring. In California the mandatory structural monitoring is manage by the California Strong Motion Instrumentation Program (CSMIP), and it use levies on building owners in order to check the condition of the structure. Such data can help to understand the structural behavior of the building, but also information about the ground motions need to be studied, to improve the knowledge about the performance during earthquake.

Due to important recent earthquake SHM system has to been improved in order to take timely information about the condition of the structure during the earthquake event. This meant the necessity to develop new autonomous sensors, embedded systems, communications, data management and mining(Kiremidjian & Straser 1998; Lynch 2005).

1.2.5 Nuclear installations

Nowadays nuclear energy is really widespread around the world, but some important disaster like Three Mile Island (1979), Chernobyl (1986) and Fukushima (2011) recalled how this technology is potentially dangerous and hence forced to stay focused on the safety of these structures.

In the UK licenses to operate nuclear reactors are granted by the Nuclear Installation Inspectorate (NII) as required by the Nuclear Installation Act of 1965. To grant the permission the performance of the prestressed concrete pressure vessel (PCPV) must be proven with structural tests and they have to be repeated every three years turning the reactors, meanwhile the online monitoring of structural response does not play an important contribution in tracking the health of the structure. Strain data are used just to obtain information about changes in other operational parameters.

1.2.6 Tunnels and excavations

Tunnel monitoring aim is to keep monitored deformations and deflections, in order to be sure they don't overpass the established limit for the stability and therefore the safety of the structure.

Monitoring of heritage and other structures during nearby tunneling or mining is a major concern: some known example are the monitoring of Mansion House in London during an extension of the underground railway, the monitoring of listed nineteenth century mining facilities in Australia close to explosive blasting in nearby open cast mining operation.

Important benefits may come out using SHM system in geotechnical constructions. In April 2004 in Singapore occurred a collapse of tunneling excavations. Post-accident examination of recordings from instrumentation showed some movements in the excavation already two months before the accident. Using online processes wired with automatic alarms might probably permitted to avoid the collapse.

1.3 Traditional and modern monitoring methods

1.3.1 The process

The structural health monitoring is a no invasive survey process of particular structural quantities subjected to known or unknown actions, in which data are taken with a preset time period. In this way several parameters can be monitored in real time or at least with short time interval, in order to be able to collect any anomaly in the structure and identify the presence of structural damages. When the sensor able to keep this type of data have to fixed in the structure, this traditional technique is also known as contact method; notice sensors able to send information in wireless mode are as well part of this category, due to the need to fix them to the structure. On the other hand, most modern methods do not need the presence of some fixed sensors into the structure: these methods are called no-contact methods.

Every SHM process, as the traditional as the most innovative, is composed by three main parts:

- Instrumentation and data acquisition;
- Signal processing and feature extraction;
- Damage detection, alarms and reports.

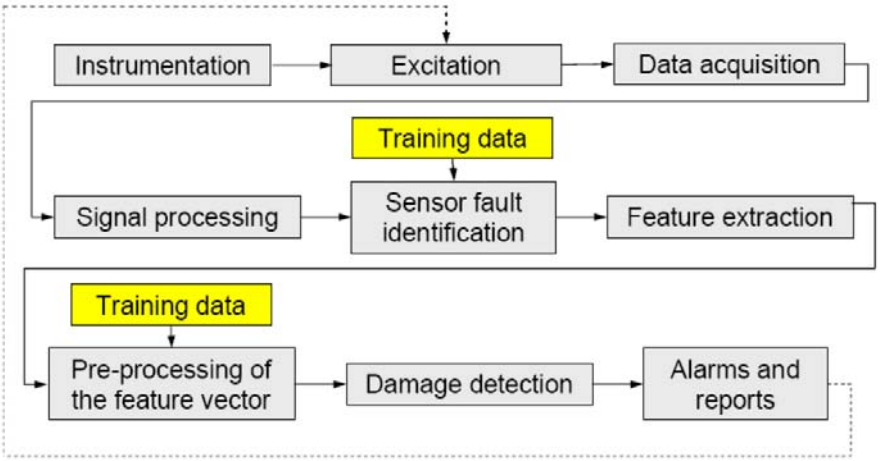

Fig. 1.5: Structural Health Monitoring process (Kullaa 2008)

1.3.2 Instrumentation and data acquisition

The first part of each SHM consists in setting the limitations about what will be monitored and how it will be accomplished, including justification for performing SHM (Farrar et al. 2001). The parts compose the monitoring system are:

- sensors (except the most modern that do not need them, how will be explain afterwards);
- acquisition unit;
- database to collect and store data.

To have a complete monitoring and to check every single point of the structure the number of the sensors should be as high as costly so, the number of points to monitor can be chosen in order to avoid useless expense that can led to overpass the maximum financial resources, but at the same time permitting to monitor efficiently the structure, controlling all the fundamental parameters.

Once points are chosen, data are recorded and, in different ways according to the chosen strategy (static, dynamic) and method(traditional, modern), information about the structure is given.

A transducer is a device able to convert a physical quantity (as displacement, strains, stresses, etc) into a proportional electrical signal, processed by the data acquisition unit. The recorded signal can be analogical or digital. Traditional and innovative sensors are now presented.

1.3.2.1 Traditional sensors

- Pendulum: exist two types of pendulum, hanging or inverted, and both permit to perform long term monitoring of horizontal structural movements in structures with important dimension such as dams, bridges and tall buildings. The pendulum is composed by a steel cable, which upper end of the steel wire is fixed to the structure, meanwhile the bottom end is free to move in an oil tank

in order to damp the cable oscillations. Displacements are measured with a portable optical readout unit or an automatic x/y coordinator.

- Inclinometers: permit to evaluate and measure the variation of inclination of a structural element. To provide the output signal the instrument considers the angle of inclination respect to the vertical direction.

- Strain gauges: measure as the strains as the elongations between couples of structural points. as reported in Ko & Ni 2005, the mainly used types of these sensors are three: electrical resistance strain gauges, vibrating wire strain gauges and, relatively to the last years, fiber optic strain gauges.

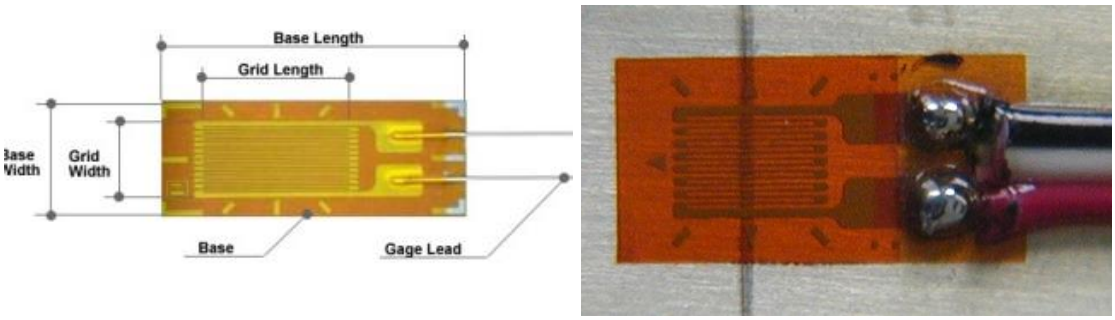

Fig. 2.1: mono directional electrical strain gauges

- Displacement transducers: permit to keep monitored a crack present in the structure, describing its development over the time. Usually is not placed just one, but rather two, both in the plane of the structure, one in the vertical direction and the other in the horizontal one, in order to split the study and identify easier contraction and expansion along the crack directions.

- Thermocouples: measure the air temperature of a particular element of the structure. Widely used in this area are thermally sensitive resistors as Thermistors and Resistance Temperature Detectors (RTD).

- Accelerometers: three main types are present: Piezoelectric accelerometers, Piezoresistive and capacitive accelerometers, Force-balance accelerometers. All three permit to obtain acceleration induced by vibrations and it is provided by a detection of inertia of a mass as a consequence of an acceleration.

Piezoelectric accelerometers produce, proportionally to the acceleration, an electric signal in a frequency band below their resonant frequency. A part of the piezoelectric material, which represent the active element of the accelerometer, is connected to the base sensor. The other side, instead, is wired to a seismic mass. In this way, when a vibration hit the accelerometer a force equal to the product of the seismic mass and the acceleration is generated. This permit to obtain a charge output, which value is proportional to the applied force. Due to inability to measure the DC components, this type of sensor is not recommended for suspension bridges or other really flexible structures.

Piezoresistive and capacitive accelerometers: contain a diaphragm which, if subject to an acceleration, behaves as a mass that undergoes flexion.

Force-Balance accelerometers: these types of sensors present a freely suspense mass constrained by an electrical equivalent mechanical spring. They cover a wide range of frequencies (from DC to 1000Hz) and accelerations (from 0.0001g up to 200g). Besides, with some alteration, it is possible to measure also angles of inclination and with a good precision.

1.3.2.2 Innovative sensors

Fiber optic sensors: in spite of the high cost, this sensors widely increased their importance during last year, because they can be used for a several different number of applications. Their main characteristic is to be easy to handle, dielectrics, immune to electromagnetic interference and capable of detecting very small deformations with high accuracy also if the observation period is long. The most important field of application of this technology is the long-term monitoring of big civil structures as bridges, dams, tunnels, geotechnical structures. Recent studies showed as fiber optic sensors are useful to study as well dynamic phenomena (Inaudi et al. 1996).

Piezoresistive cement-based strain sensors: piezoresistive cement-based material is a quite recent material in civil engineering. Differently from the traditional cement-based, it involves the insertion of carbon fibers in the cement paste. Many studies have been done to develop properties and focused measurement methods, but the research is still going on.

Corrosion monitoring sensors: In civil engineering structures, the presence of a corroded element have to be avoided because could lead to a deterioration of the structural performance. Trying to avoid the arise of this phenomenon, a sensor was developed by Qiao & Ou in the 2007. It is able to find the presence of corrosion using a time-frequency analysis approach thanks to the wavelet transform.

GPS systems: The use of the GPS technology gave a new approach of displacement measuring and more generally to SHM in civil engineering. In fact this technique permit to have a direct measurement of the request parameters, resolving in this way many of the main problems which traditional methods were affected by, because no sensor are required to be fixed to the

studied structure. Important results were showed in some recent project, such as a ratio tower in Japan (Li et al. 2004) and a group of three high-rise buildings in Chicago(Kijewski et al. 2003). Low frequencies and slow displacements own of the long-span suspended bridges induct by environmental vibrations permit the best apply of this method, as reported by Wong et al. in 2001 with same applications example.

Wireless sensor Network(WSN): it consist in a wireless network able to connect different types of sensors, which can communicate each other through elements called nodes, detecting, sharing and processing data obtained from the single points of the structure. Although nodes still need a battery to work, the absence of connecting cables has been an important development because it prevents wires tear or breakage typical of the traditional systems. Besides installation time and costs are significantly reduced (Celebi, 2002). This technology has been widely used in civil engineering field during last period, especially for Structural Health Monitoring.

Digital Image Correlation (DIC): this recent and innovative technology, as explain for the GPS system, permit a direct measurement of the request parameters, without the need of install any weather-sensible sensor to the structure, often difficulty to place and costly. Although with this monitoring process there is no need to use an external technology such as GPS: the required equipment is based to some cameras, which cost is widely lower than all the other used technologies. Due to this reason, DIC technologies is the one chosen for carry on this thesis: a wider description of this method is discussed in the paragraph 1.4.

1.3.3 Signal processing

Although most modern technologies such as GPS and DIC systems work in a different way, is presented in this section how signal is processing to obtain information we need. Signal processing provides some useful information from the time histories using stochastic properties (Kullaa 2008).

Most of the sensor acquired information in time domain, but due to computation requirements frequency domain is preferred. The conversion signal is made possible without information loss using The Fast Fourier Transform FTT (Cooley & Tukey 1965). Some problems, known as leakage error, derived because FTT is supposed to be used by time series of infinite length, but techniques have been developed to reduce them to acceptable values.

1.3.4 Damage identification

For a civil building, damage means a variation of the initial and undamaged state that might lead to compromise the integrity of the structure. The rule of the Structural Health Monitoring consists exactly in a continuously check of the structure, in order to notice when parameter values start to differ from the initials or expected ones. Different part of the structure are usually sensible to different kind of damage, so the fundamental step in order to furnish a well monitored system is the choice of the parameters to check. Development of automatic and continuously monitoring methods of last period permitted to find easily and quickly many types of damage.

1.4 Digital Image Correlation (DIC)

Digital Image Correlation is a modern no-contact technology of structural health monitoring. As for the GPS-system this method allows to check the structure without a direct contact to the building and at the same time no-one sensor is required to be located into the bridge. Once the measurement point is chosen, it has to be marked with a target panel of known geometry or painted with same spray, in order to define points will permit to identify, though the camera and the software, displacement of single points. A commercial digital camera with telescopic lens is installed on a fixed point as the coast, or on a pier (abutment) that can be considered as fixed point as well (in this case the camera will be without telescopic lens). The technique of digital image correlation allows to calculate the displacement of the chosen point comparing several motion pictures of the target; displacement are furnished with a process involves the use of texture recognition algorithms, projection of the captured images, calculation of the actual displacement based on the number of the pixel moved. Image processing software as MATLAB and ARAMIS permit nowadays to have all this functions.

This bridges monitoring system is basically composed by hardware (digital camera, laptop computer, target object, telescopic lens) and software (continuous image capturing, target recognition algorithm, calculation of a trigonometric transformation matrix from pre captured images, actual displacement calculation from online image data. This equipment cost is really economic amount comparing to other bridges health monitoring techniques.

Target panel/sprayed area dimension is determined in order to the distance of the camera, the expected maximum displacement and the performance of the camera considering the telescopic lens. A light source can be used to brighten white spots on the target. In the case of target panel, to recognize the white

spots on a threshold for the white and black image is calculated basing on the brightness of background and target region as:

$$\theta = median[\mu_B + 3\sigma_B, \mu_T - 3\sigma_T]$$

μ_B= average of brightness in background region
σ_B= standard deviation of brightness in background region
μ_T= average of brightness in target region
σ_T= standard deviation of brightness in target region

Direction vectors permit to have actual horizontal and vertical direction, basing calculation on pixel coordinates (x,y). Actual displacement ($[dxdy]^T$) are calculated basing on the number of pixel of target movement and using the trigonometric transformation matrix (T) and the scaling factors (SFx, SFy):

$$T = \begin{bmatrix} X_1 & X_2 \\ Y_1 & Y_2 \end{bmatrix}^{-1}$$

$$\mathrm{SF_x} = L_x/\sqrt{(x_1^2 + y_1^2)},\ \mathrm{SF}_y = L_y/\sqrt{(x_2^2 + y_2^2)}$$

The accuracy of the system is correlated to the hardware performance and the distance to the target. Using a commercial digital camera with 30x optical zoom and telescopic lens with 8x optical zoom it is possible to have a resolution of 0.021mm/pixel at the distance of 10m. It means that basing on the expected displacement, the camera could be placed at the distance of several tens of meters in the case of a normal bridge, till a couple of hundreds for the case of long-spam ones, where expected displacement are about tens of centimeters.
Displacements of the considered point are calculated from correlation of image frames using image processing techniques. It provides displacement after a process of recognition and calculation, where the information quality of the result is related to the number of pixel for frame and to the number of frame for second.

Chapter 2

Conceptual framework

2.1 Experiment background

The present thesis takes its inspiration to a real bridge in the south part of Denmark, the Storstrøm Bridge (figure 2.1). In the structure occurred a problem of cracking in several of the steel beams, but this problem was discovered just when the cracks came out from the plates used as junction between beams through bolting (figure 2.2). The discovery of these cracks leads to check all the bridge, in order to understand the entity of the problem. Quick interventions of rehabilitation have been done in order to guarantee the restore of the safe conditions, but vehicles speed limit had to be reduced from 120km/h to 80km/h. From this case born the idea of this thesis, mainly focus on discover if it is possible to understand the presence of a crack also when it is not visible because hidden from plates. The structural health monitoring in which the thesis focused on is a no-contact technology based on the digital image correlation (DIC), in order to have a not fixed set of sensors to the studied structure, but based on a no contact technology that could permit to check the bridge when is request.

Fig. 2.1: the Storstrøm Bridge

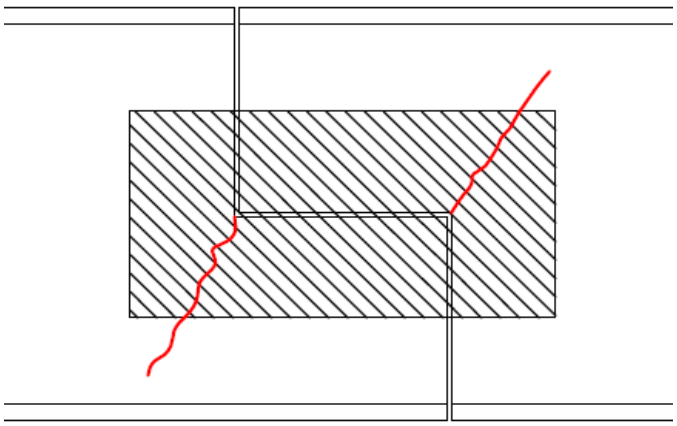

Fig. 2.2: simplified scheme of the problem occurred in the Storstrøm Bridge

2.2 The project

2.2.1 Description of the structure

The model used and tested in the laboratory does not reproduce exactly the structure of the Storstrøm Bridge, but is a simplified structure that permit as well to study the request problem. The structure built in the laboratory consists in three plates of 10mm thickness. The main one is 850mm long and 150mm high: one edge is free and the other one is bolted with the other two plates (both are 300mm long and 150mm high) through 9 high resistance bolts. The structure is finally welded to a fixed plate through the two smaller plates.
The load applied needed to induce in the joint actions of shear forces and in the same time bending moment so, due to these requests, the load was applied in the external free edge of the main plate (called in the rest of the work as beam). After a first solution made with a hole in the upper part of the beam but this one was a little too wide and the gap could not permit to have a precise load application point. In this way a second solution with a 16mm hole, close to the middle of the beam high, has been preferred because in this way there was no variation of the load application point and the force was applied exactly in the vertical direction.

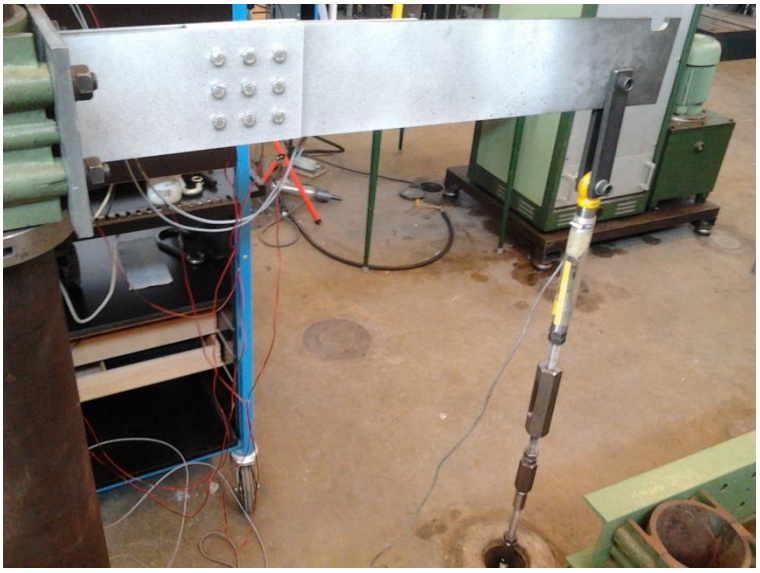

Fig. 2.3: structure during test

2.2.2 Application of the load

To applied the load to the beam there were two different set up to choose between: a mechanical one and an hydraulic jack. Instead the hydraulic jack could have been easier to use, it was as well harder to control. In fact, due to the reduced maximum value of the load (13,10KN for the undamaged condition and 5,57 KN for the damaged one), the mechanical set up was easier to control increasing manually in every step the actual force, and vibration due to the load increase (vibration were responsible of noise in the strain diagram) was much lower than using the hydraulic solution. The measurement of the load was carried out using strain gauges, as showed in figure 2.17. In order to compare strain gauges technology with digital image correlation method, photographs were taken exactly in the same moment in which strain gauges were taking data.

2.2.3 Undamaged and damaged conditions

In order to understand if it is possible to understand the presence of a crack also when it is not visible because hidden from plates, the project presents two main part: the undamaged and the damaged. These two states differ from a crack, from the more external and upper bolt going almost in vertical direction, in order to take data from each condition and be able to compare and analyze results.

The place creation of the crack has been decided studying a 3D fem model (Abaqus) and looking at the location of the main stresses in the beam, in order to have a crack in the most stressed point of the structure(figure 2.4a).

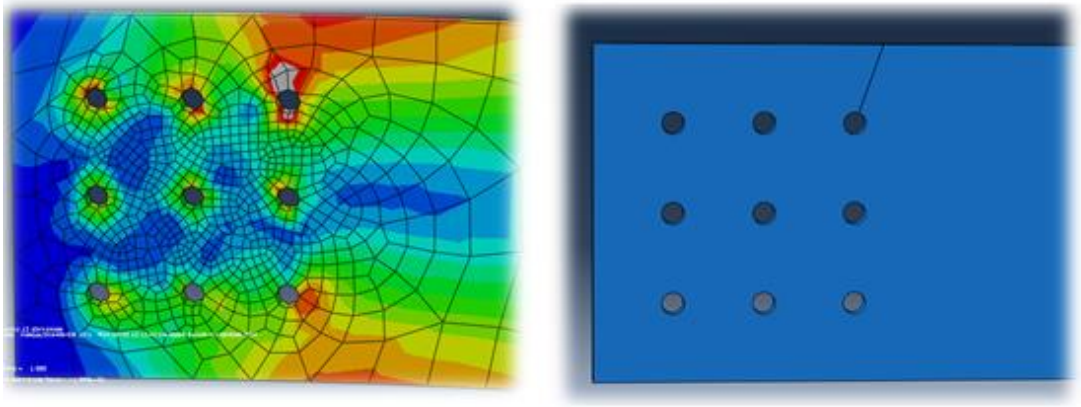

Fig. 2.4: (a) Von Mises stresses in the undamaged state and (b) damaged beam in Abaqus

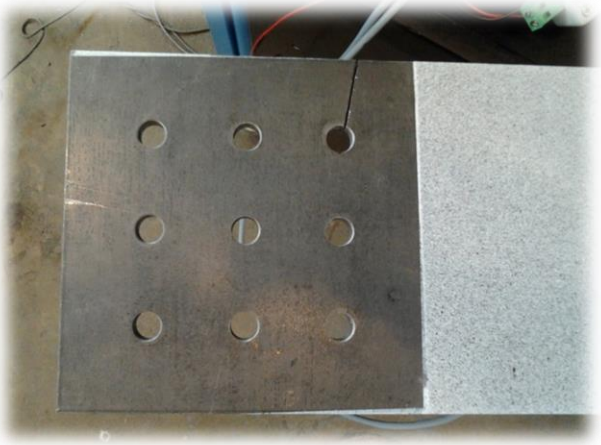

Fig. 2.5: Damaged real beam

Due to the crack, in the damaged condition the structure is subjected to a different distribution of the strain and this lead to overpass the plasticization of the section. In order to avoid this situation, tests in damaged and undamaged condition have been performed reaching different values of the maximum load. The choice of the maximum load has been based in order to reach in both cases the 70% of the load that lead the structure to yield.

2.3 Design of the structure

After the choice of the dimension of plates and the calculation of the maximum load to apply, 9 high resistance M10 bolts of class 8.8 have been selected for the joint, in order they worked below their yield stress to have the same initial condition for every test.

Maximum shear force applied on bolts (due to shear and bending moment): 27,26KN

Shear resistance of a M10 8.8 class(EC3): $\frac{0,6*f_{ub}*A_s}{\gamma_{Mb}} = \mathbf{44,54}\boldsymbol{KN}$

Preload of bolts(EC3) : $\boldsymbol{F_{p.Cd} = 0,7 * f_{ub} * A_s = 32,50\ KN}$

Tightening of bolts(EC3) : $\boldsymbol{M = \frac{d*P*K}{100} = 63,0\ Nm}$

Burr plates(EC3): $\boldsymbol{F_{b,Rd} = \frac{2,5*\alpha*f_{ub}*d*t}{\gamma_{Mb}} = 101\ KN}$

2.4 Materials and hypothesis

2.4.1 Elasticity theory

In order to valuate Aramis results is given a brief explication of elasticity and deformations, parameters on which Aramis mainly works and gives results. Generally a strain can be defined as a tensor quantity, decomposed in normal and shear components. The state of strain in a material point of a continuum body is defined as the totally of all changes in length of material lines or fibers:

$$\boldsymbol{\varepsilon} = \frac{\boldsymbol{\partial}}{\boldsymbol{\partial X}}(\boldsymbol{x} - \boldsymbol{X})$$

The engineering meaning of strain is usually defined as the ratio between the variation of length during the process and the total initial length:

$$\varepsilon = \frac{\boldsymbol{\Delta L}}{\boldsymbol{L}} = \frac{\boldsymbol{l} - \boldsymbol{L}}{\boldsymbol{L}}$$

Values of strain Aramis provides (called green strain) are obtained as:

$$\boldsymbol{\varepsilon_G} = {}^{\mathbf{1}}/_{\mathbf{2}}\left(\frac{\boldsymbol{l^2} - \boldsymbol{L^2}}{\boldsymbol{l^2}}\right)$$

2.4.2 Materials

The materials used in the tested model:

- Plates: Steel S355/Fe510;
- Bolts: M10 class 8.8

2.5 Aramis

2.5.1 A new project

Aramis set up has been the part needed longest time to be understand. Not having found previous cases of study about steel plate strain using Aramis, has been necessary to exploit other Aramis works knowledge, as for bridges cables but also for concrete structure. Differently from found studies, this work presents a range of strain with a low value: in fact obtained strain oscillate between 0.12% (higher value of the undamaged condition test) and 0.009% (lower value of the damaged condition test), where this last is really close to the low declared limit of Aramis(0.005%).

2.5.2 Set up

Many tests have been done on the structure to understand the correct set up to provide good results. First attempts have been focused trying to capture, with a single photograph, all the studied part of the structure, but results were not close to strain values provide with strain gauges and strain diagram presented many noise due to the difficulties to notice with a good approximation displacement in the x direction. Another problem due to a single picture was the focus: being the two plates not in the same plane, just one was on focus.
Aramis works comparing photographs of every step, and more precisely observing how single pixels move one to the other during test. For this reason the main attention was about the pattern. This was built using two different color, a completely and uniform white background to hide any possible imperfection of the steel plates and the a discontinuous use of a black spray. The latter have to be used in order to create black points of dimension dependent from which distance digital cameras take photographs. Due to the

low range of strain values, to obtain good results the only way found in this work was to place the camera really close to the structure (from 10cm to 30cm) and so the pattern needed to contain black points with a very limited coverage area, otherwise the processing of Aramis was not able to give as good results. The used digital camera was a Nikon D800 and three lens with different focal distance has been used: 24mm, 60mm, 105mm. The best obtained results have been provided with the 60mm lens. Tripod were used in order to have the control directly from the laptop and avoiding in this way vibrations due to the manual release photo.

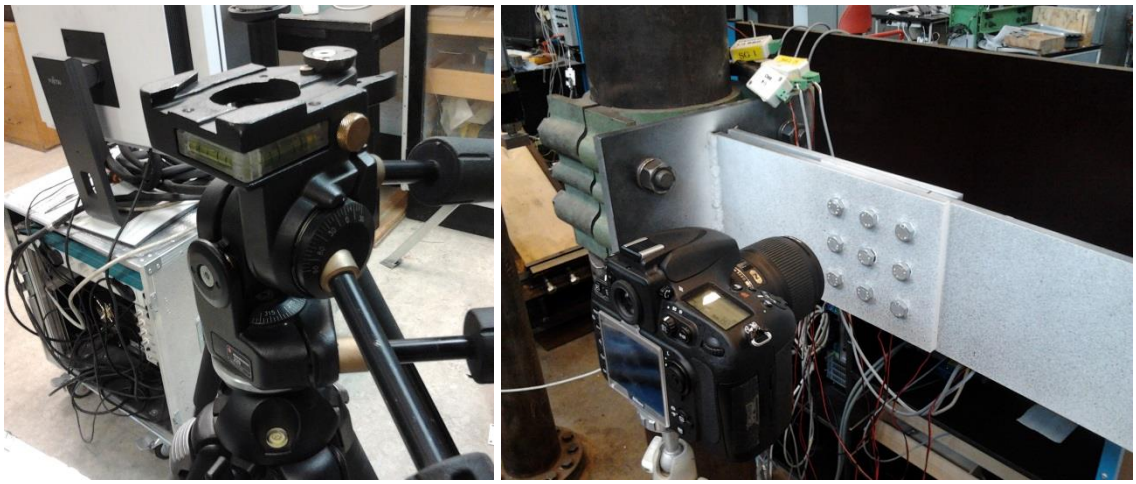

Fig 2.6: (a) one of the used tripods and (b) a release during tests.

Many types of pattern has been tried, and better results have been provided every time a finer pattern has been created.

The final selected set up was taking pictures around 10cm from the structure. This permitted to take photos just to one small area of the structure, so two cameras were used at the same time: one in the beam part, the other on the joint, but in this way not all the structure points has been possible to be checked at the same time.

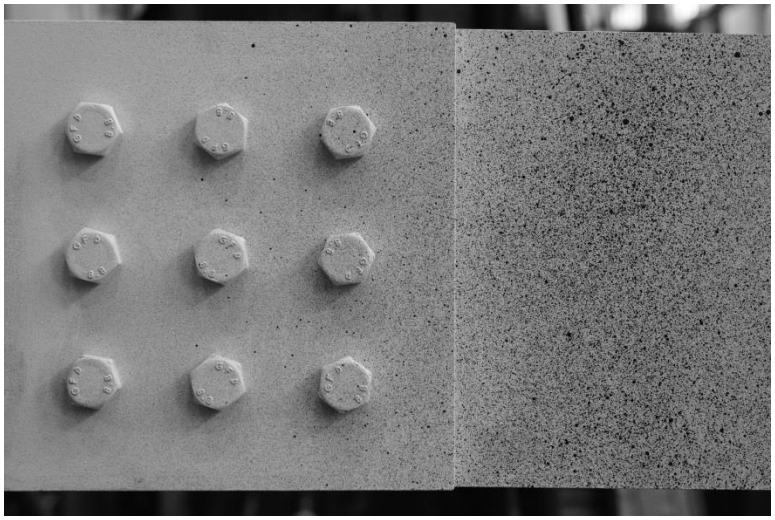

Fig. 2.7: first pattern on the beam part, test 1

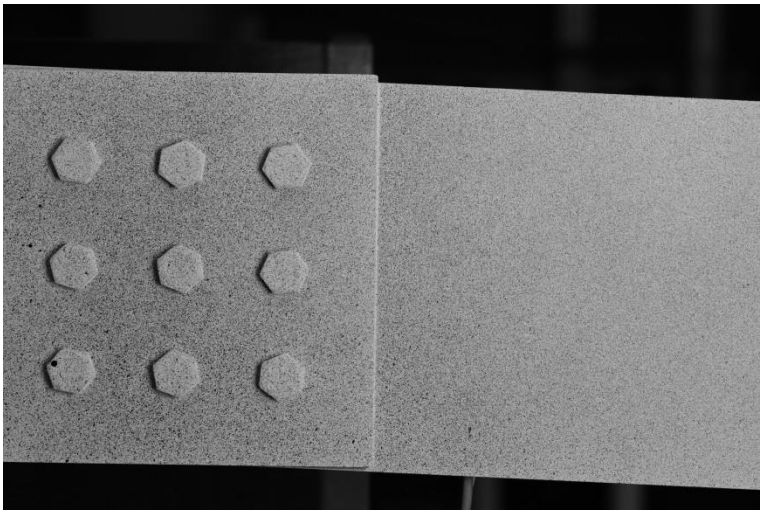

Fig. 2.8: trying different solutions of pattern

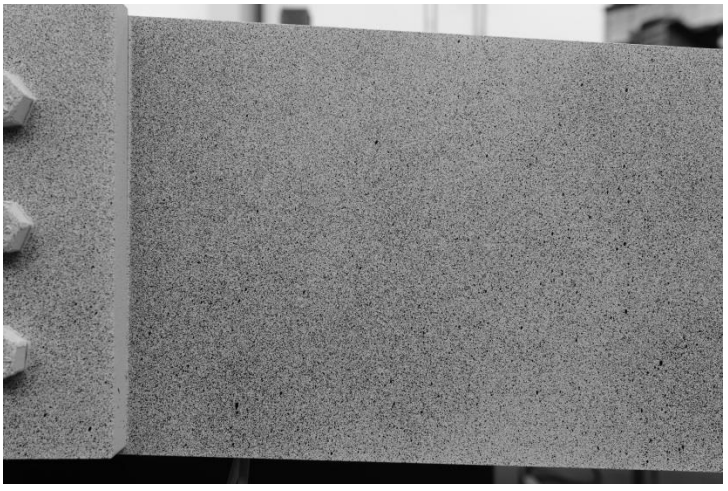

Fig.2.9 : focusing just on the beam, test 10

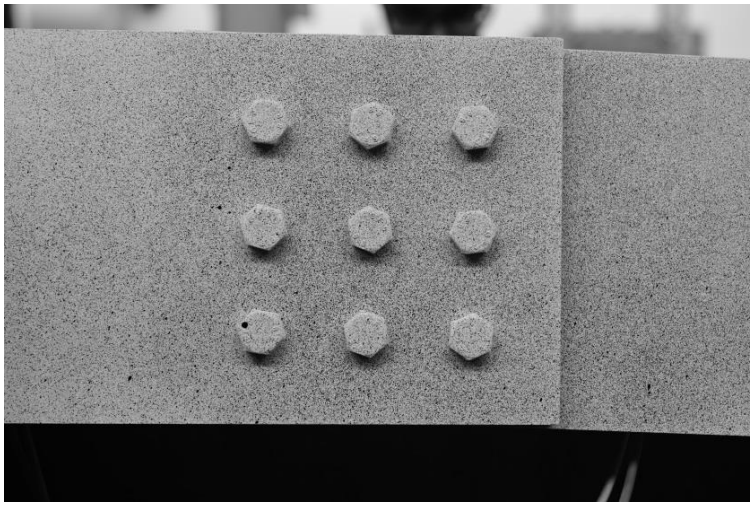

Fig.2.10 : focusing on the joint, test11

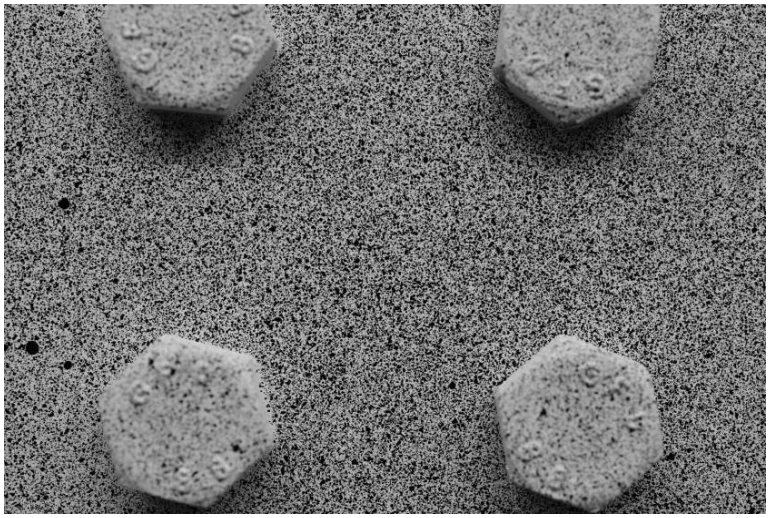

Fig. 2.11: final solution for the middle joint, camera really close to the structure

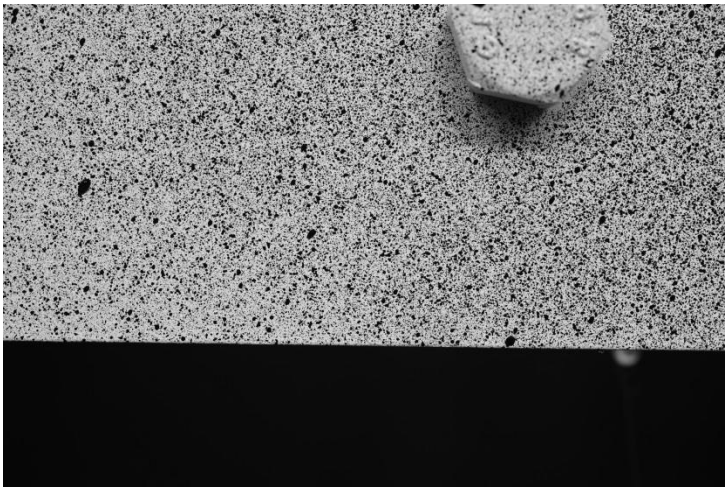

Fig. 2.12: final solution for the bottom joint, camera really close to the structure

2.6 Other technologies

The finite element model of the structure and the strain gauges have been used in this work in support of the digital image correlation method. The choice of strain gauges is due to the reliability of the technology to evaluate strains, meanwhile the 3D finite element method is basically due to place the strain gauges in the most interesting point of the structure, that is where high variation of stress are present.

2.6.1 Abaqus

Trying to have a more precise model as possible, the finite element model created in Abaqus is not a simplified one, but present all the characteristics the real structure has.
In this study a 0.2 coefficient friction has been used between plates, as suggest in the Eurocode 3 part 6.5.8.3.
The model presents two different steps:

- Preload of bolts;
- Application of the load.

An important point of the experiment was to not overpass the yield stress of the structure. Especially for the damaged condition, due to the presence of the crack, could have been quite hard to obtain the exact value of the load lead the structure to yield, but the model permitted to obtain this limit value. In order to do this the load application step was defined with fixed increments of 0.01.
In this way the fem model permit to obtain the limit load value:

- Undamaged condition: 18,71KN;
- Damaged condition: 7,95KN.

Another important contribute of the model for the project was the possibility to have a general all-round stresses and strains view, and this permit to have an easier results valuation from strain gauges and DIC technology, especially for the comparison between undamaged and damaged conditions.

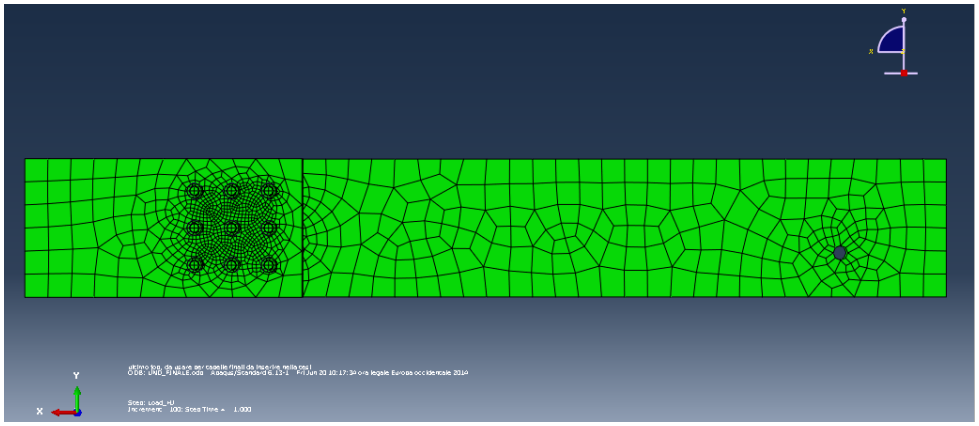

Fig. 2.13: mesh of the model

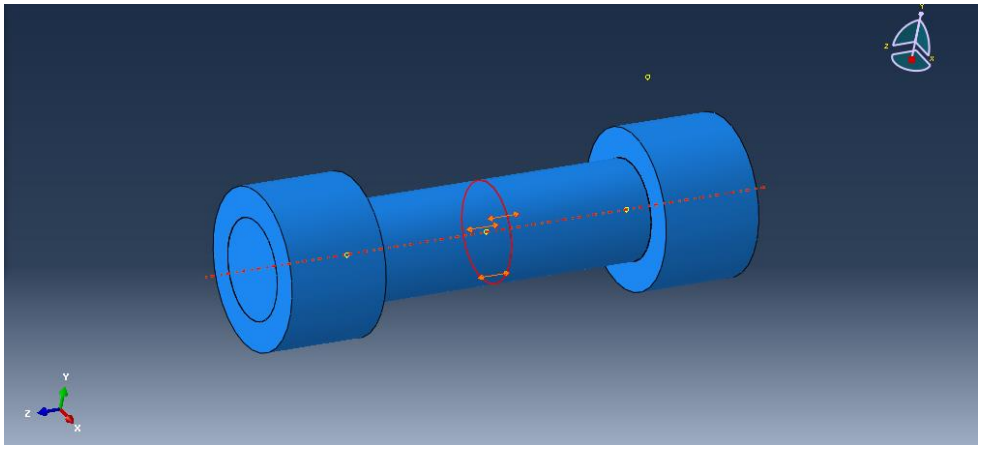

Fig. 2.14: application of bolts pre-stress

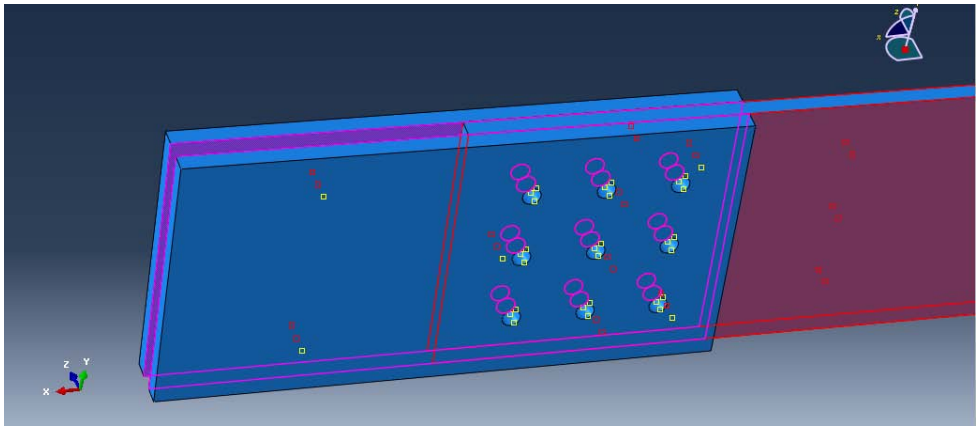

Fig. 2.15: defining friction between plates

2.6.2 Strain gauges

Strain gauges represented in this work an important part. The reliability of this technology permitted, especially at the beginning of the tests, to understand if Aramis results were correct. At the same time, comparing diagrams of strain gauges with Aramis ones was possible to understand the main problem in the first part of the tests (despite the trend line was close to strain gauges one) that was the wide oscillation of Aramis values.

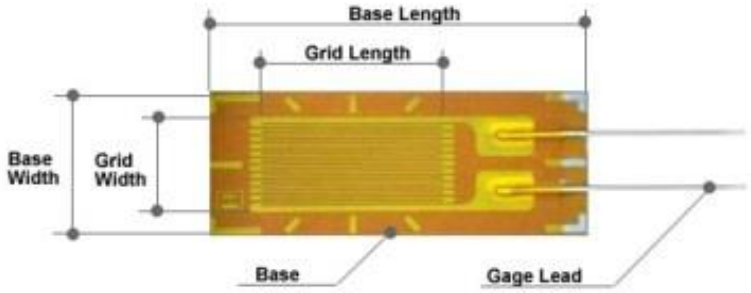

Fig. 2.16: a mono directional strain gauges

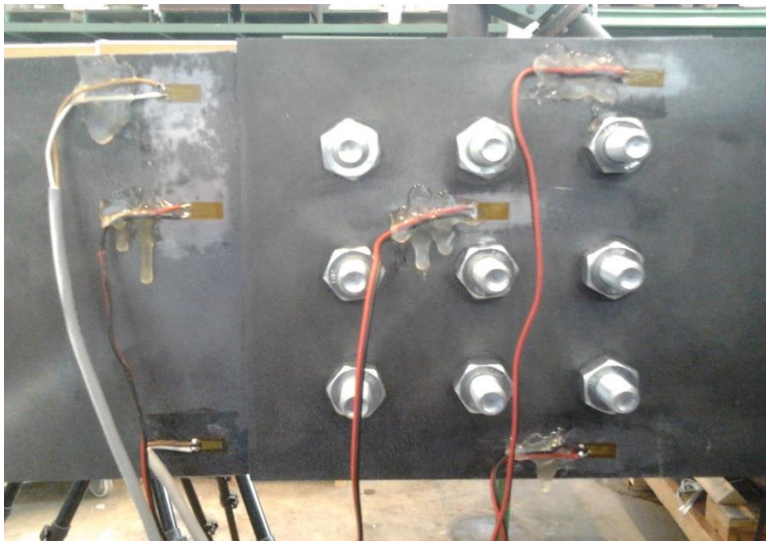

Fig. 2.17: photo of the six applied strain gauges

Chapter 3

Undamaged condition

3.1 Conduct of the test

This chapter present all the final tests have been done on the structure in undamaged condition, that means without the crack in the beam at the joint. Measured loads were plotted in graphs with load as a function of strains obtained from digital image correlation method and also with those obtained from strain gauges. For every test, due to the close proximity required from camera and structure to obtain good results, just two restricted areas were analyzed: one in the main beam, the other in the joint part.

As explained in the chapter 2, six points of particular importance were analyzed, three of them in the joint part of the structure and the other three in the beam, as with Aramis as with strain gauges. These points, due to the positioning respect to the height of the structure will be called as top beam, mid beam, bottom beam, top joint, mid joint and bottom joint. Two tests for each single relevant point are presented in this chapter. Every test presents a comparison graph with both technologies used.

3.2 Experiment results

3.2.1 Top beam

Test 21	Strain gauges	Aramis				
Load (KN)	Strain (%)	Strain (%)	Δ Lenght x (mm)	Δ Lenght y (mm)	Displ x (mm)	Displ y (mm)
0,066	0,000	0,000	0,00000	0,000	0,00	0,00
0,341	0,002	0,008	0,00263	0,004	0,04	-0,12
0,967	0,007	-0,005	-0,00175	0,016	0,12	-0,49
1,601	0,011	0,031	0,00436	0,029	0,23	-0,87
2,301	0,016	0,036	0,00563	0,044	0,34	-1,32
3,157	0,022	0,020	0,00172	0,062	0,48	-1,88
3,886	0,028	0,022	0,00251	0,077	0,60	-2,33
4,510	0,032	0,019	0,00112	0,090	0,70	-2,70
5,163	0,037	0,041	0,00518	0,104	0,80	-3,08
5,686	0,041	0,018	0,00376	0,115	0,87	-3,39
6,146	0,043	0,020	0,00330	0,124	0,94	-3,65
6,846	0,048	0,040	0,00523	0,138	1,04	-4,05
7,473	0,054	0,048	0,00504	0,164	1,13	-4,41
8,127	0,058	0,053	0,00506	0,180	1,22	-4,77
8,925	0,064	0,062	0,00555	0,193	1,33	-5,22
9,612	0,069	0,073	0,00504	0,205	1,43	-5,61
10,255	0,073	0,076	0,00526	0,218	1,51	-5,97
10,884	0,078	0,089	0,00667	0,228	1,60	-6,30
11,375	0,082	0,094	0,00578	0,236	1,66	-6,57
11,805	0,085	0,100	0,00826	0,245	1,72	-6,82
12,316	0,090	0,111	0,00757	0,255	1,78	-7,09
12,798	0,094	0,103	0,00780	0,262	1,85	-7,36
13,237	0,095	0,110	0,01005	0,263	1,91	-7,59

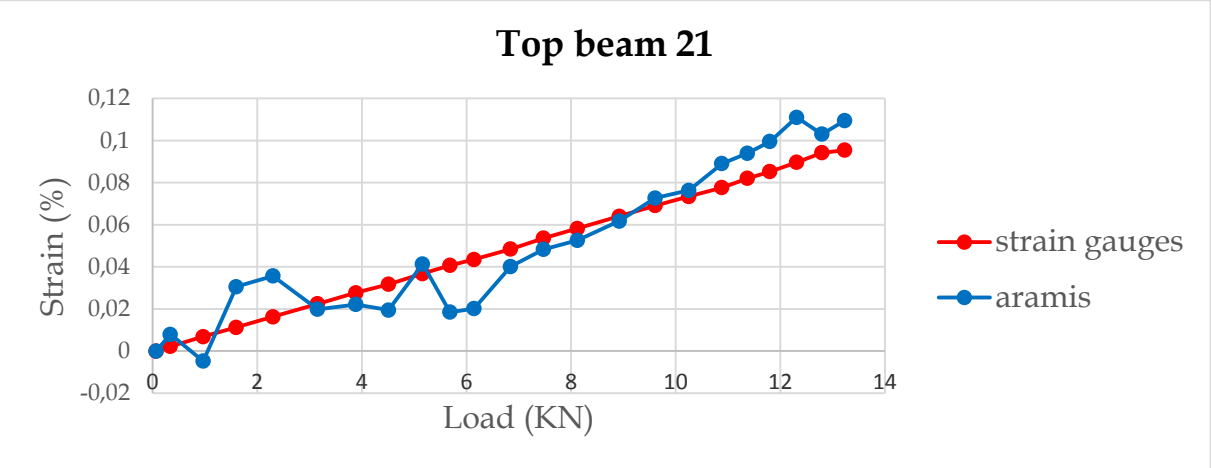

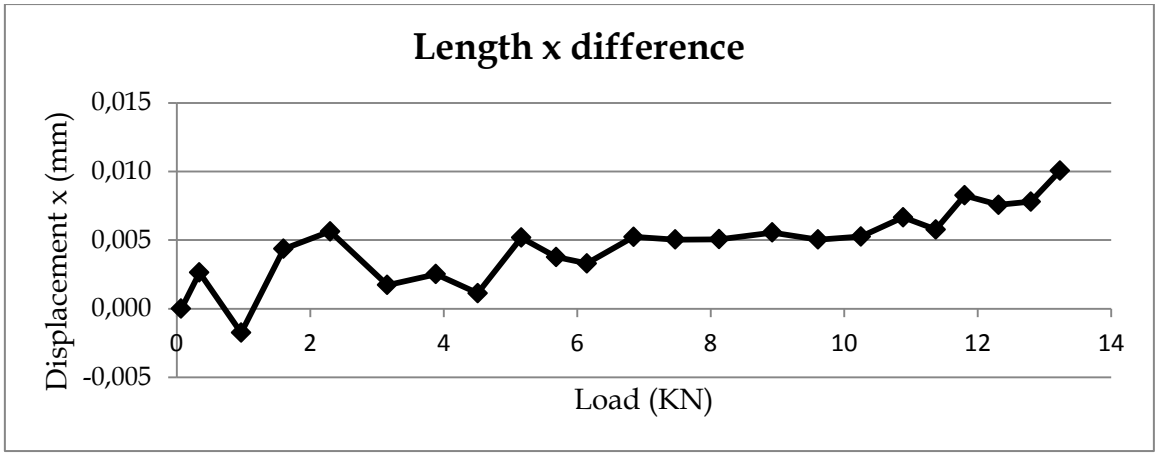
Length x difference
Displacement x (mm)
0,015
0,010
0,005
0,000
-0,005
0
2
4
6
8
10
12
14
Load (KN)

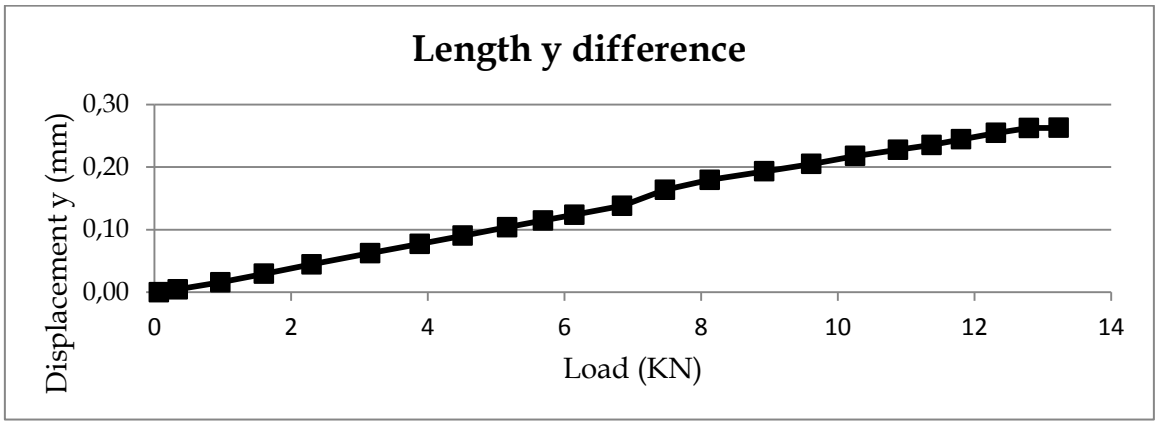
Length y difference
Displacement y (mm)
0,30
0,20
0,10
0,00
0
2
4
6
8
10
12
14
Load (KN)

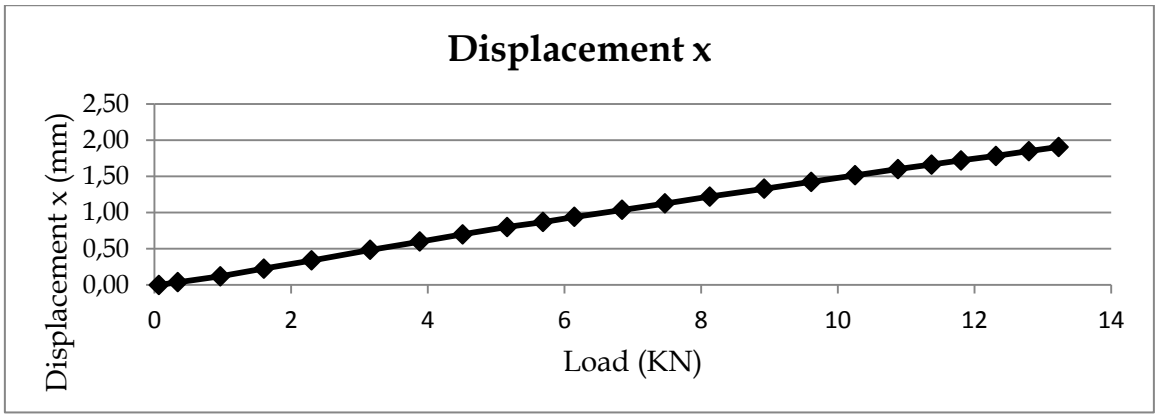
Displacement x
Displacement x (mm)
2,50
2,00
1,50
1,00
0,50
0,00
0
2
4
6
8
10
12
14
Load (KN)

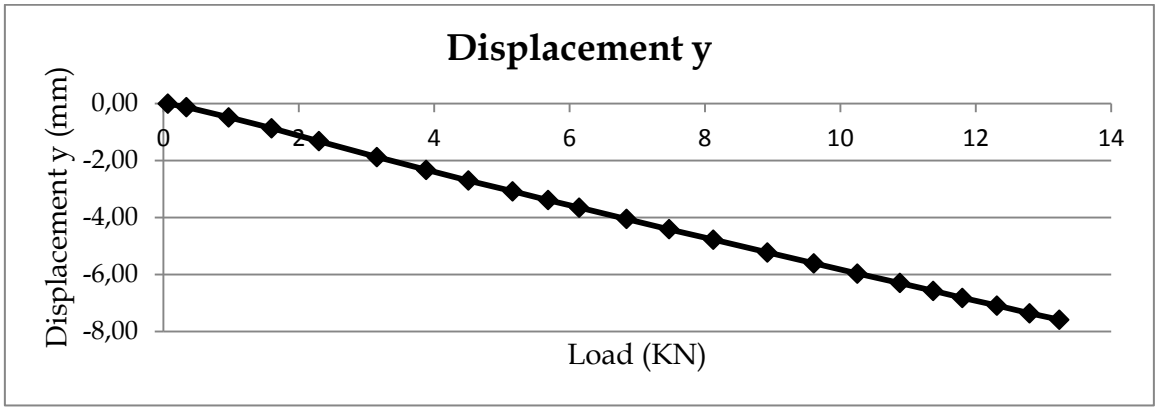
Displacement y
Displacement y (mm)
0,00
-2,00
-4,00
-6,00
-8,00
0
2
4
6
8
10
12
14
Load (KN)

Test 25

	Strain gauges	Aramis				
Load (KN)	Strain (%)	Strain (%)	Δ Lenght x (mm)	Δ Lenght y (mm)	Displ x (mm)	Displ y (mm)
0,064	0,000	0,000	0,0000	0,000	0,00	0,00
0,476	0,003	-0,006	0,0017	0,008	0,06	-0,21
1,013	0,007	0,010	0,0013	0,020	0,14	-0,52
1,515	0,011	0,019	0,0013	0,032	0,22	-0,85
2,211	0,016	0,009	0,0035	0,052	0,35	-1,35
2,873	0,020	0,012	0,0037	0,067	0,47	-1,81
3,710	0,026	0,022	0,0043	0,088	0,61	-2,39
4,578	0,033	0,016	0,0038	0,110	0,75	-2,95
5,284	0,037	0,023	0,0042	0,127	0,87	-3,39
5,886	0,042	0,027	0,0044	0,141	0,95	-3,75
6,554	0,046	0,032	0,0054	0,155	1,05	-4,14
7,059	0,050	0,036	0,0056	0,169	1,13	-4,44
7,554	0,054	0,034	0,0050	0,181	1,20	-4,72
8,057	0,057	0,048	0,0070	0,193	1,26	-4,98
8,658	0,062	0,060	0,0078	0,206	1,34	-5,31
9,122	0,065	0,068	0,0083	0,217	1,41	-5,56
9,644	0,069	0,068	0,0082	0,230	1,48	-5,87
10,057	0,072	0,069	0,0081	0,241	1,54	-6,08
10,522	0,075	0,080	0,0088	0,251	1,60	-6,32
10,979	0,078	0,090	0,0094	0,262	1,66	-6,57
11,561	0,083	0,094	0,0095	0,276	1,74	-6,89
11,948	0,085	0,105	0,0102	0,285	1,79	-7,08
12,309	0,089	0,094	0,0123	0,292	1,83	-7,25
12,676	0,091	0,098	0,0125	0,300	1,88	-7,45
12,833	0,093	0,111	0,0111	0,304	1,90	-7,54

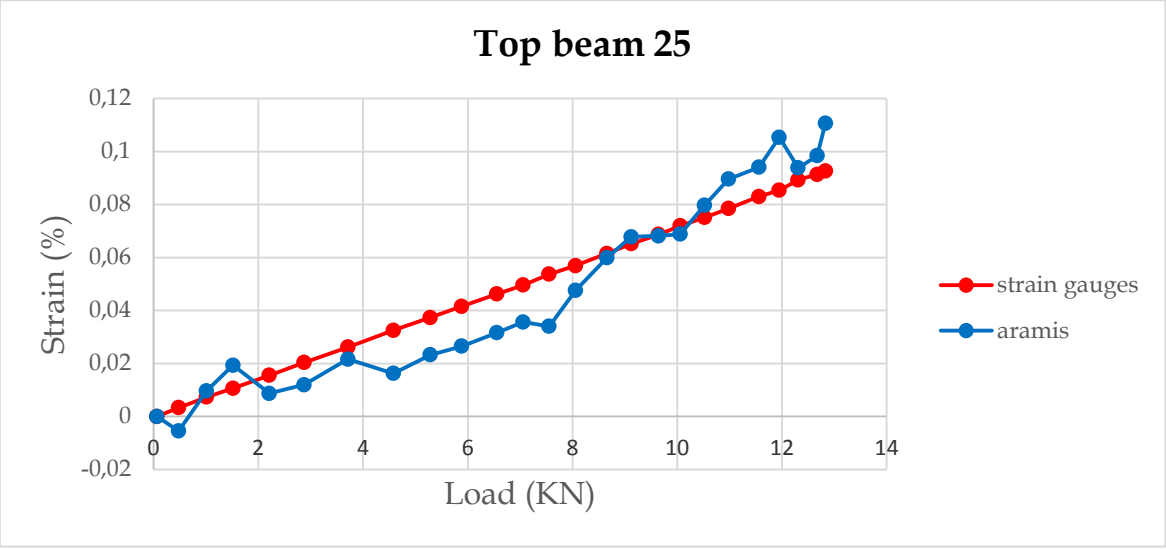

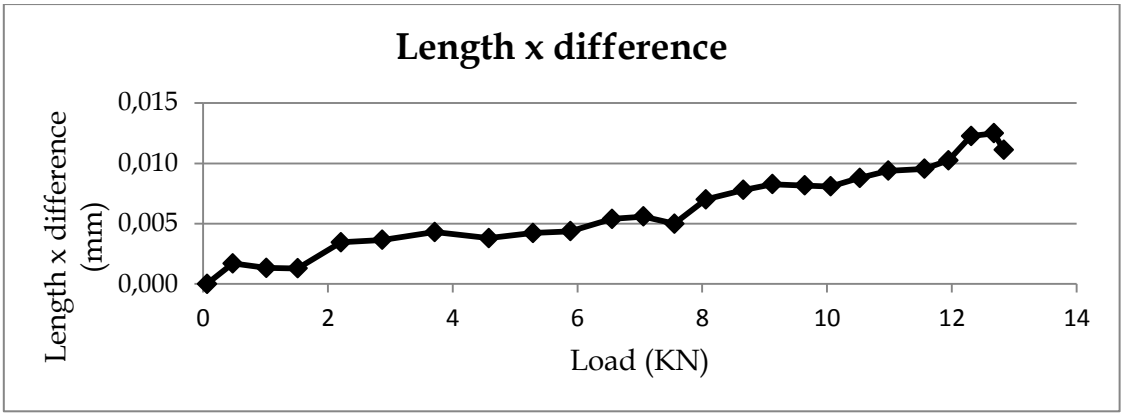
Length x difference
Length x difference (mm)
0,015
0,010
0,005
0,000
0
2
4
6
8
10
12
14
Load (KN)

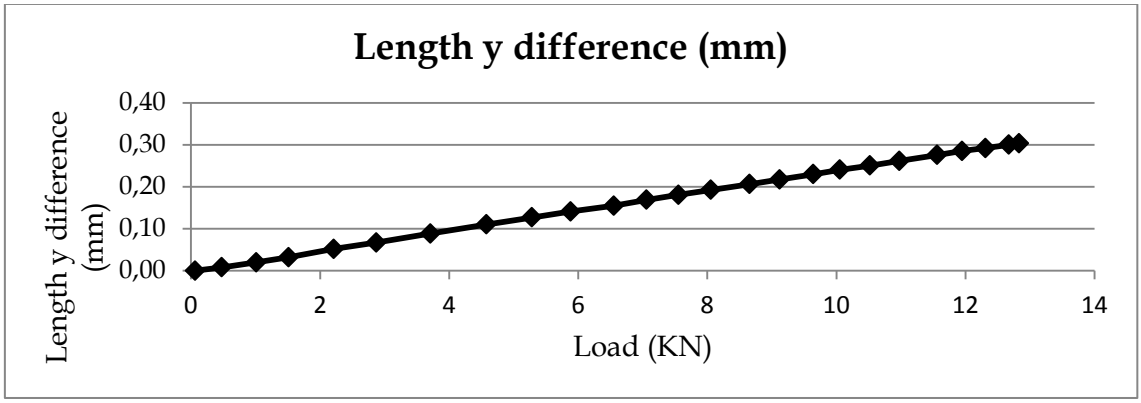
Length y difference (mm)
Length y difference (mm)
0,40
0,30
0,20
0,10
0,00
0
2
4
6
8
10
12
14
Load (KN)

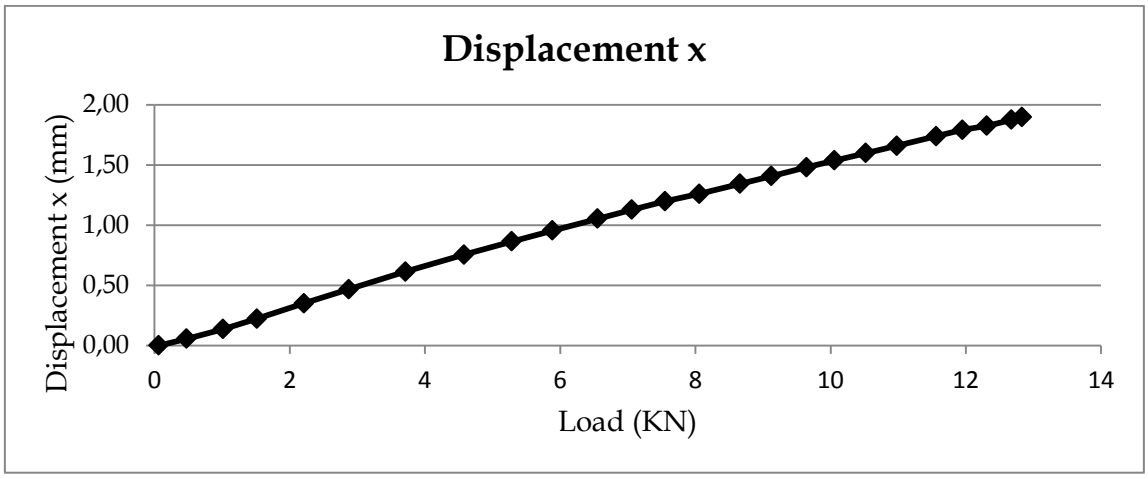
Displacement x
Displacement x (mm)
2,00
1,50
1,00
0,50
0,00
0
2
4
6
8
10
12
14
Load (KN)

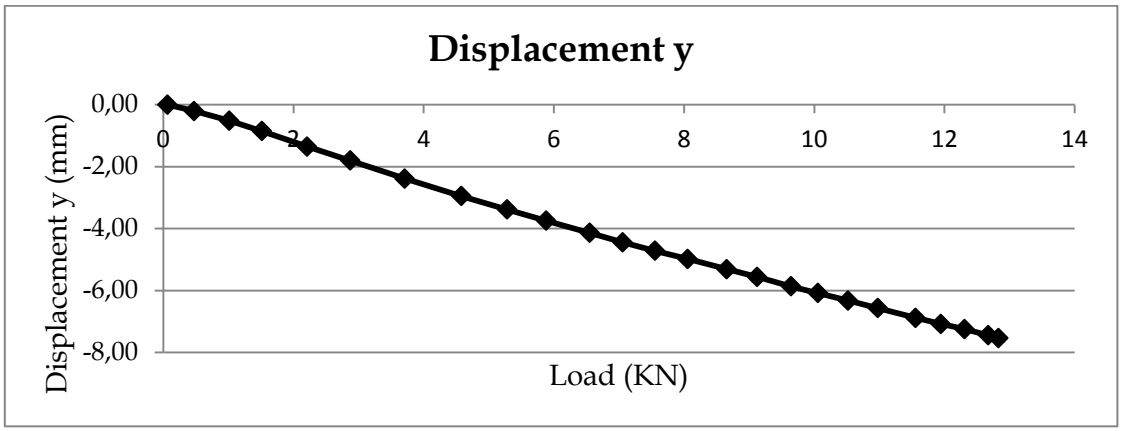
Displacement y
Displacement y (mm)
0,00
-2,00
-4,00
-6,00
-8,00
0
2
4
6
8
10
12
14
Load (KN)

3.2.2 Mid beam

Test 18

	Strain gauges	Aramis				
Load (KN)	Strain (%)	Strain (%)	Δ Lenght x (mm)	Δ Lenght y (mm)	Displ x (mm)	Displ y (mm)
0,026	0,000	0,003	0,00000	0,000	0,00	0,00
0,700	0,003	-0,009	-0,00065	-0,014	0,04	-0,36
1,154	0,004	-0,009	-0,00055	-0,023	0,08	-0,63
1,630	0,006	0,008	0,00075	-0,033	0,12	-0,93
2,242	0,008	0,020	0,00097	-0,048	0,18	-1,34
2,777	0,010	0,010	0,00033	-0,060	0,22	-1,68
3,177	0,010	0,010	0,00045	-0,069	0,26	-1,93
3,545	0,012	0,013	0,00073	-0,078	0,29	-2,16
4,057	0,013	0,014	0,00091	-0,087	0,33	-2,47
4,456	0,014	0,006	0,00038	-0,096	0,36	-2,71
4,800	0,015	0,013	0,00096	-0,105	0,39	-2,92
5,218	0,016	0,016	0,00123	-0,114	0,42	-3,16
5,558	0,017	0,014	0,00119	-0,121	0,45	-3,36
5,865	0,018	0,015	0,00129	-0,128	0,47	-3,54
6,244	0,019	0,014	0,00130	-0,137	0,50	-3,76
6,579	0,020	0,011	0,00090	-0,143	0,52	-3,95
6,979	0,021	0,015	0,00095	-0,152	0,55	-4,18
7,362	0,023	0,016	0,00105	-0,160	0,57	-4,41
7,785	0,024	0,016	0,00158	-0,171	0,60	-4,65
8,047	0,024	0,017	0,00167	-0,175	0,62	-4,80
8,432	0,026	0,019	0,00182	-0,183	0,65	-5,02
8,813	0,026	0,020	0,00193	-0,191	0,67	-5,23
9,216	0,029	0,032	0,00279	-0,200	0,70	-5,47
9,593	0,029	0,024	0,00226	-0,208	0,72	-5,67
9,926	0,030	0,026	0,00243	-0,215	0,74	-5,86
10,223	0,032	0,037	0,00317	-0,222	0,76	-6,03
10,583	0,033	0,034	0,00296	-0,230	0,78	-6,23
10,901	0,033	0,042	0,00353	-0,237	0,80	-6,40
11,302	0,035	0,041	0,00404	-0,244	0,83	-6,63
11,672	0,036	0,040	0,00406	-0,249	0,85	-6,83
12,154	0,038	0,046	0,00383	-0,256	0,88	-7,09
12,589	0,039	0,041	0,00431	-0,267	0,91	-7,35
12,937	0,040	0,049	0,00472	-0,273	0,92	-7,53

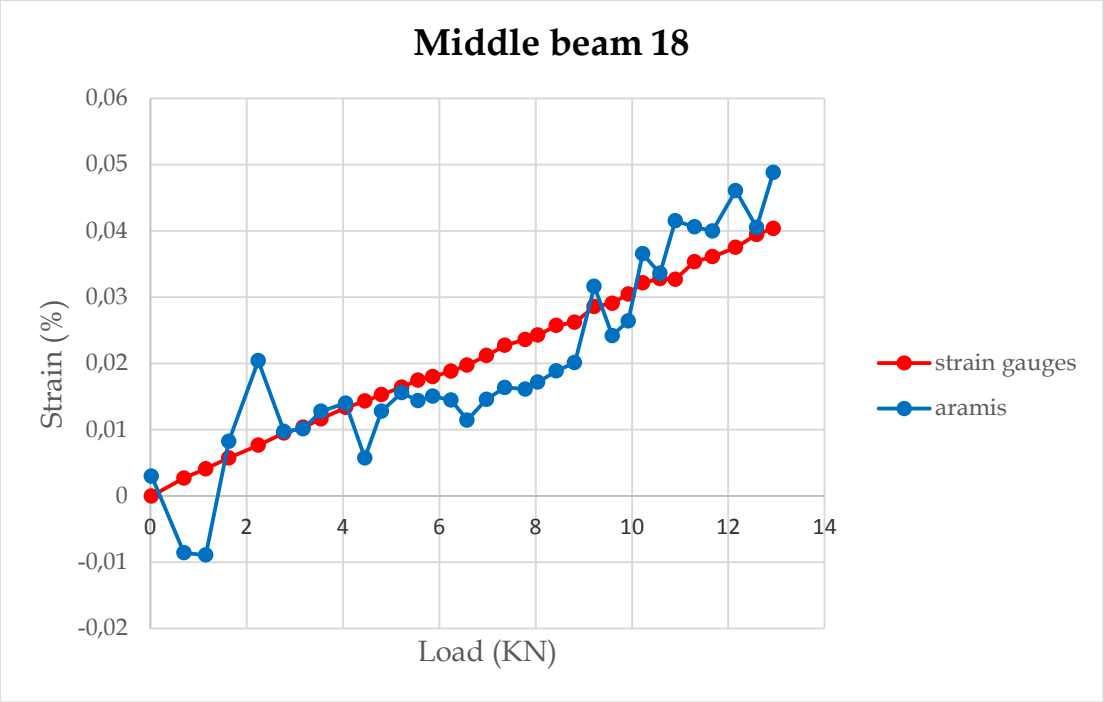
Middle beam 18
0,06
0,05
0,04
0,03
0,02
0,01
0
-0,01
-0,02
Strain (%)
0
2
4
6
8
10
12
14
Load (KN)
strain gauges
aramis

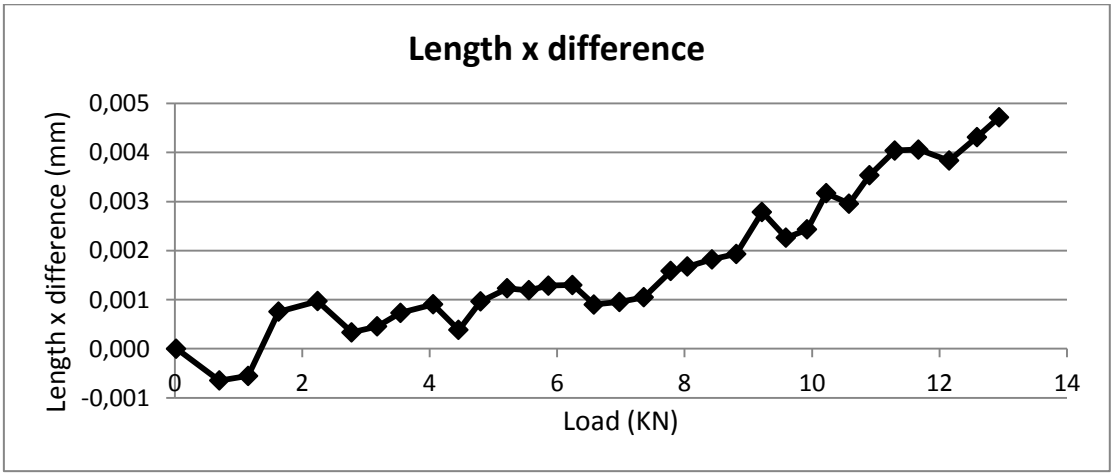
Length x difference
0,005
0,004
0,003
0,002
0,001
0,000
-0,001
Length x difference (mm)
0
2
4
6
8
10
12
14
Load (KN)

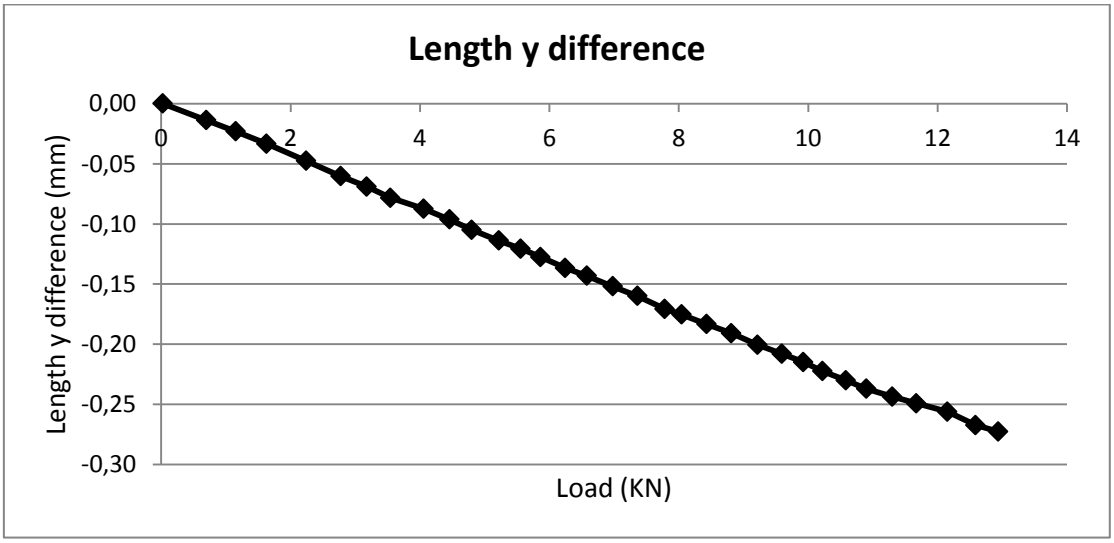
Length y difference
0,00
-0,05
-0,10
-0,15
-0,20
-0,25
-0,30
Length y difference (mm)
0
2
4
6
8
10
12
14
Load (KN)

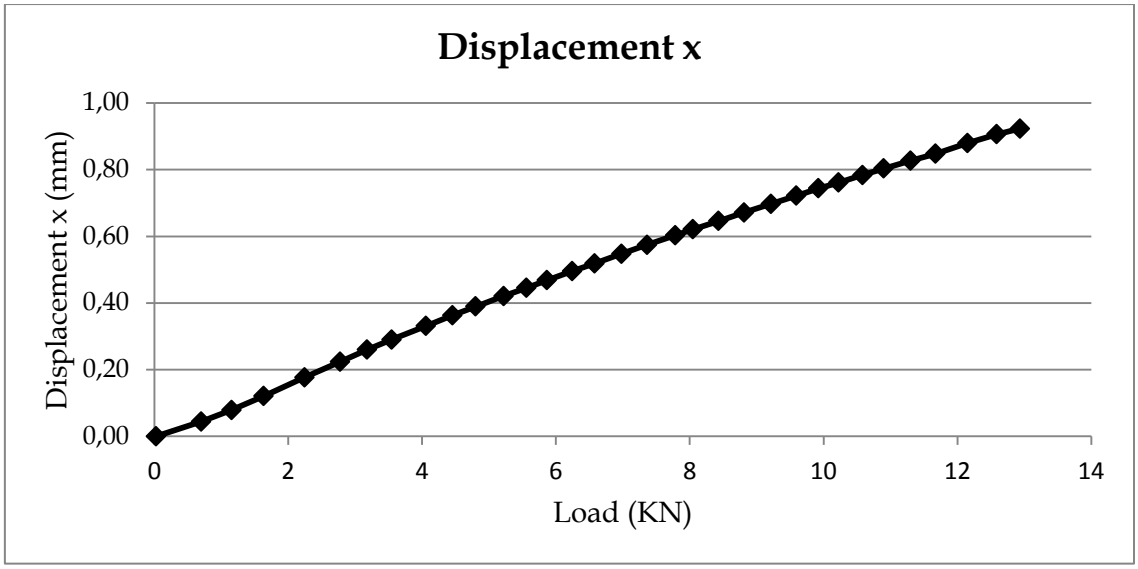
Displacement x
1,00
0,80
0,60
0,40
0,20
0,00
Displacement x (mm)
0
2
4
6
8
10
12
14
Load (KN)

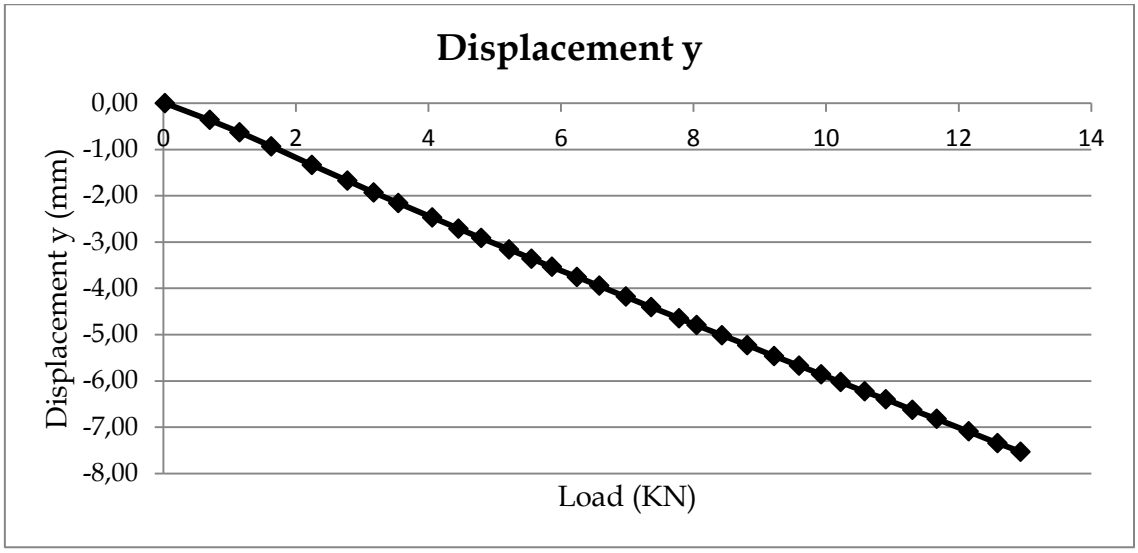
Displacement y
0,00
-1,00
-2,00
-3,00
-4,00
-5,00
-6,00
-7,00
-8,00
Displacement y (mm)
0
2
4
6
8
10
12
14
Load (KN)

Test 25

	Strain gauges	Aramis				
Load (KN)	Strain (%)	Strain (%)	Δ Lenght x (mm)	Δ Lenght y (mm)	Displ x (mm)	Displ y (mm)
0,0636	0,0000	0,0000	0,0000	0,000	0,00	0,00
0,4762	0,0018	-0,0184	-0,0020	0,007	0,03	-0,20
1,0128	0,0038	0,0032	0,0009	0,018	0,07	-0,51
1,5151	0,0053	0,0207	0,0029	0,029	0,11	-0,86
2,2109	0,0076	0,0116	0,0020	0,045	0,17	-1,35
2,8728	0,0098	0,0060	0,0009	0,059	0,23	-1,80
3,7105	0,0121	0,0045	0,0006	0,078	0,31	-2,38
4,5784	0,0149	0,0198	0,0012	0,096	0,38	-2,94
5,2843	0,0167	0,0107	0,0001	0,111	0,43	-3,40
5,8857	0,0184	0,0180	0,0008	0,124	0,48	-3,74
6,5536	0,0203	0,0094	0,0007	0,139	0,53	-4,13
7,0588	0,0215	0,0211	0,0019	0,149	0,56	-4,44
7,5539	0,0233	0,0093	0,0011	0,160	0,60	-4,71
8,0574	0,0245	0,0256	0,0040	0,170	0,63	-4,94
8,6582	0,0265	0,0377	0,0040	0,183	0,67	-5,30
9,1224	0,0282	0,0360	0,0037	0,192	0,70	-5,58
9,6437	0,0295	0,0239	0,0017	0,202	0,74	-5,86
10,0569	0,0310	0,0377	0,0035	0,213	0,77	-6,09
10,5223	0,0322	0,0398	0,0035	0,222	0,80	-6,31
10,9794	0,0336	0,0473	0,0042	0,231	0,83	-6,56
11,5606	0,0356	0,0429	0,0045	0,244	0,87	-6,88
11,9483	0,0365	0,0341	0,0023	0,251	0,90	-7,07
12,3092	0,0387	0,0488	0,0050	0,258	0,91	-7,25
12,6755	0,0393	0,0433	0,0053	0,265	0,94	-7,44
12,8329	0,0398	0,0418	0,0051	0,269	0,95	-7,51

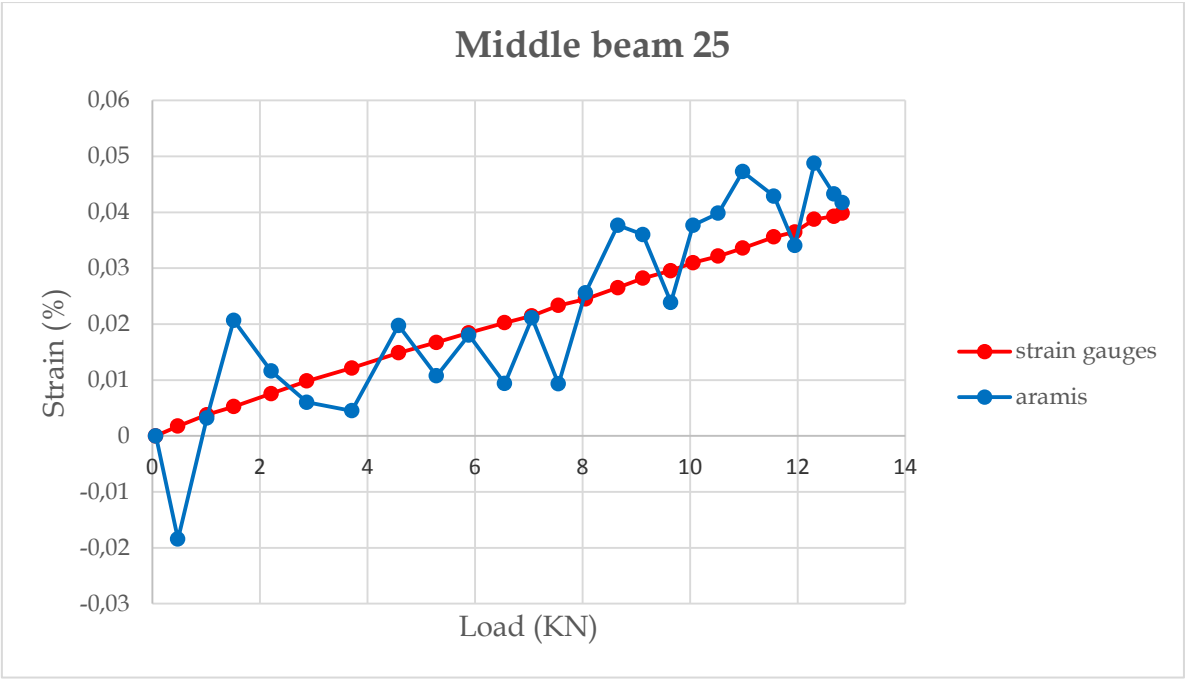
Middle beam 25
0,06
0,05
0,04
0,03
0,02
0,01
0
-0,01
-0,02
-0,03
Strain (%)
0
2
4
6
8
10
12
14
Load (KN)
strain gauges
aramis

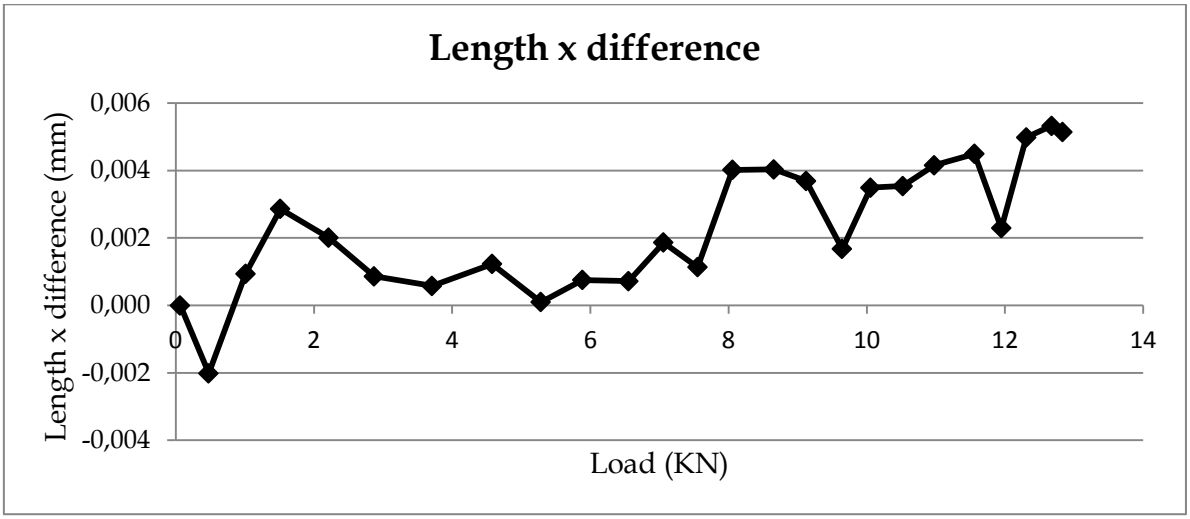
Length x difference
0,006
0,004
0,002
0,000
-0,002
-0,004
Length x difference (mm)
0
2
4
6
8
10
12
14
Load (KN)

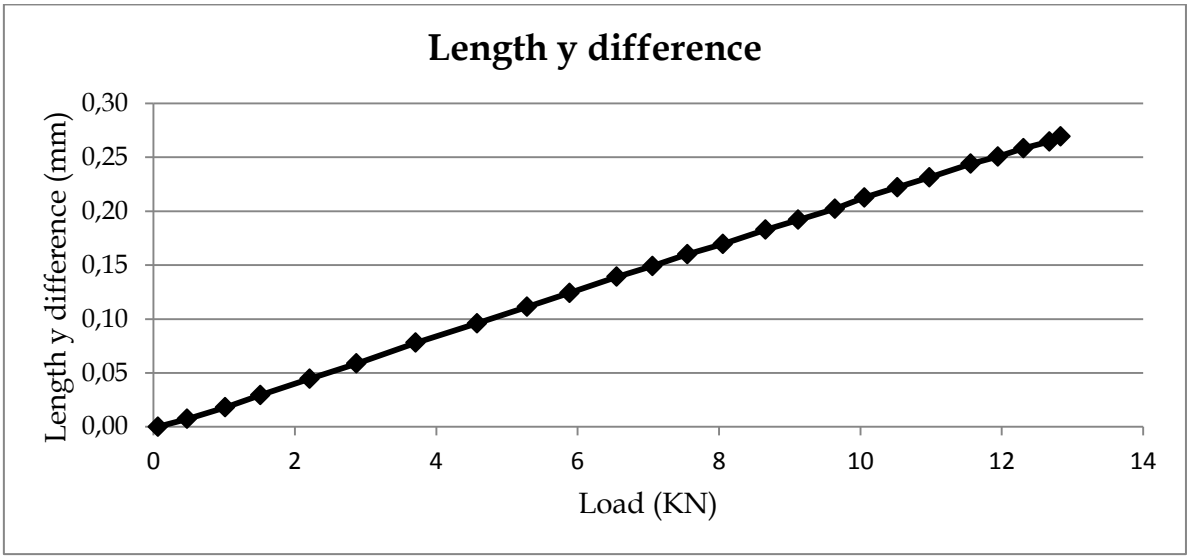
Length y difference
0,30
0,25
0,20
0,15
0,10
0,05
0,00
Length y difference (mm)
0
2
4
6
8
10
12
14
Load (KN)

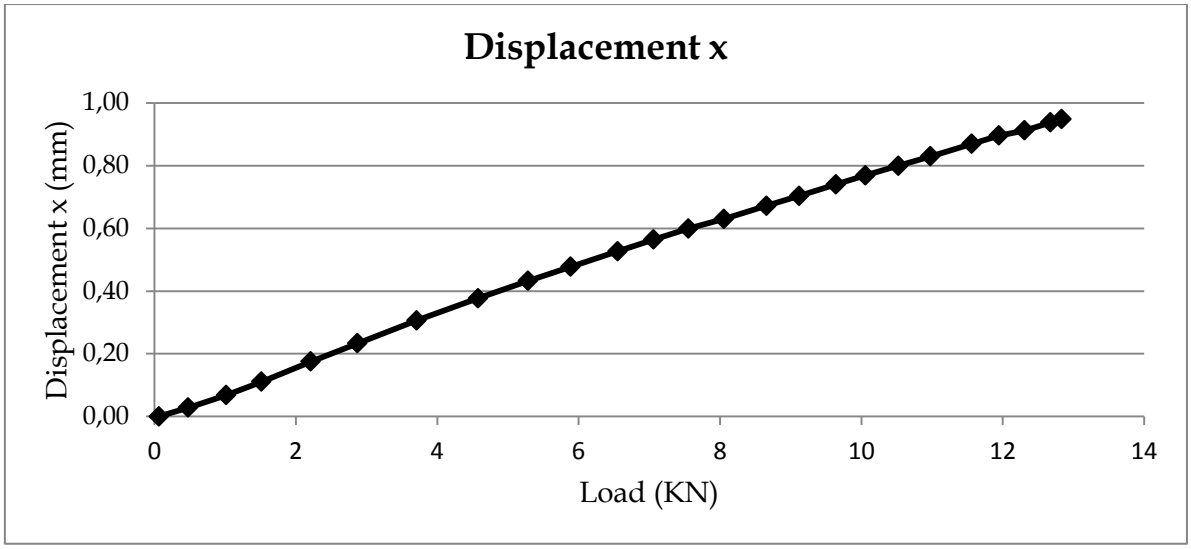
Displacement x
Displacement x (mm)
1,00
0,80
0,60
0,40
0,20
0,00
0
2
4
6
8
10
12
14
Load (KN)

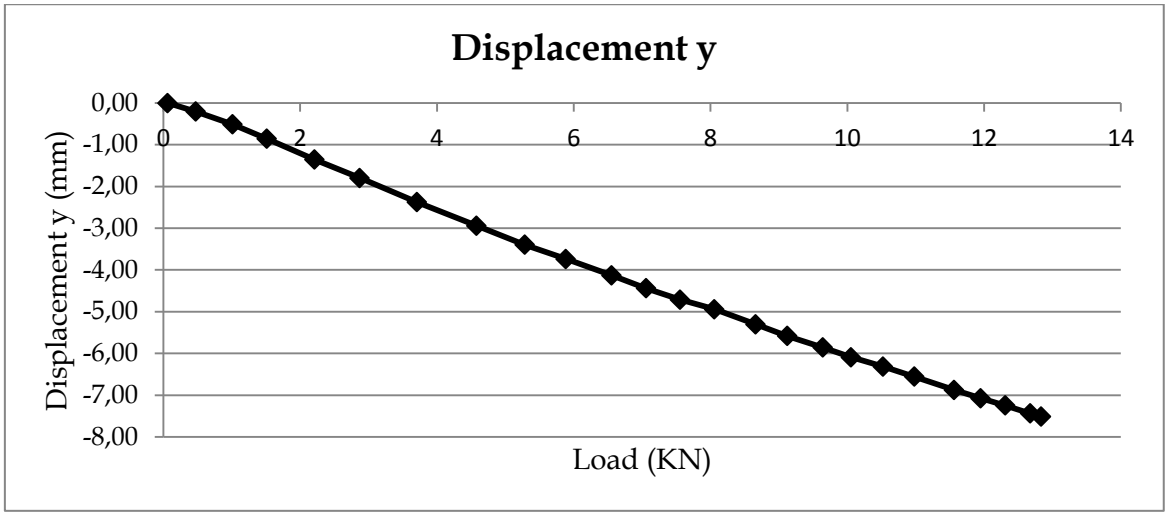
Displacement y
Displacement y (mm)
0,00
-1,00
-2,00
-3,00
-4,00
-5,00
-6,00
-7,00
-8,00
0
2
4
6
8
10
12
14
Load (KN)

3.2.3 Bottom beam

Test 32

	Strain gauges	Aramis				
Load (KN)	Strain (%)	Strain (%)	Δ Lenght x (mm)	Δ Lenght y (mm)	Displ x (mm)	Displ y (mm)
0,1295	0,0000	0,0000	0,0000	0,000	0,00	0,00
0,5148	-0,0018	-0,0127	-0,0002	0,006	-0,02	-0,20
1,2301	-0,0055	-0,0193	-0,0007	0,019	-0,06	-0,61
2,1283	-0,0106	-0,0187	-0,0013	0,037	-0,11	-1,19
2,9090	-0,0152	-0,0204	-0,0018	0,052	-0,16	-1,69
3,5460	-0,0186	-0,0237	-0,0021	0,066	-0,20	-2,09
4,2994	-0,0229	-0,0263	-0,0024	0,079	-0,24	-2,56
4,9584	-0,0270	-0,0275	-0,0026	0,092	-0,28	-2,95
5,2612	-0,0311	-0,0422	-0,0035	0,098	-0,30	-3,11
5,5182	-0,0297	-0,0311	-0,0029	0,102	-0,32	-3,28
6,1303	-0,0333	-0,0304	-0,0031	0,114	-0,35	-3,63
6,7483	-0,0368	-0,0406	-0,0035	0,126	-0,39	-3,98
7,4524	-0,0403	-0,0396	-0,0037	0,139	-0,44	-4,39
8,0871	-0,0438	-0,0425	-0,0040	0,151	-0,48	-4,74
8,7799	-0,0475	-0,0465	-0,0043	0,164	-0,53	-5,13
9,3272	-0,0506	-0,0498	-0,0045	0,174	-0,57	-5,44
9,9832	-0,0541	-0,0456	-0,0047	0,185	-0,61	-5,81
10,4706	-0,0569	-0,0598	-0,0057	0,195	-0,64	-6,07
10,8179	-0,0592	-0,0518	-0,0051	0,201	-0,67	-6,26
11,4793	-0,0623	-0,0553	-0,0054	0,213	-0,71	-6,62
11,9073	-0,0646	-0,0558	-0,0055	0,220	-0,74	-6,85
12,3769	-0,0670	-0,0595	-0,0058	0,229	-0,77	-7,11
12,9261	-0,0701	-0,0650	-0,0061	0,238	-0,81	-7,40
13,4123	-0,0728	-0,0655	-0,0063	0,247	-0,84	-7,66

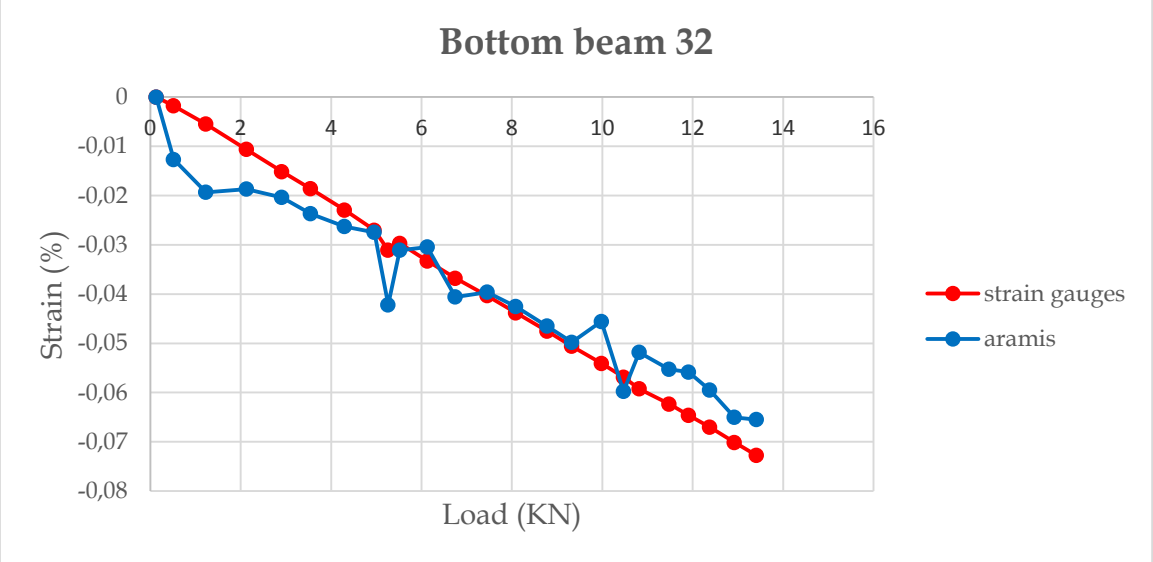

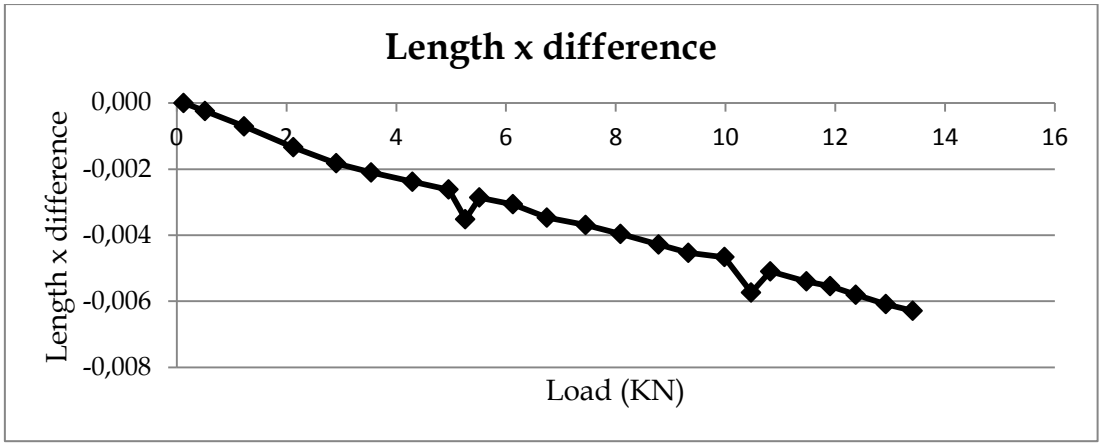
Length x difference
0,000
-0,002
-0,004
-0,006
-0,008
Length x difference
0
2
4
6
8
10
12
14
16
Load (KN)

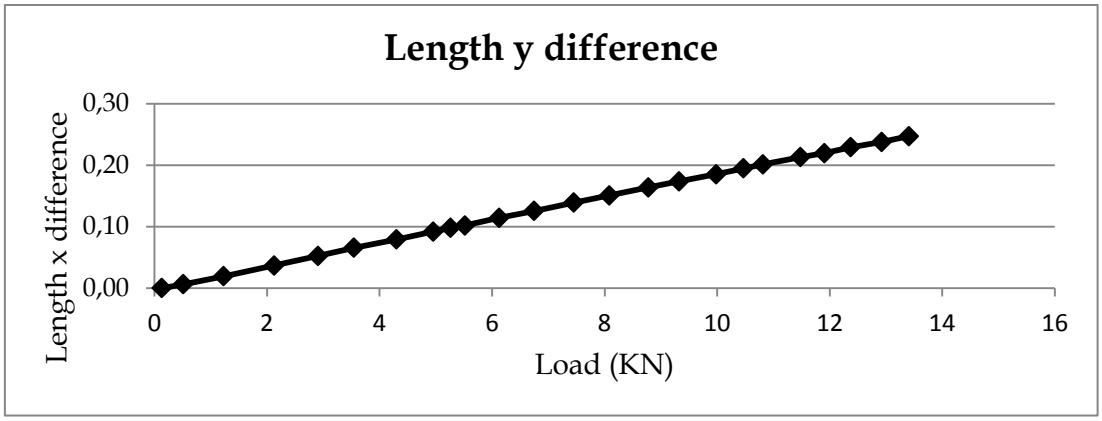
Length y difference
0,30
0,20
0,10
0,00
Length x difference
0
2
4
6
8
10
12
14
16
Load (KN)

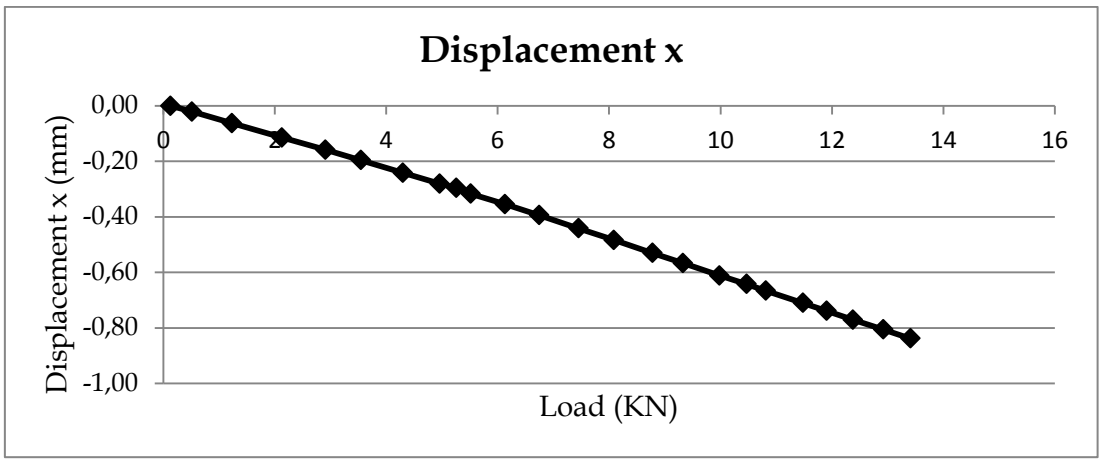
Displacement x
0,00
-0,20
-0,40
-0,60
-0,80
-1,00
Displacement x (mm)
0
2
4
6
8
10
12
14
16
Load (KN)

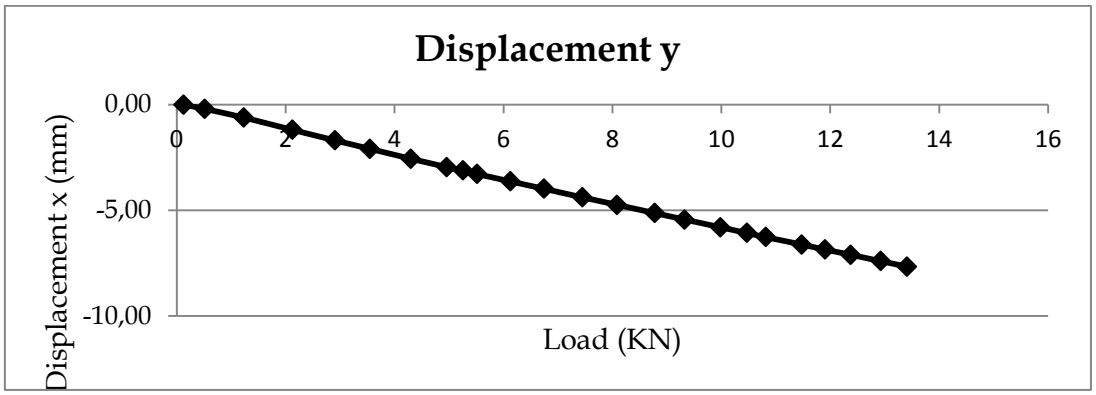
Displacement y
0,00
-5,00
-10,00
Displacement x (mm)
0
2
4
6
8
10
12
14
16
Load (KN)

Test 34

	Strain gauges	Aramis				
Load (KN)	Strain (%)	Strain (%)	Δ Lenght x (mm)	Δ Lenght y (mm)	Displ x (mm)	Displ y (mm)
0,1283	0,0000	0,0000	0,0000	0,000	0,00	0,00
0,2755	-0,0007	-0,0120	0,0003	0,001	-0,01	-0,07
0,9042	-0,0038	-0,0081	-0,0004	0,014	-0,05	-0,42
1,5531	-0,0074	-0,0135	-0,0007	0,029	-0,10	-0,81
2,0524	-0,0101	-0,0164	-0,0009	0,042	-0,13	-1,14
2,4786	-0,0127	-0,0186	-0,0013	0,051	-0,16	-1,41
3,1275	-0,0163	-0,0066	-0,0017	0,068	-0,20	-1,82
3,8714	-0,0204	-0,0171	-0,0022	0,087	-0,25	-2,29
4,6687	-0,0251	-0,0191	-0,0024	0,105	-0,31	-2,77
5,4179	-0,0295	-0,0257	-0,0029	0,122	-0,36	-3,20
5,9783	-0,0323	-0,0278	-0,0042	0,134	-0,41	-3,53
6,7596	-0,0368	-0,0462	-0,0052	0,153	-0,47	-3,96
7,3847	-0,0406	-0,0419	-0,0039	0,166	-0,51	-4,33
8,0140	-0,0434	-0,0577	-0,0045	0,181	-0,56	-4,68
8,6035	-0,0466	-0,0441	-0,0043	0,193	-0,61	-5,02
9,3011	-0,0504	-0,0503	-0,0041	0,210	-0,67	-5,41
9,8693	-0,0534	-0,0541	-0,0046	0,223	-0,71	-5,72
10,4457	-0,0566	-0,0478	-0,0050	0,235	-0,75	-6,04
10,9076	-0,0586	-0,0556	-0,0054	0,246	-0,79	-6,29
11,5161	-0,0631	-0,0601	-0,0053	0,258	-0,83	-6,62
12,0771	-0,0650	-0,0555	-0,0058	0,272	-0,87	-6,92
12,6518	-0,0681	-0,0625	-0,0062	0,283	-0,92	-7,23
13,3013	-0,0719	-0,0825	-0,0070	0,299	-0,97	-7,57

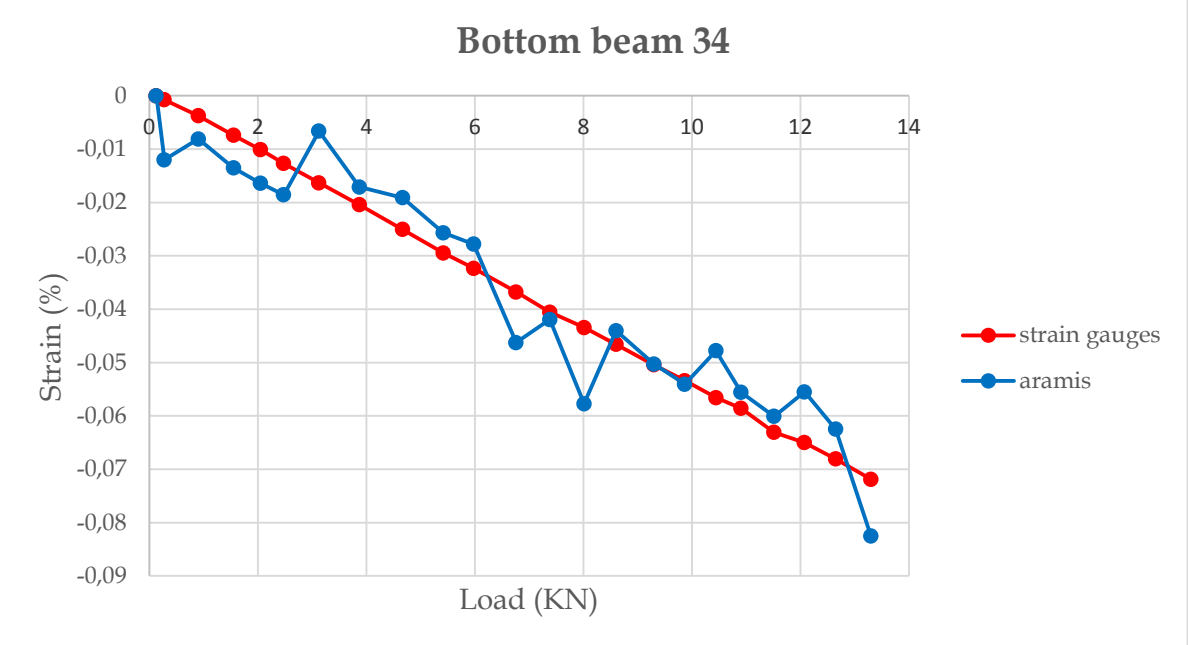

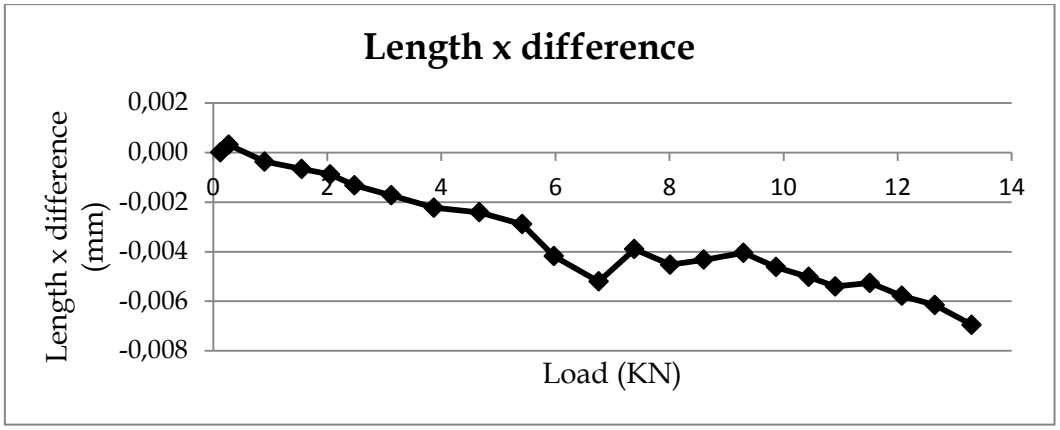
Length x difference
Length x difference (mm)
0,002
0,000
-0,002
-0,004
-0,006
-0,008
0
2
4
6
8
10
12
14
Load (KN)

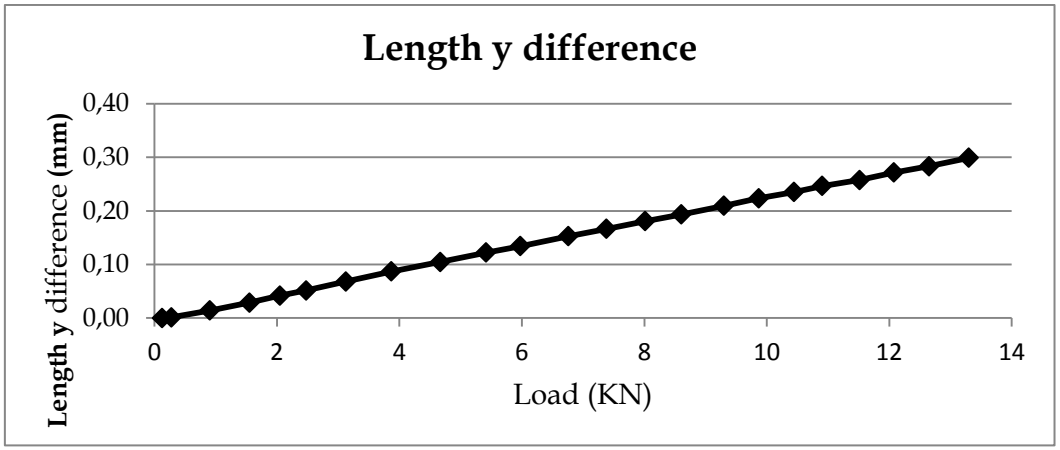
Length y difference
Length y difference (mm)
0,40
0,30
0,20
0,10
0,00
0
2
4
6
8
10
12
14
Load (KN)

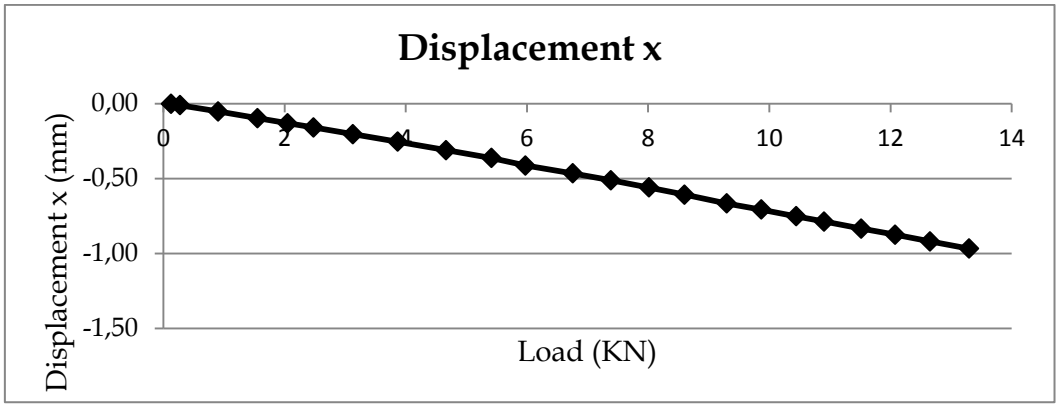
Displacement x
Displacement x (mm)
0,00
-0,50
-1,00
-1,50
0
2
4
6
8
10
12
14
Load (KN)

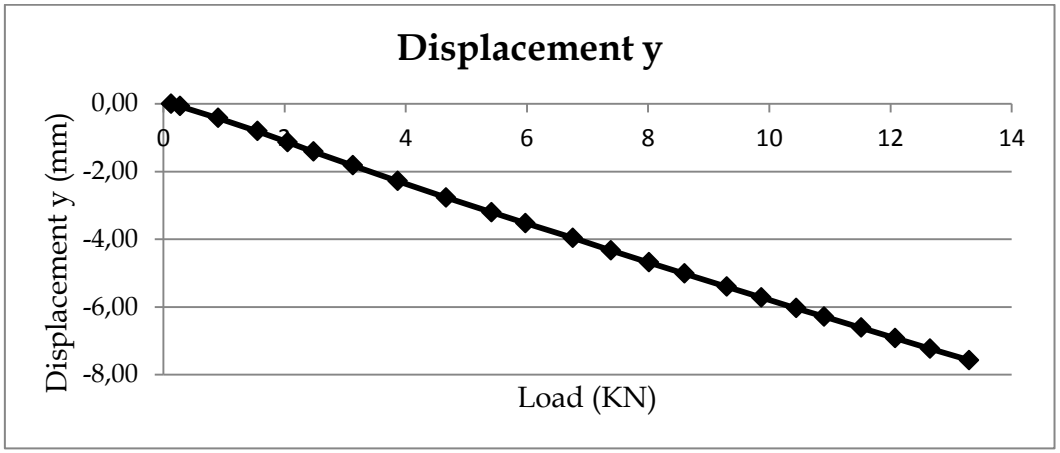
Displacement y
Displacement y (mm)
0,00
-2,00
-4,00
-6,00
-8,00
0
4
6
8
10
12
14
Load (KN)

3.2.4 Top joint

Test 31

	Strain gauges	Aramis				
Load (KN)	Strain (%)	Strain (%)	Δ Lenght x (mm)	Δ Lenght y (mm)	Displ x (mm)	Displ y (mm)
0,1419	0,0000	0,0000	0,0000	0,000	0,00	0,00
0,4791	0,0008	0,0033	0,0003	0,006	0,04	-0,10
0,9659	0,0020	0,0026	0,0003	0,016	0,09	-0,27
1,8297	0,0040	-0,0059	-0,0005	0,034	0,22	-0,59
2,4287	0,0054	0,0076	0,0008	0,048	0,31	-0,82
3,2261	0,0074	0,0159	0,0015	0,066	0,44	-1,12
3,9521	0,0091	0,0143	0,0016	0,080	0,55	-1,39
4,5731	0,0106	0,0033	0,0009	0,095	0,64	-1,61
5,3811	0,0125	0,0186	0,0021	0,111	0,76	-1,89
6,1089	0,0140	0,0140	0,0016	0,126	0,86	-2,13
6,7649	0,0156	0,0156	0,0015	0,138	0,95	-2,35
7,4708	0,0171	0,0144	0,0016	0,152	1,04	-2,59
8,0544	0,0183	0,0174	0,0019	0,163	1,12	-2,78
8,6285	0,0196	0,0247	0,0027	0,174	1,20	-2,97
9,3100	0,0211	0,0198	0,0022	0,187	1,28	-3,19
9,9399	0,0226	0,0165	0,0019	0,198	1,37	-3,40
10,4095	0,0238	0,0280	0,0031	0,207	1,43	-3,55
10,8743	0,0249	0,0244	0,0027	0,215	1,49	-3,70
11,4021	0,0262	0,0244	0,0027	0,225	1,55	-3,87
11,8385	0,0272	0,0248	0,0028	0,234	1,61	-4,01
12,3003	0,0283	0,0289	0,0032	0,242	1,68	-4,16
12,6839	0,0292	0,0428	0,0038	0,249	1,73	-4,28
13,2235	0,0305	0,0418	0,0046	0,261	1,80	-4,45

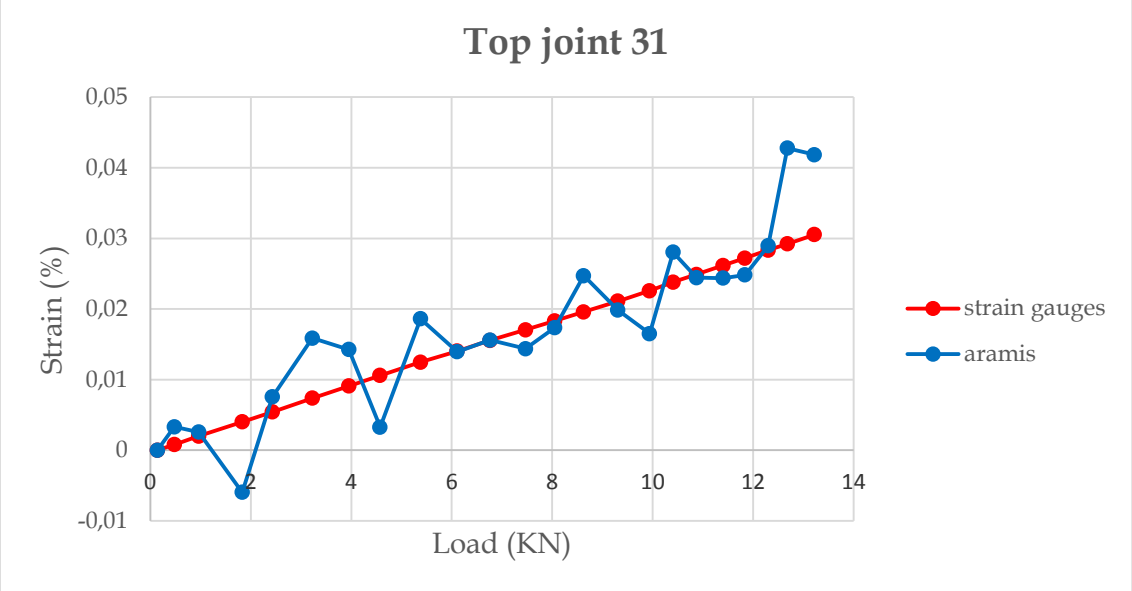

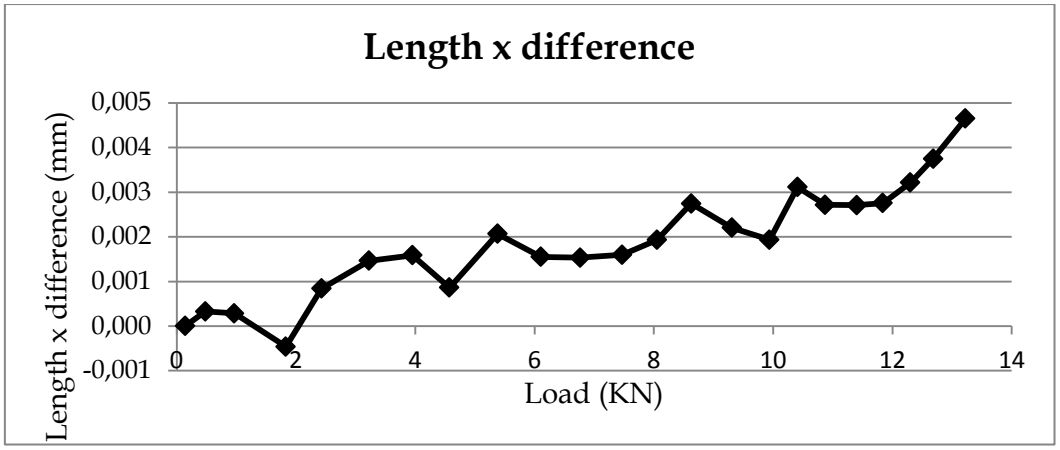
Length x difference
Length x difference (mm)
0,005
0,004
0,003
0,002
0,001
0,000
-0,001
0
2
4
6
8
10
12
14
Load (KN)

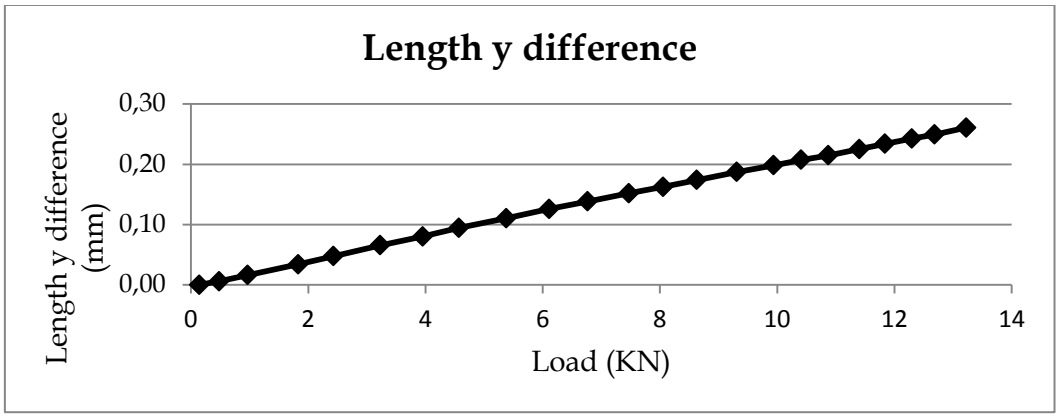
Length y difference
Length y difference (mm)
0,30
0,20
0,10
0,00
0
2
4
6
8
10
12
14
Load (KN)

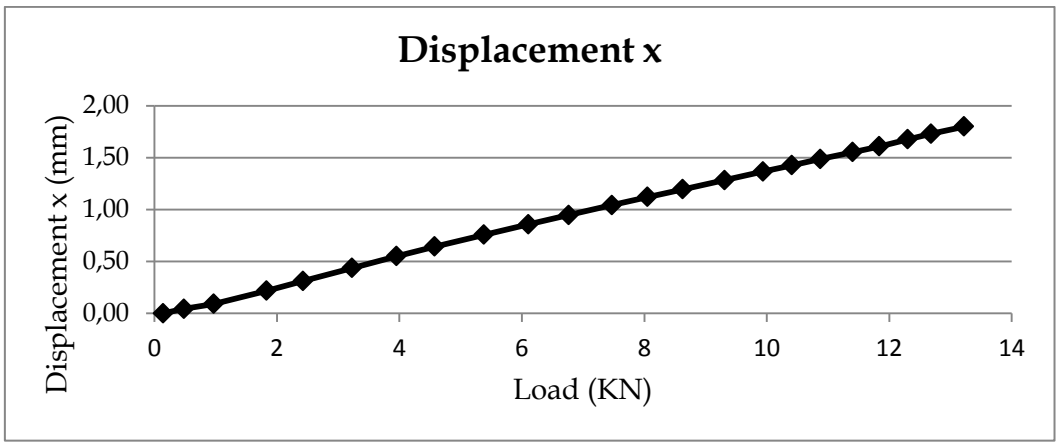
Displacement x
Displacement x (mm)
2,00
1,50
1,00
0,50
0,00
0
2
4
6
8
10
12
14
Load (KN)

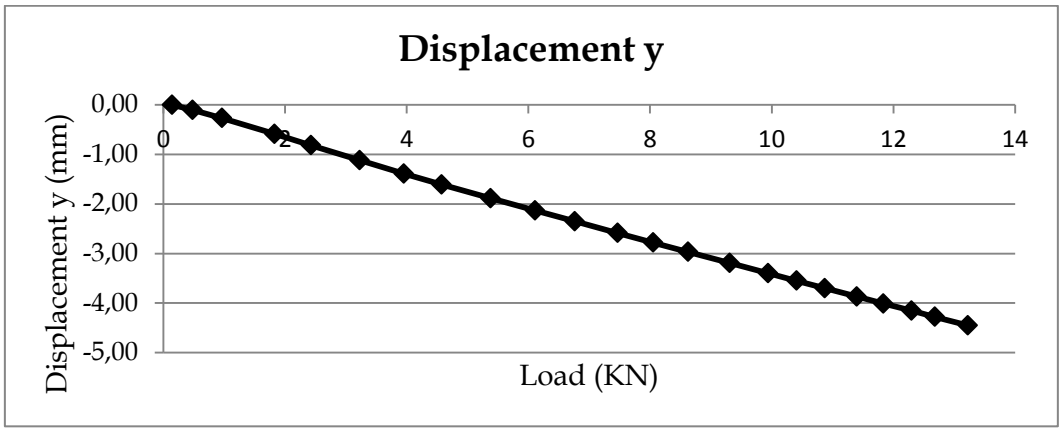
Displacement y
Displacement y (mm)
0,00
-1,00
-2,00
-3,00
-4,00
-5,00
0
2
4
6
8
10
12
14
Load (KN)

Test 33

	Strain gauges	Aramis				
Load (KN)	Strain (%)	Strain (%)	Δ Lenght x (mm)	Δ Lenght y (mm)	Displ x (mm)	Displ y (mm)
0,1295	0,0000	0,0000	0,0000	0,000	0,00	0,00
0,5148	0,0008	-0,0055	-0,0016	0,007	0,04	-0,12
1,2301	0,0025	0,0066	-0,0043	0,021	0,12	-0,37
2,1283	0,0046	0,0039	-0,0072	0,040	0,25	-0,73
2,9090	0,0064	0,0015	-0,0094	0,057	0,35	-1,04
3,5460	0,0079	0,0092	-0,0104	0,071	0,44	-1,28
4,2994	0,0097	0,0136	-0,0118	0,087	0,54	-1,57
4,9584	0,0113	0,0069	-0,0133	0,101	0,63	-1,81
5,2612	0,0117	0,0042	-0,0136	0,101	0,63	-1,81
5,5182	0,0127	0,0093	-0,0136	0,112	0,70	-2,01
6,1303	0,0141	0,0070	-0,0145	0,124	0,77	-2,22
6,7483	0,0155	0,0133	-0,0145	0,136	0,84	-2,44
7,4524	0,0171	0,0139	-0,0158	0,150	0,93	-2,68
8,0871	0,0185	0,0170	-0,0163	0,162	1,00	-2,89
8,7799	0,0198	0,0153	-0,0165	0,176	1,08	-3,13
9,3272	0,0211	0,0209	-0,0164	0,186	1,15	-3,32
9,9832	0,0226	0,0256	-0,0166	0,198	1,22	-3,54
10,4706	0,0238	0,0233	-0,0174	0,207	1,28	-3,70
10,8179	0,0246	0,0267	-0,0174	0,213	1,32	-3,82
11,4793	0,0262	0,0311	-0,0177	0,225	1,39	-4,04
11,9073	0,0272	0,0311	-0,0182	0,233	1,44	-4,18
12,3769	0,0284	0,0320	-0,0186	0,242	1,49	-4,34
12,9261	0,0297	0,0317	-0,0193	0,252	1,55	-4,52
13,4123	0,0308	0,0306	-0,0201	0,262	1,60	-4,67

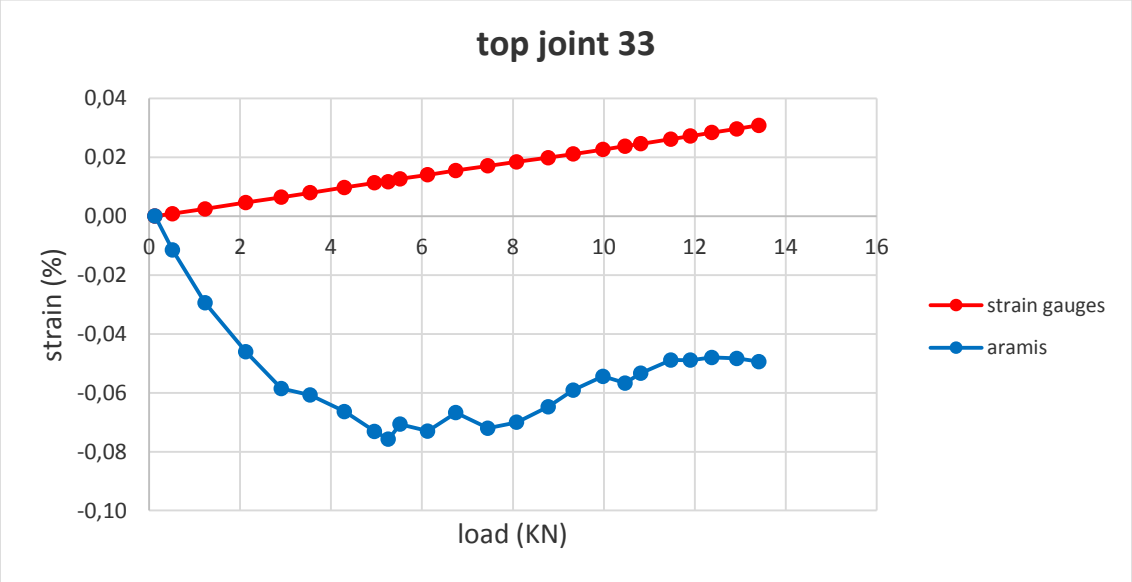

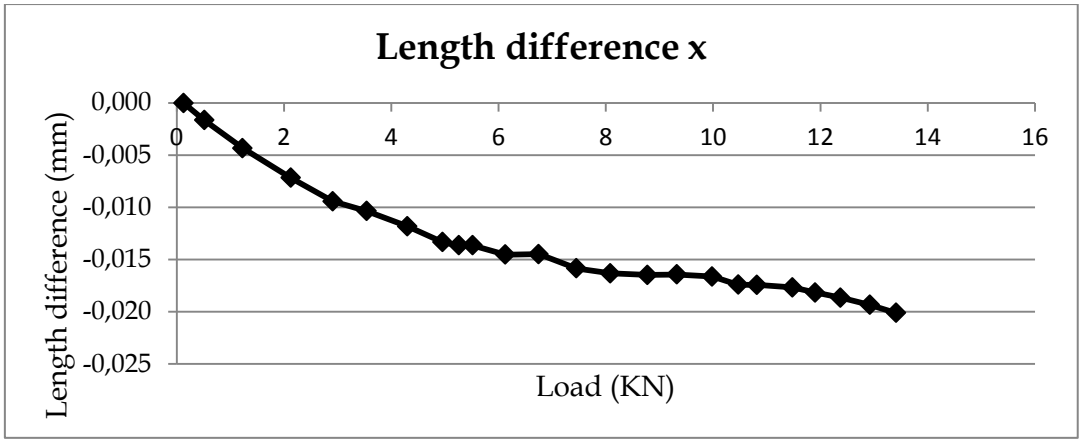
Length difference x
Length difference (mm)
0,000
-0,005
-0,010
-0,015
-0,020
-0,025
0
2
4
6
8
10
12
14
16
Load (KN)

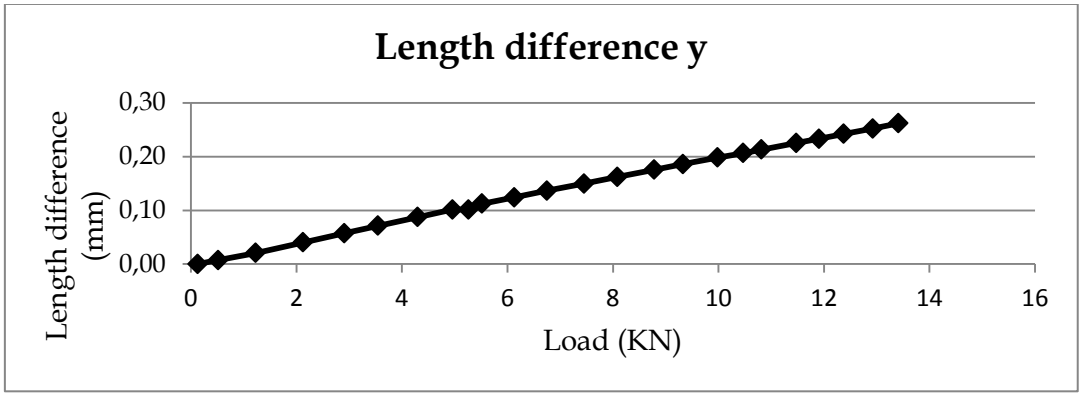
Length difference y
Length difference (mm)
0,30
0,20
0,10
0,00
0
2
4
6
8
10
12
14
16
Load (KN)

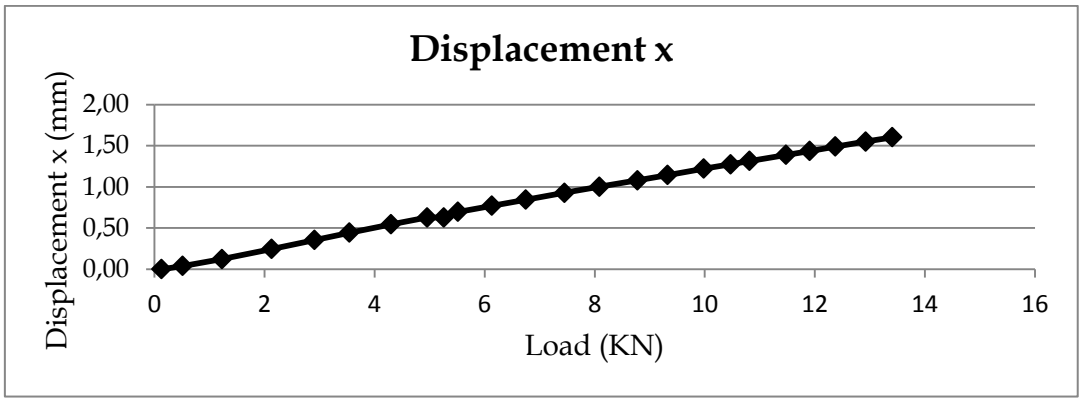
Displacement x
Displacement x (mm)
2,00
1,50
1,00
0,50
0,00
0
2
4
6
8
10
12
14
16
Load (KN)

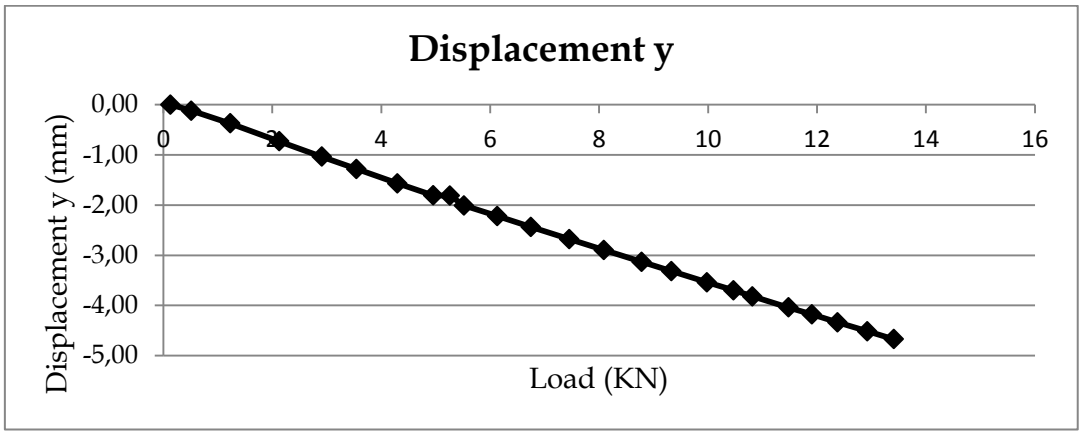
Displacement y
Displacement y (mm)
0,00
-1,00
-2,00
-3,00
-4,00
-5,00
0
4
6
8
10
12
14
16
Load (KN)

3.2.5 Mid joint

Test 13	Strain gauges	Aramis				
Load (KN)	Strain (%)	Strain (%)	Δ Lenght x (mm)	Δ Lenght y (mm)	Displ x (mm)	Displ y (mm)
0,01	0,0000	0,0000	0,0000	0,000	0,00	0,00
0,18	0,0002	-0,0009	0,0001	0,001	0,01	-0,06
0,49	0,0005	-0,0016	0,0000	0,006	0,03	-0,18
0,97	0,0010	0,0015	-0,0001	0,014	0,06	-0,38
1,45	0,0015	0,0003	0,0003	0,022	0,10	-0,59
2,11	0,0023	0,0005	0,0000	0,034	0,16	-0,90
2,37	0,0025	0,0005	0,0000	0,038	0,18	-1,02
2,97	0,0031	0,0003	0,0000	0,049	0,24	-1,30
3,61	0,0037	0,0003	0,0000	0,060	0,30	-1,59
4,15	0,0042	0,0015	0,0001	0,069	0,34	-1,83
4,63	0,0047	0,0021	0,0001	0,077	0,38	-2,03
5,25	0,0055	0,0025	0,0001	0,087	0,43	-2,30
5,67	0,0058	0,0038	0,0001	0,094	0,46	-2,48
6,33	0,0065	0,0048	0,0002	0,105	0,51	-2,75
6,91	0,0069	0,0042	0,0003	0,114	0,55	-2,99
7,33	0,0073	0,0064	0,0003	0,121	0,58	-3,16
7,79	0,0076	0,0058	0,0004	0,127	0,62	-3,35
8,34	0,0081	0,0065	0,0006	0,136	0,66	-3,58
8,85	0,0086	0,0081	0,0008	0,144	0,69	-3,78
9,48	0,0090	0,0096	0,0008	0,153	0,74	-4,03
10,33	0,0098	0,0130	0,0012	0,167	0,80	-4,38
10,90	0,0103	0,0139	0,0012	0,175	0,83	-4,61
11,56	0,0110	0,0153	0,0016	0,186	0,88	-4,88
12,06	0,0116	0,0171	0,0016	0,192	0,91	-5,08
12,46	0,0119	0,0165	0,0019	0,198	0,94	-5,24
12,86	0,0125	0,0183	0,0017	0,205	0,97	-5,40
13,16	0,0127	0,0181	0,0019	0,209	0,99	-5,53

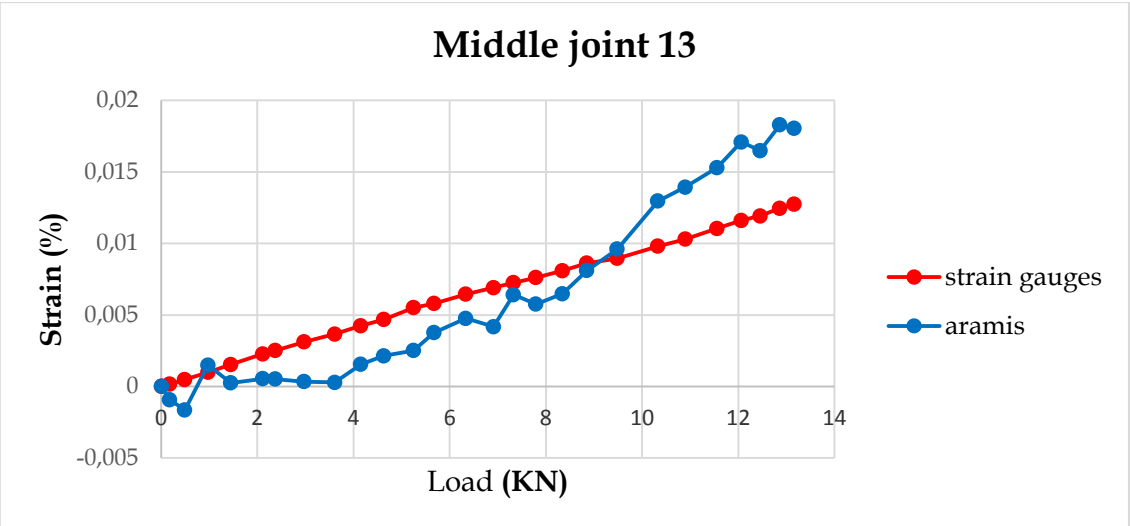

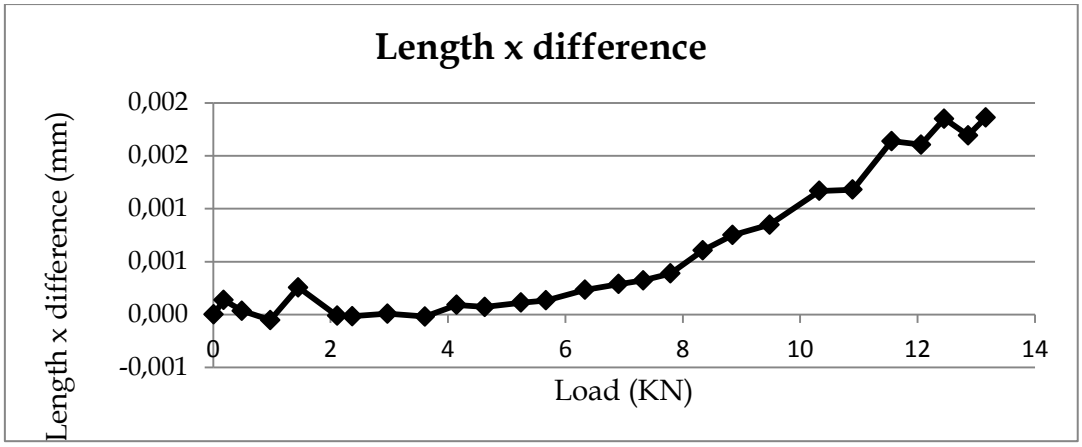
Length x difference
Length x difference (mm)
0,002
0,002
0,001
0,001
0,000
-0,001
0
2
4
6
8
10
12
14
Load (KN)

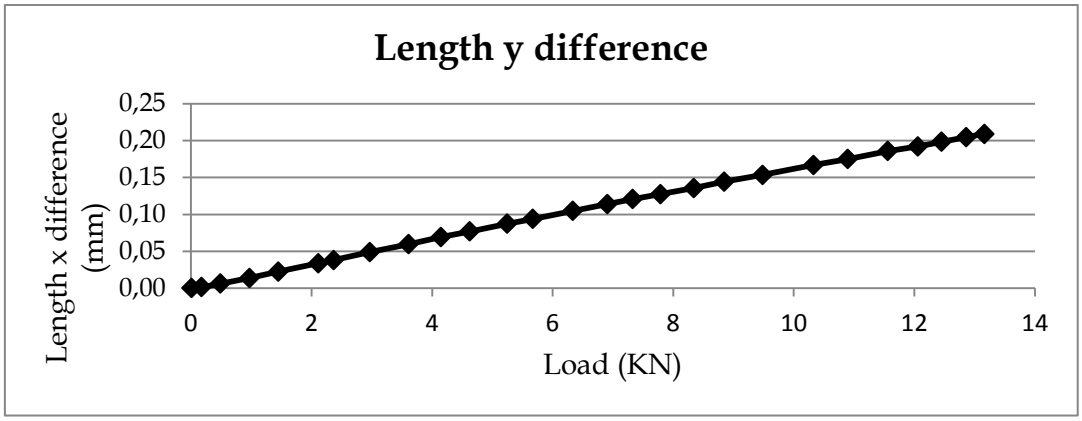
Length y difference
Length x difference (mm)
0,25
0,20
0,15
0,10
0,05
0,00
0
2
4
6
8
10
12
14
Load (KN)

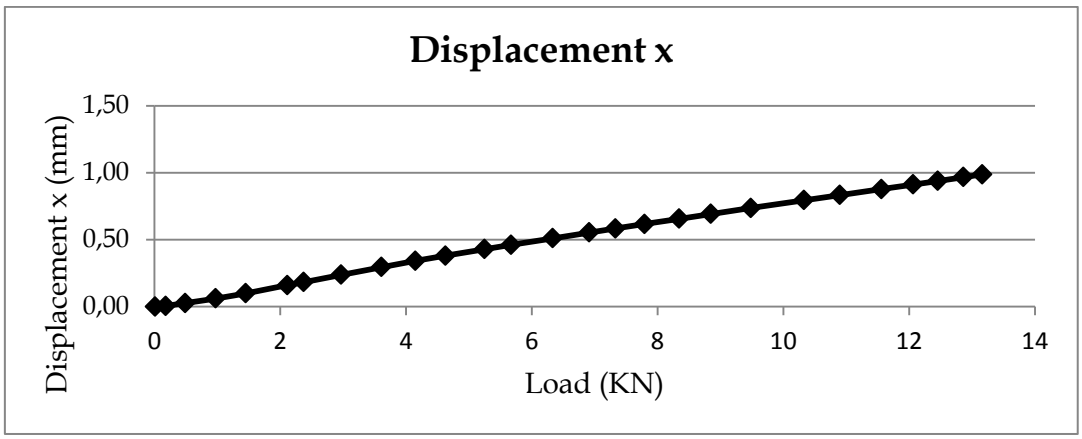
Displacement x
Displacement x (mm)
1,50
1,00
0,50
0,00
0
2
4
6
8
10
12
14
Load (KN)

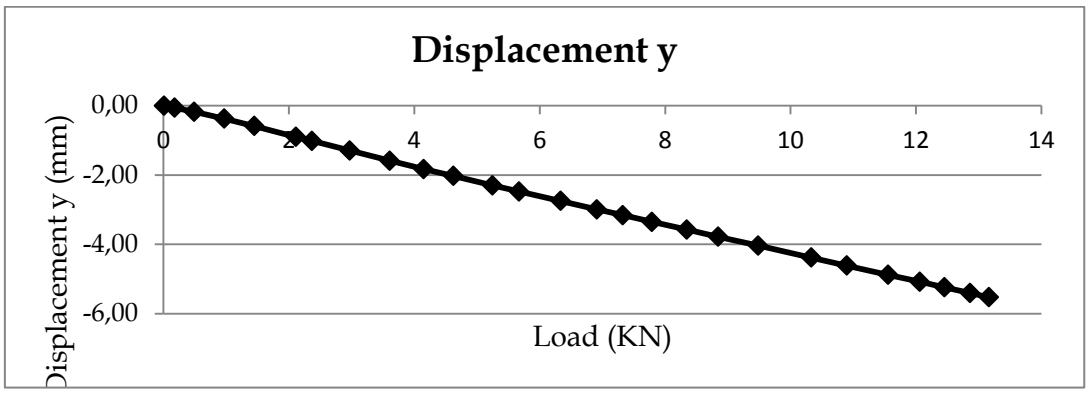
Displacement y
Displacement y (mm)
0,00
-2,00
-4,00
-6,00
0
4
6
8
10
12
14
Load (KN)

Test 40

	Strain gauges	Aramis				
Load (KN)	Strain (%)	Strain (%)	Δ Lenght x (mm)	Δ Lenght y (mm)	Displ x (mm)	Displ y (mm)
0,12	0,0000	0,000	0,0000	0,000	0,00	0,00
0,46	0,0003	-0,019	-0,0018	0,006	0,01	-0,12
1,17	0,0012	-0,038	-0,0037	0,018	0,05	-0,42
2,27	0,0023	-0,065	-0,0064	0,038	0,12	-0,93
3,26	0,0033	-0,093	-0,0091	0,056	0,19	-1,38
4,17	0,0042	-0,101	-0,0101	0,074	0,25	-1,79
4,99	0,0051	-0,111	-0,0112	0,088	0,30	-2,14
5,87	0,0060	-0,117	-0,0119	0,102	0,34	-2,50
6,41	0,0065	-0,121	-0,0124	0,112	0,37	-2,72
7,06	0,0069	-0,134	-0,0138	0,123	0,41	-2,98
7,57	0,0073	-0,130	-0,0135	0,131	0,44	-3,19
8,02	0,0076	-0,136	-0,0141	0,138	0,46	-3,37
8,62	0,0080	-0,145	-0,0152	0,148	0,49	-3,61
9,15	0,0086	-0,146	-0,0155	0,157	0,52	-3,82
9,67	0,0089	-0,147	-0,0157	0,166	0,54	-4,03
10,15	0,0094	-0,145	-0,0155	0,172	0,57	-4,22
10,79	0,0100	-0,151	-0,0163	0,183	0,60	-4,47
11,47	0,0107	-0,148	-0,0163	0,194	0,63	-4,73
11,98	0,0112	-0,145	-0,0161	0,201	0,66	-4,93
12,55	0,0118	-0,157	-0,0175	0,212	0,68	-5,15
13,12	0,0121	-0,153	-0,0173	0,220	0,71	-5,36

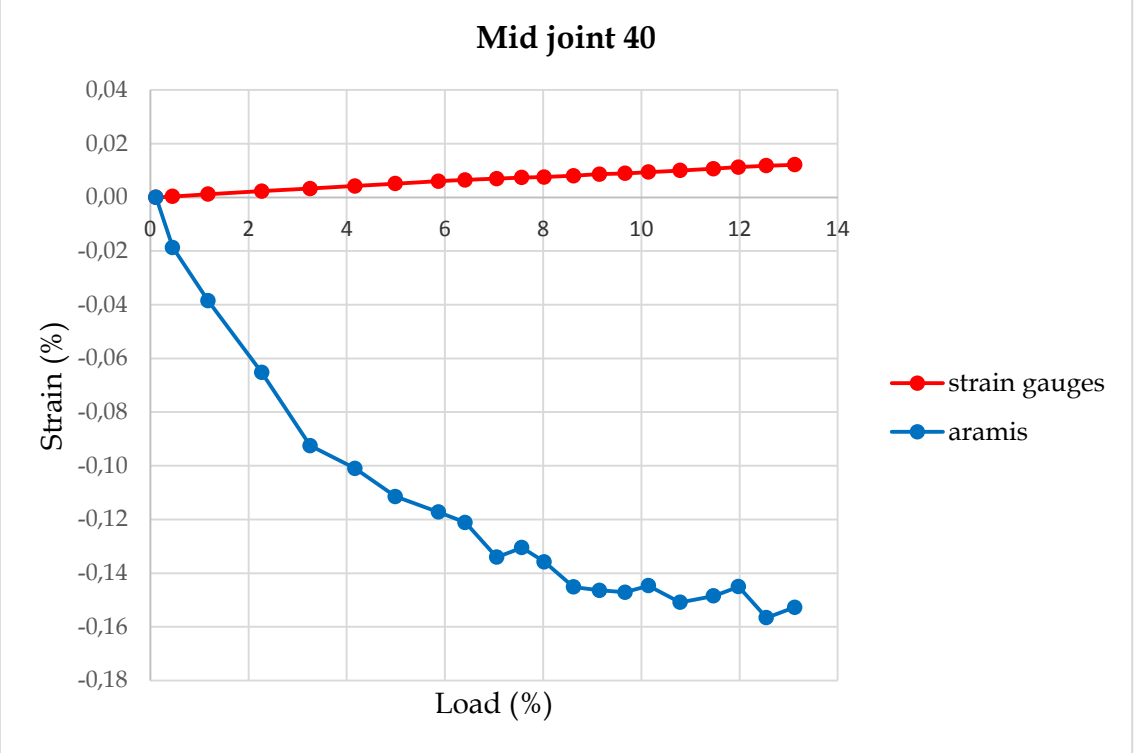

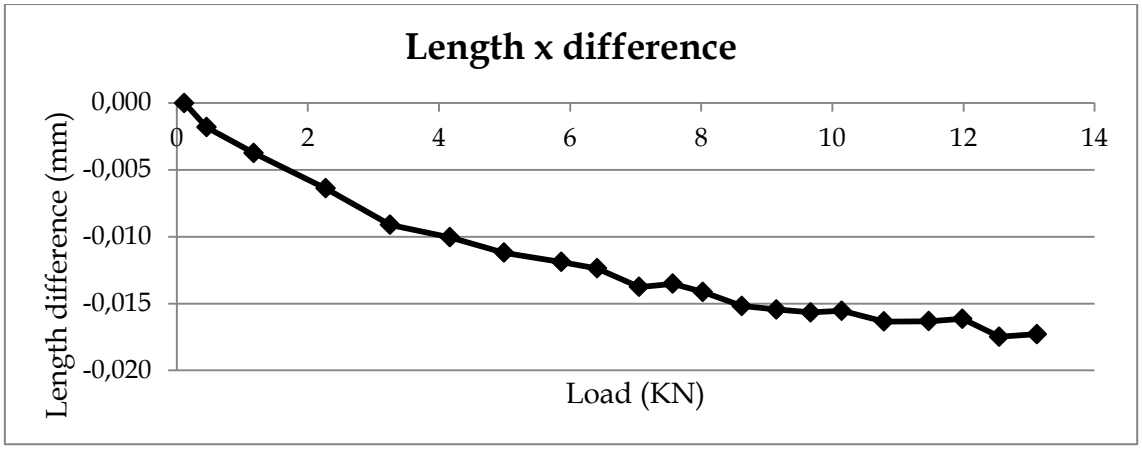
Length x difference
Length difference (mm)
0,000
-0,005
-0,010
-0,015
-0,020
0
2
4
6
8
10
12
14
Load (KN)

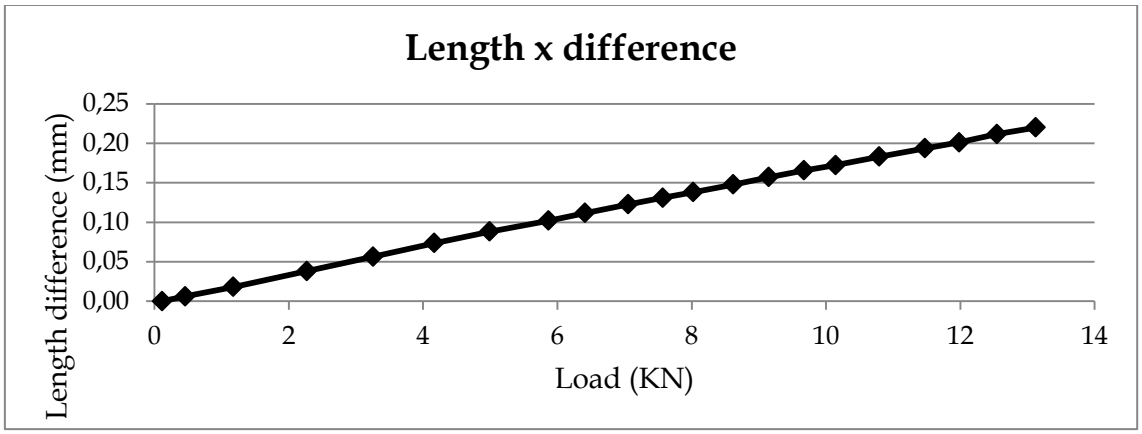
Length x difference
Length difference (mm)
0,25
0,20
0,15
0,10
0,05
0,00
0
2
4
6
8
10
12
14
Load (KN)

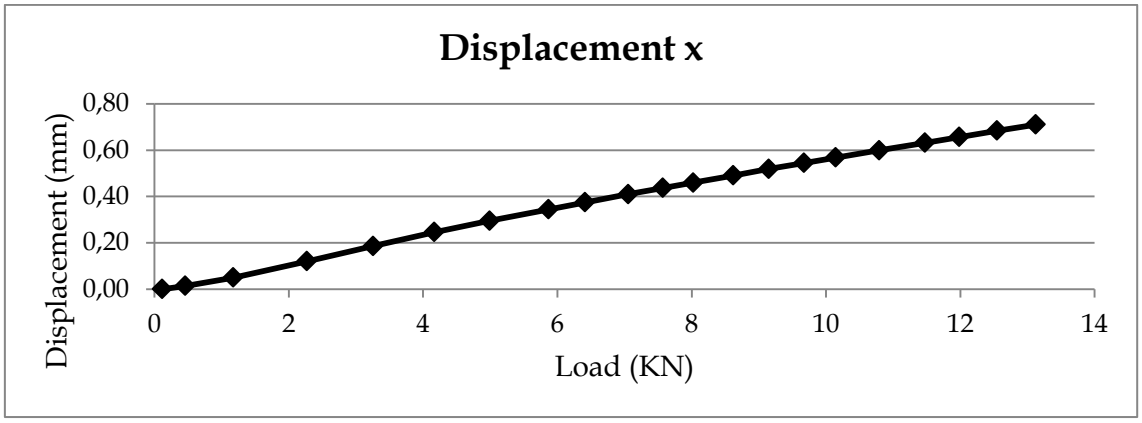
Displacement x
Displacement (mm)
0,80
0,60
0,40
0,20
0,00
0
2
4
6
8
10
12
14
Load (KN)

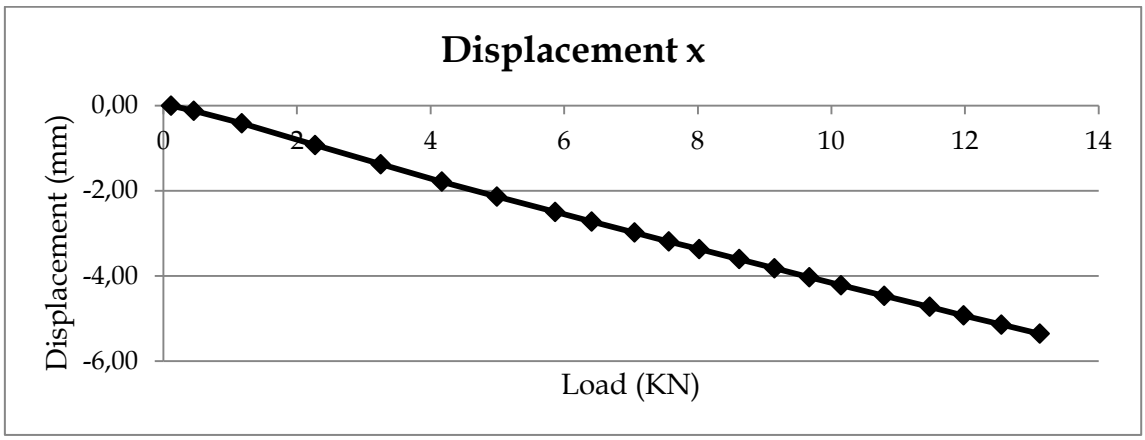
Displacement x
Displacement (mm)
0,00
-2,00
-4,00
-6,00
0
2
4
6
8
10
12
14
Load (KN)

3.2.6 Bottom joint

Test 16	Strain gauges	Aramis				
Load (KN)	Strain (%)	Strain (%)	Δ Lenght x (mm)	Δ Lenght y (mm)	Displ x (mm)	Displ y (mm)
0,00	0,0000	0,0000	0,00000	0,000	0,00	0,00
0,27	-0,0006	-0,0022	-0,00004	0,006	-0,02	-0,08
0,62	-0,0015	0,0042	0,00009	0,014	-0,04	-0,19
1,30	-0,0031	0,0011	-0,00003	0,030	-0,09	-0,43
2,14	-0,0051	-0,0065	-0,00031	0,053	-0,16	-0,74
2,70	-0,0065	-0,0017	-0,00042	0,068	-0,20	-0,95
3,25	-0,0079	-0,0047	-0,00049	0,083	-0,24	-1,15
3,86	-0,0095	-0,0061	-0,00055	0,098	-0,28	-1,37
4,51	-0,0111	-0,0084	-0,00061	0,115	-0,33	-1,60
5,00	-0,0123	-0,0125	-0,00070	0,127	-0,36	-1,77
5,63	-0,0138	-0,0144	-0,00076	0,142	-0,41	-1,98
6,29	-0,0153	-0,0150	-0,00081	0,158	-0,45	-2,20
6,80	-0,0167	-0,0157	-0,00085	0,169	-0,49	-2,37
6,79	-0,0167	-0,0152	-0,00084	0,170	-0,49	-2,37
7,31	-0,0179	-0,0188	-0,00093	0,182	-0,53	-2,54
7,94	-0,0194	-0,0190	-0,00097	0,196	-0,57	-2,74
8,45	-0,0203	-0,0225	-0,00105	0,208	-0,61	-2,90
8,90	-0,0213	-0,0221	-0,00108	0,218	-0,64	-3,04
9,46	-0,0226	-0,0256	-0,00116	0,231	-0,68	-3,22
9,93	-0,0236	-0,0262	-0,00121	0,242	-0,71	-3,37
10,55	-0,0251	-0,0253	-0,00124	0,256	-0,75	-3,57
11,12	-0,0262	-0,0301	-0,00135	0,268	-0,79	-3,75
11,63	-0,0274	-0,0323	-0,00142	0,280	-0,83	-3,91
12,12	-0,0286	-0,0338	-0,00148	0,291	-0,86	-4,06
12,66	-0,0300	-0,0360	-0,00155	0,303	-0,90	-4,23
13,17	-0,0311	-0,0405	-0,00166	0,315	-0,93	-4,39

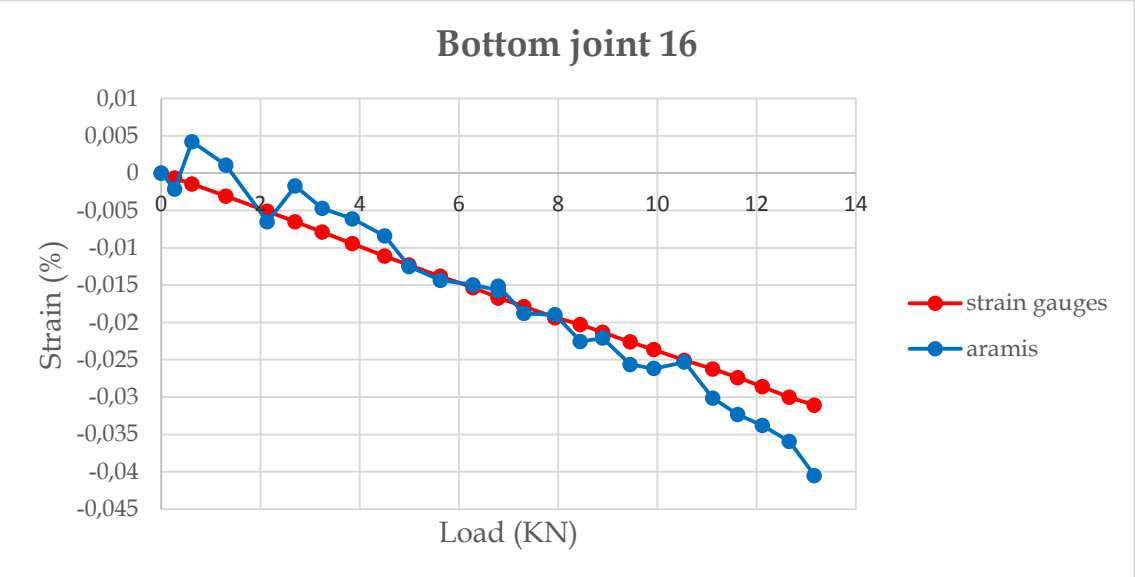

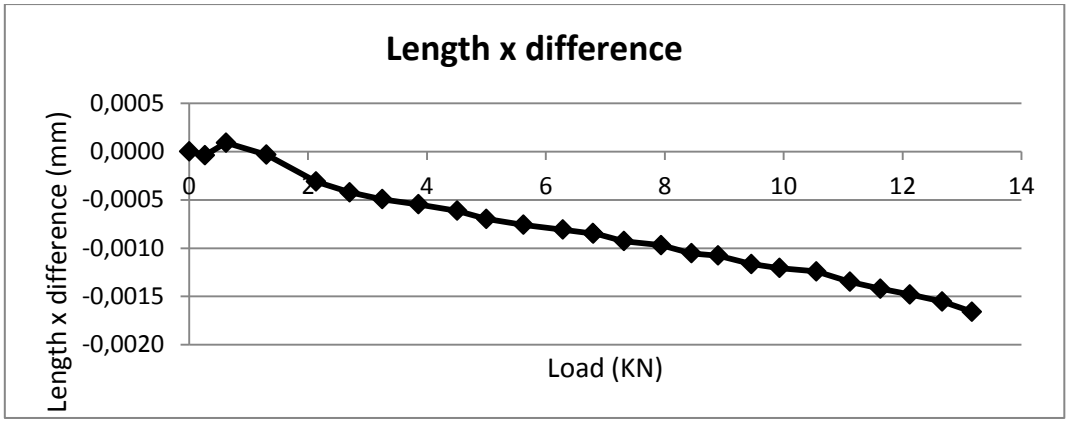
Length x difference
Length x difference (mm)
0,0005
0,0000
-0,0005
-0,0010
-0,0015
-0,0020
0
2
4
6
8
10
12
14
Load (KN)

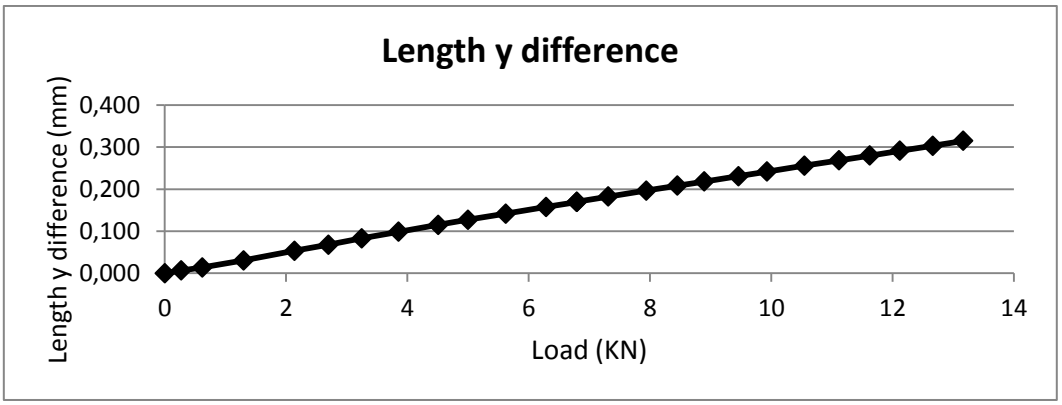
Length y difference
Length y difference (mm)
0,400
0,300
0,200
0,100
0,000
0
2
4
6
8
10
12
14
Load (KN)

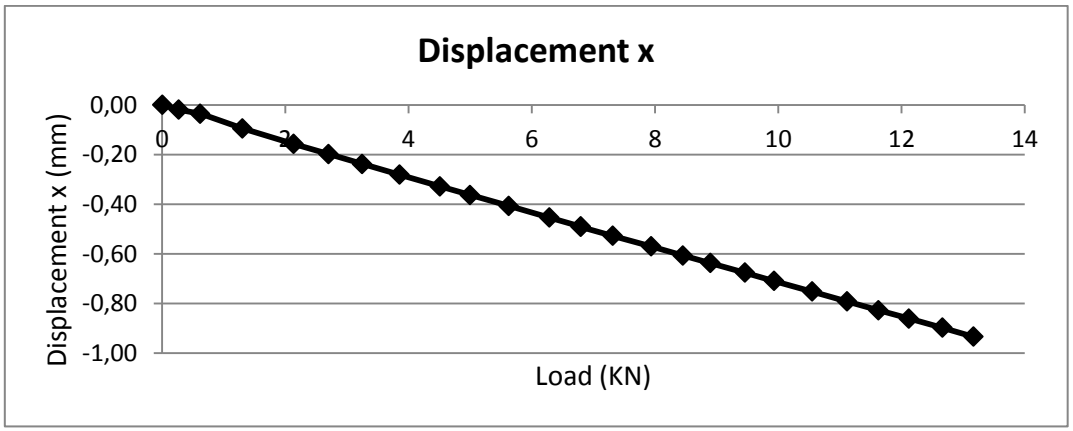
Displacement x
Displacement x (mm)
0,00
-0,20
-0,40
-0,60
-0,80
-1,00
0
2
4
6
8
10
12
14
Load (KN)

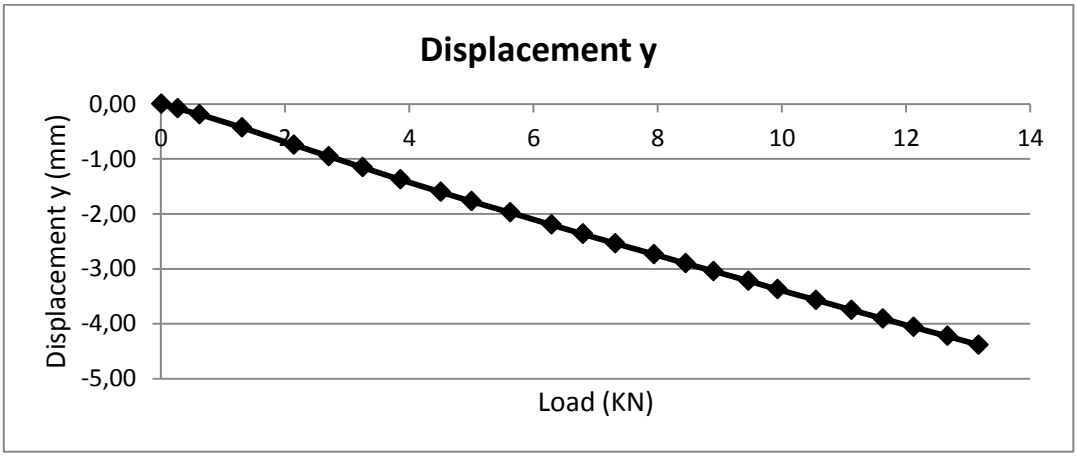
Displacement y
Displacement y (mm)
0,00
-1,00
-2,00
-3,00
-4,00
-5,00
0
2
4
6
8
10
12
14
Load (KN)

Test 44

	Strain gauges	Aramis				
Load (KN)	Strain (%)	Strain (%)	Δ Lenght x (mm)	Δ Lenght y (mm)	Displ x (mm)	Displ y (mm)
0,08	0,0000	0,0000	0,0000	0,000	0,00	0,00
0,46	-0,0008	0,0010	0,0001	0,005	-0,03	-0,11
0,89	-0,0018	-0,0014	-0,0001	0,009	-0,06	-0,25
1,43	-0,0031	-0,0030	-0,0003	0,019	-0,10	-0,44
1,91	-0,0042	-0,0026	-0,0003	0,031	-0,14	-0,62
2,59	-0,0059	-0,0066	-0,0006	0,042	-0,19	-0,88
3,14	-0,0073	-0,0102	-0,0009	0,053	-0,23	-1,08
3,80	-0,0090	-0,0121	-0,0010	0,064	-0,28	-1,32
4,35	-0,0103	-0,0111	-0,0010	0,075	-0,32	-1,51
5,06	-0,0121	-0,0120	-0,0011	0,086	-0,38	-1,75
5,59	-0,0134	-0,0148	-0,0013	0,094	-0,42	-1,92
6,25	-0,0151	-0,0177	-0,0016	0,108	-0,46	-2,14
6,82	-0,0166	-0,0154	-0,0015	0,116	-0,51	-2,33
7,20	-0,0175	-0,0181	-0,0017	0,124	-0,53	-2,45
7,74	-0,0188	-0,0205	-0,0019	0,130	-0,57	-2,62
8,19	-0,0198	-0,0175	-0,0017	0,134	-0,61	-2,77
8,77	-0,0210	-0,0183	-0,0018	0,142	-0,65	-2,95
9,21	-0,0220	-0,0220	-0,0021	0,154	-0,68	-3,09
9,65	-0,0229	-0,0244	-0,0023	0,159	-0,72	-3,23
10,13	-0,0240	-0,0224	-0,0022	0,167	-0,75	-3,38
10,68	-0,0252	-0,0242	-0,0024	0,174	-0,79	-3,55
11,26	-0,0264	-0,0223	-0,0023	0,183	-0,83	-3,73
11,85	-0,0279	-0,0253	-0,0025	0,191	-0,87	-3,91
12,21	-0,0288	-0,0274	-0,0027	0,197	-0,90	-4,02
12,79	-0,0301	-0,0272	-0,0028	0,208	-0,94	-4,19
13,11	-0,0310	-0,0268	-0,0028	0,215	-0,96	-4,29

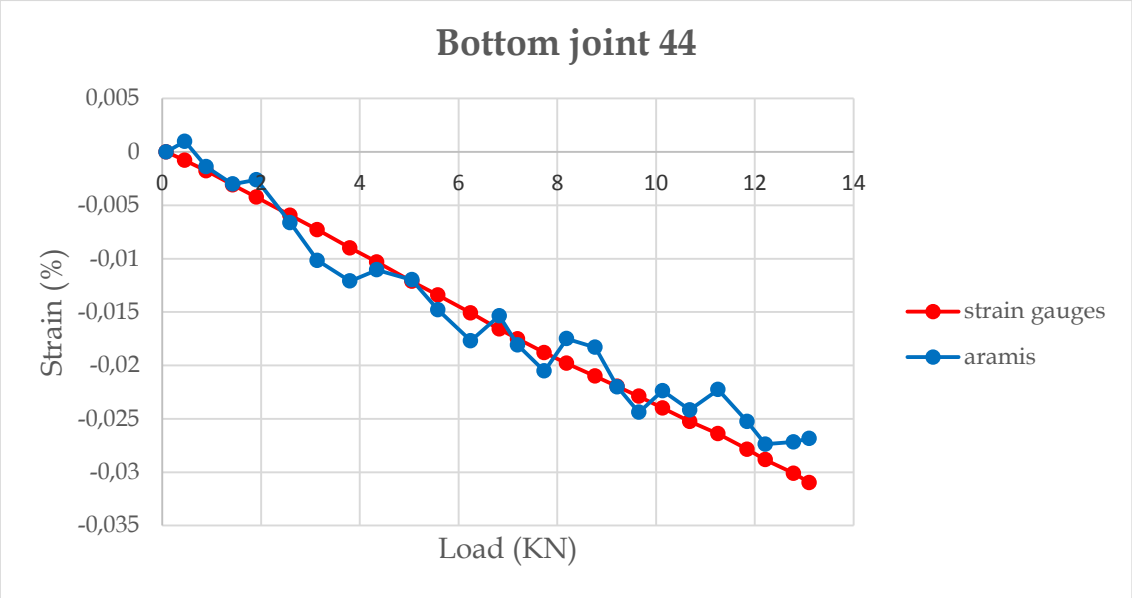

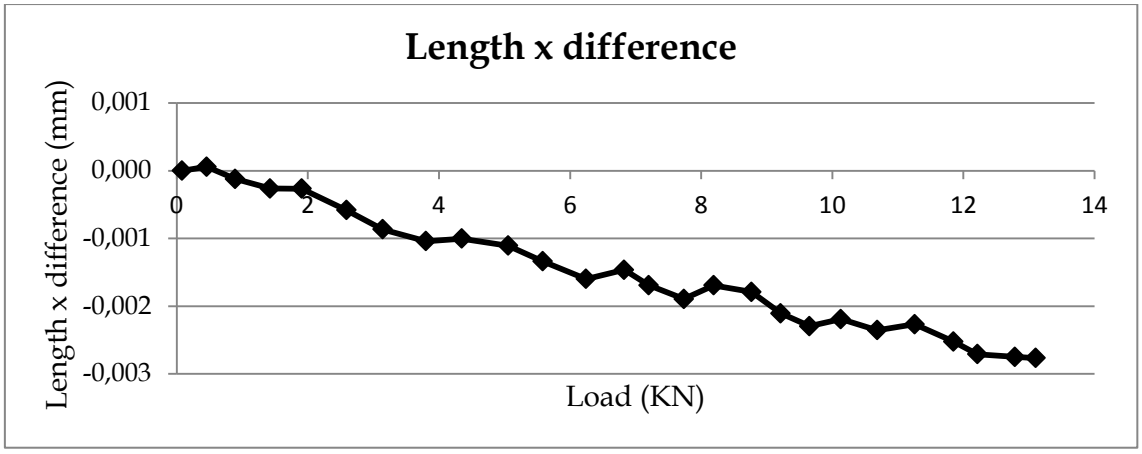
Length x difference
Length x difference (mm)
0,001
0,000
-0,001
-0,002
-0,003
0
2
4
6
8
10
12
14
Load (KN)

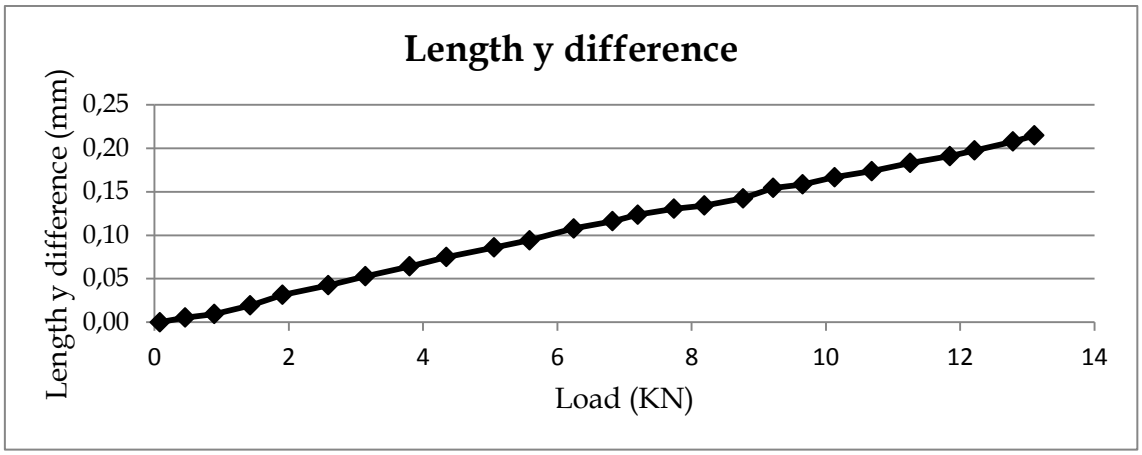
Length y difference
Length y difference (mm)
0,25
0,20
0,15
0,10
0,05
0,00
0
2
4
6
8
10
12
14
Load (KN)

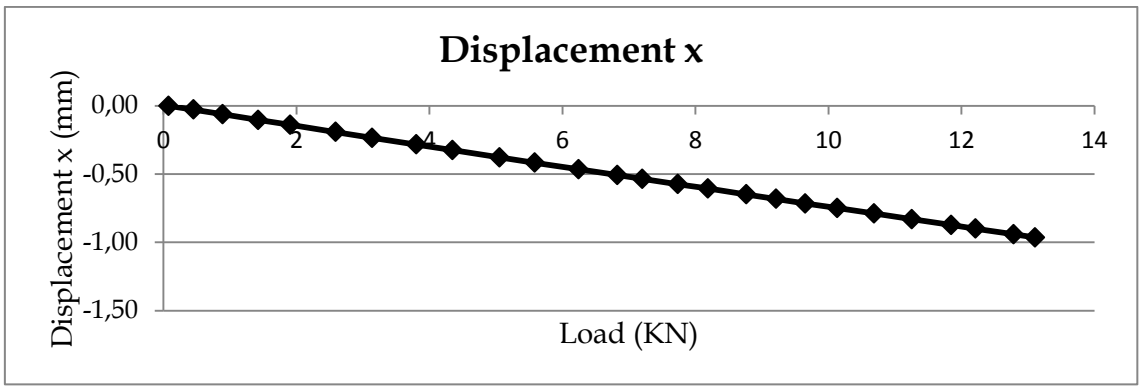
Displacement x
Displacement x (mm)
0,00
-0,50
-1,00
-1,50
0
2
4
6
8
10
12
14
Load (KN)

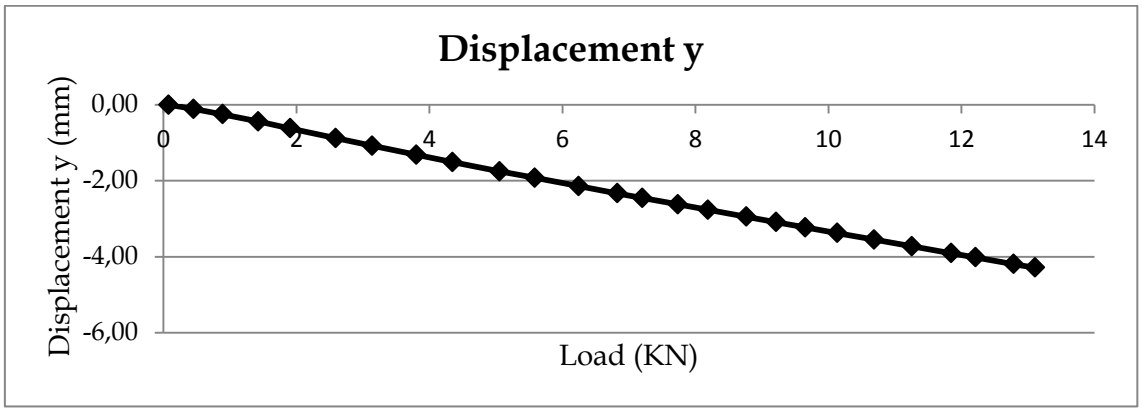
Displacement y
Displacement y (mm)
0,00
-2,00
-4,00
-6,00
0
2
4
6
8
10
12
14
Load (KN)

3.3 Considerations

Graphs presented in the previous paragraph show a general good comparison between strain data obtained from strain gauges and whom obtained from digital image correlation.

All the test in the undamaged condition were carried out loading the beam up to 13,10KN which coincides with the 70% of the yield strength.

Some considerations relatively to strain comparison in different parts of the structure: good results were given in all the beam parts of the structure, as taking photos really close to the beam as taking farther in order to take data of top and mid beam with the same photos. Relatively to the joint part, a good comparison of values was obtained, but have to be considered that some of the test gave a not good result. This problem was present in some tests of the tense part, but especially into the middle area of the joint, the one subjected to lower strain (up to 0,015%). The compressed part gave better result if compared to the same range of strain. In general, good comparison was found until 0.035% strain values, while with lower values the reliability was not guaranteed.

Chapter 4

Damaged condition

4.1 Conduct of the test

This chapter present all the final tests have been done on the structure in damaged condition, that means with the crack in the beam at the joint. Measured loads were plotted in graphs with load as a function of strains obtained from digital image correlation method and also with those obtained from strain gauges. As explained in the previous chapter, just two restricted areas were analyzed in the same time, due to the close proximity required from camera and structure to obtain good results: one in the main beam, the other in the joint part.

The six points of particular importance analyzed in this chapter are exactly the same of the previous one in order to compare the two condition: three of them are in the joint part of the structure and the other three in the beam, as with Aramis as with strain gauges. The name of these points is the same, due to the positioning respect to the height of the structure will be called as top beam, mid beam, bottom beam, top joint, mid joint and bottom joint. Two tests for each single relevant point are presented. Every test presents a comparison graph with both technologies used.

4.2 Experiment results

4.2.1 Top beam

Test 103	Strain gauges	Aramis				
Load (KN)	Strain (%)	Strain (%)	Δ Lenght x (mm)	Δ Lenght y (mm)	Displ x (mm)	Displ y (mm)
0,20	0,0000	0,0000	0,0000	0,000	0,000	0,000
0,30	0,0005	0,0021	0,0002	-0,002	0,007	-0,050
0,56	0,0020	0,0022	0,0006	-0,007	0,033	-0,190
0,76	0,0032	0,0051	0,0006	-0,011	0,053	-0,296
1,14	0,0053	0,0087	0,0013	-0,019	0,097	-0,517
1,57	0,0078	0,0102	0,0018	-0,029	0,149	-0,776
1,80	0,0095	0,0133	0,0020	-0,035	0,185	-0,932
2,03	0,0107	0,0151	0,0019	-0,040	0,213	-1,072
2,25	0,0121	0,0138	0,0023	-0,046	0,245	-1,214
2,41	0,0131	0,0173	0,0024	-0,050	0,268	-1,318
2,63	0,0148	0,0178	0,0025	-0,055	0,300	-1,463
2,91	0,0164	0,0186	0,0027	-0,063	0,340	-1,642
3,15	0,0180	0,0198	0,0027	-0,069	0,374	-1,797
3,39	0,0197	0,0196	0,0028	-0,074	0,406	-1,946
3,73	0,0217	0,0267	0,0024	-0,082	0,453	-2,159
3,96	0,0232	0,0288	0,0029	-0,088	0,483	-2,300
4,18	0,0246	0,0276	0,0030	-0,093	0,512	-2,432
4,40	0,0259	0,0279	0,0031	-0,098	0,539	-2,561
4,62	0,0276	0,0276	0,0029	-0,103	0,568	-2,694
4,87	0,0291	0,0272	0,0031	-0,109	0,599	-2,841
5,18	0,0314	0,0296	0,0030	-0,116	0,637	-3,023
5,37	0,0320	0,0300	0,0034	-0,120	0,660	-3,133

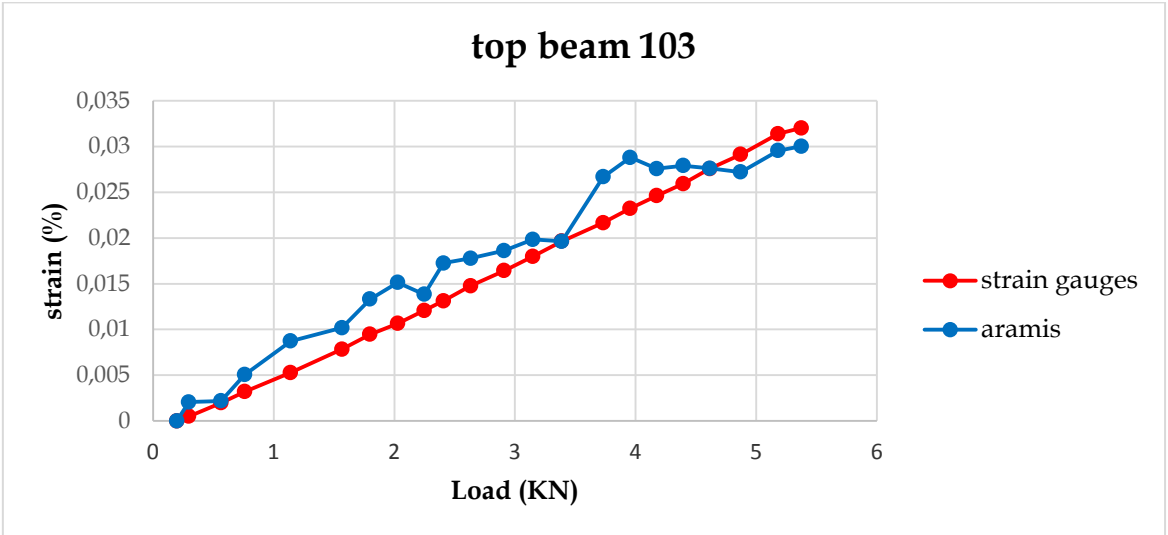

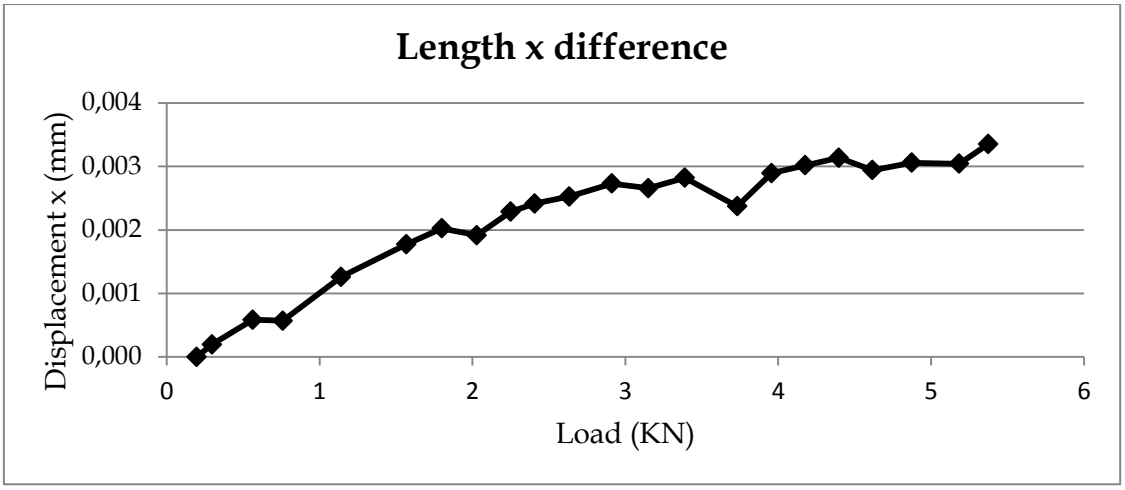
Length x difference
Displacement x (mm)
0,004
0,003
0,002
0,001
0,000
0
1
2
3
4
5
6
Load (KN)

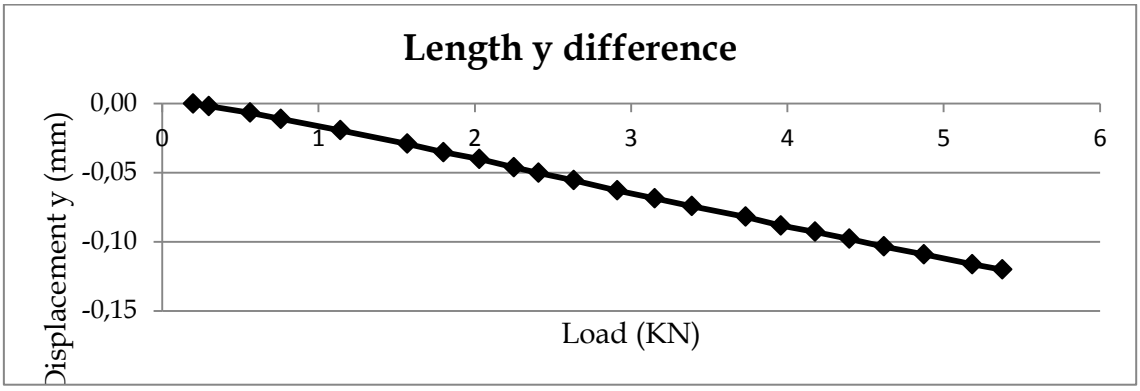
Length y difference
Displacement y (mm)
0,00
-0,05
-0,10
-0,15
0
1
2
3
4
5
6
Load (KN)

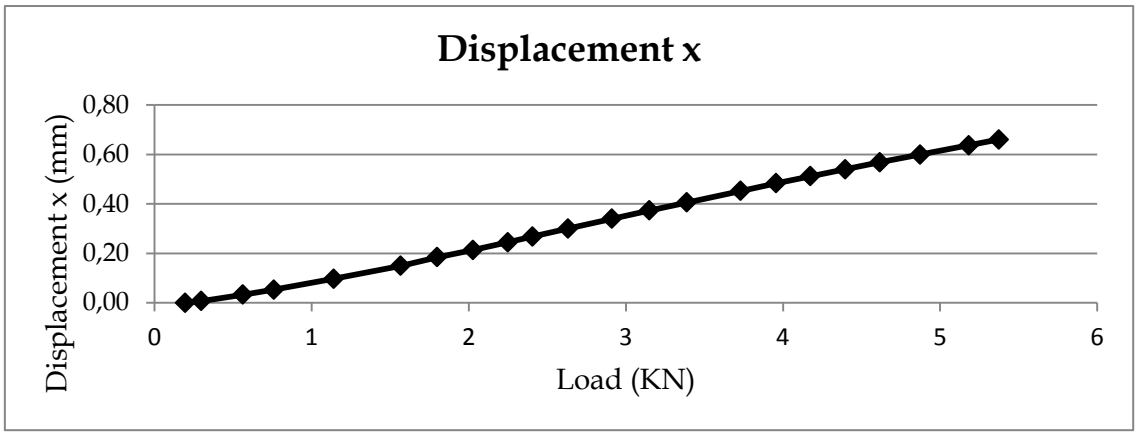
Displacement x
Displacement x (mm)
0,80
0,60
0,40
0,20
0,00
0
1
2
3
4
5
6
Load (KN)

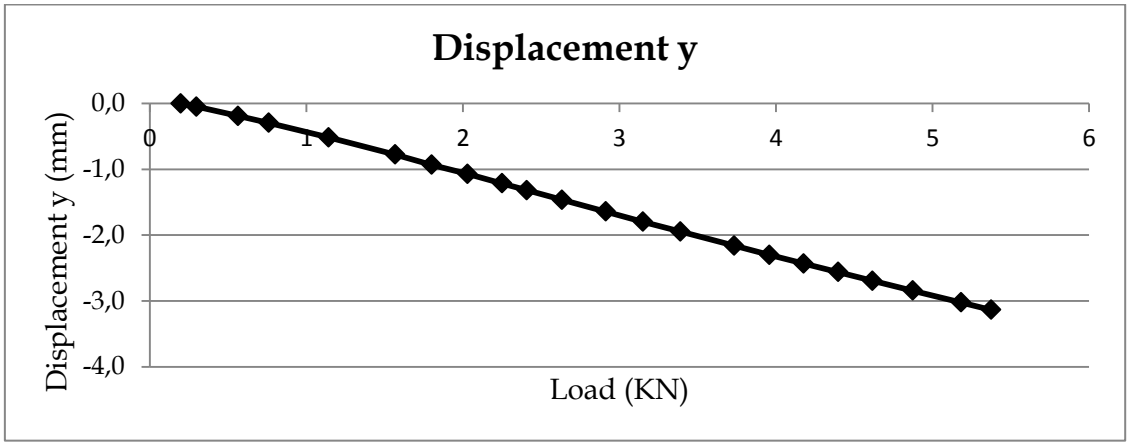
Displacement y
Displacement y (mm)
0,0
-1,0
-2,0
-3,0
-4,0
0
1
2
3
4
5
6
Load (KN)

Test 113

	Strain gauges	Aramis				
Load (KN)	Strain (%)	Strain (%)	Δ Lenght x (mm)	Δ Lenght y (mm)	Displ x (mm)	Displ y (mm)
0,15	0,0000	0,000	0,0000	0,000	0,000	0,000
0,32	0,0012	-0,017	-0,0021	0,004	0,011	-0,089
0,53	0,0027	-0,024	-0,0030	0,009	0,032	-0,201
0,77	0,0043	-0,034	-0,0042	0,014	0,063	-0,340
1,08	0,0060	-0,043	-0,0052	0,021	0,104	-0,524
1,70	0,0093	-0,045	-0,0056	0,038	0,193	-0,916
2,23	0,0121	-0,071	-0,0087	0,050	0,279	-1,277
2,75	0,0147	-0,065	-0,0082	0,065	0,361	-1,625
3,19	0,0172	-0,073	-0,0092	0,076	0,430	-1,920
3,56	0,0188	-0,079	-0,0100	0,085	0,488	-2,163
3,93	0,0206	-0,075	-0,0096	0,095	0,542	-2,396
4,32	0,0225	-0,083	-0,0106	0,106	0,599	-2,640
4,60	0,0240	-0,086	-0,0111	0,112	0,638	-2,814
4,90	0,0255	-0,084	-0,0109	0,120	0,679	-2,991
5,13	0,0266	-0,080	-0,0104	0,126	0,711	-3,136
5,33	0,0279	-0,093	-0,0121	0,130	0,738	-3,254
5,58	0,0288	-0,073	-0,0097	0,136	0,781	-3,401

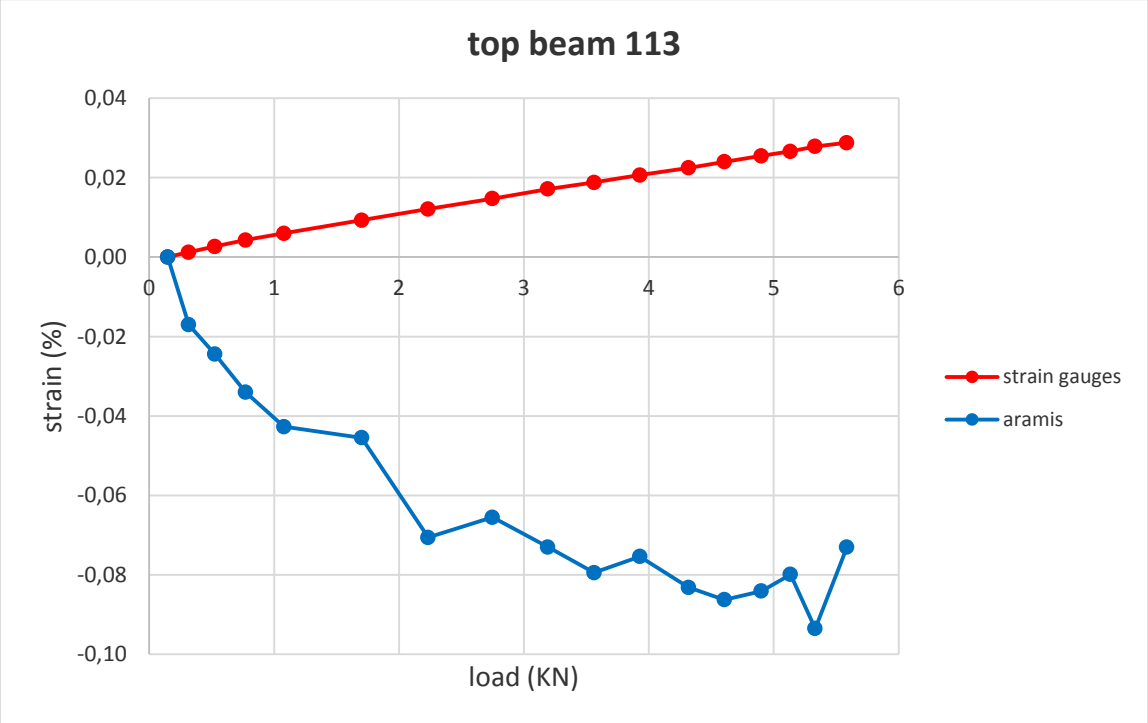

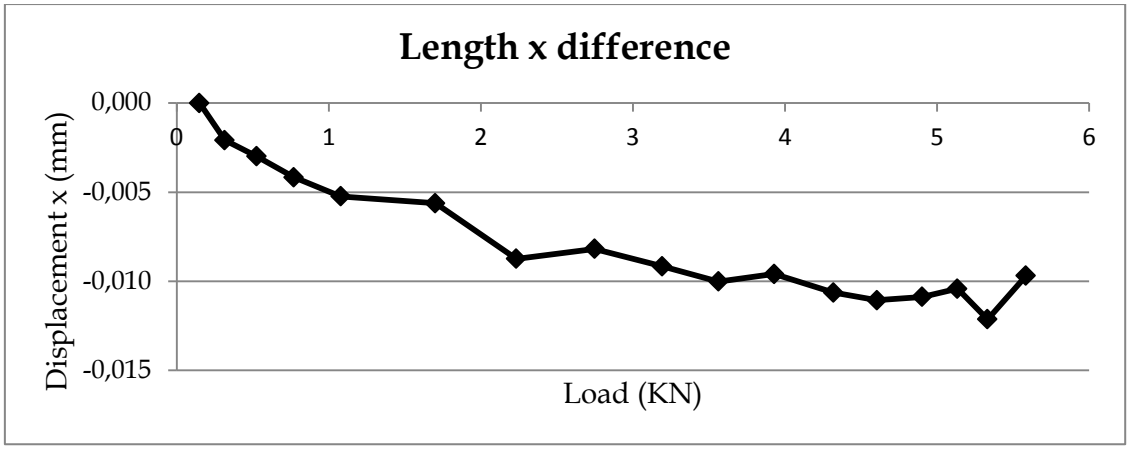
Length x difference
Displacement x (mm)
0,000
-0,005
-0,010
-0,015
0
1
2
3
4
5
6
Load (KN)

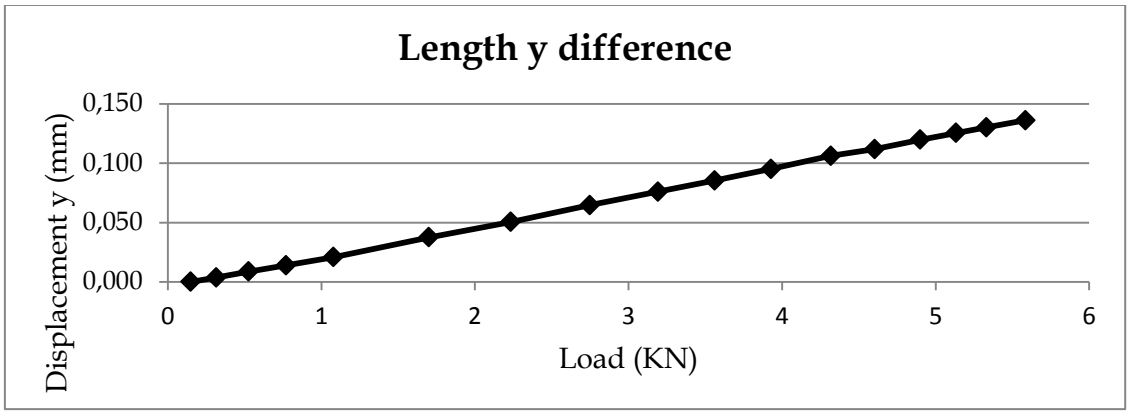
Length y difference
Displacement y (mm)
0,150
0,100
0,050
0,000
0
1
2
3
4
5
6
Load (KN)

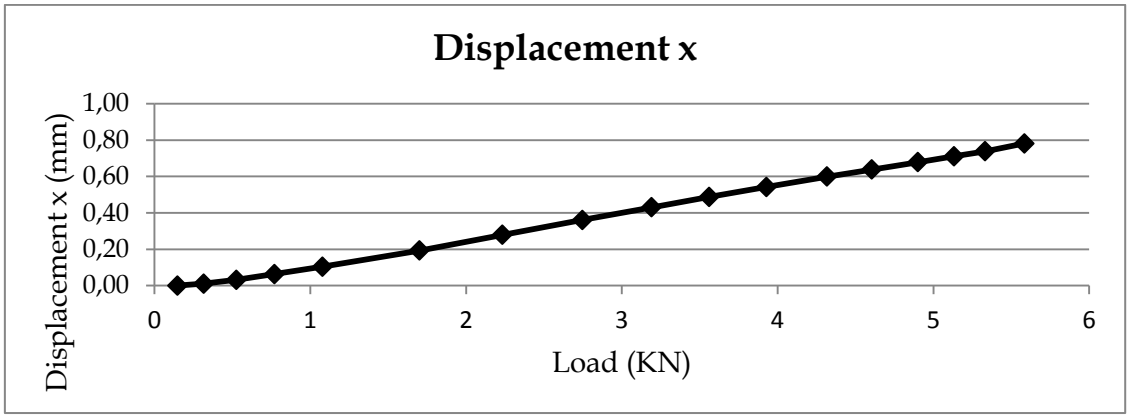
Displacement x
Displacement x (mm)
1,00
0,80
0,60
0,40
0,20
0,00
0
1
2
3
4
5
6
Load (KN)

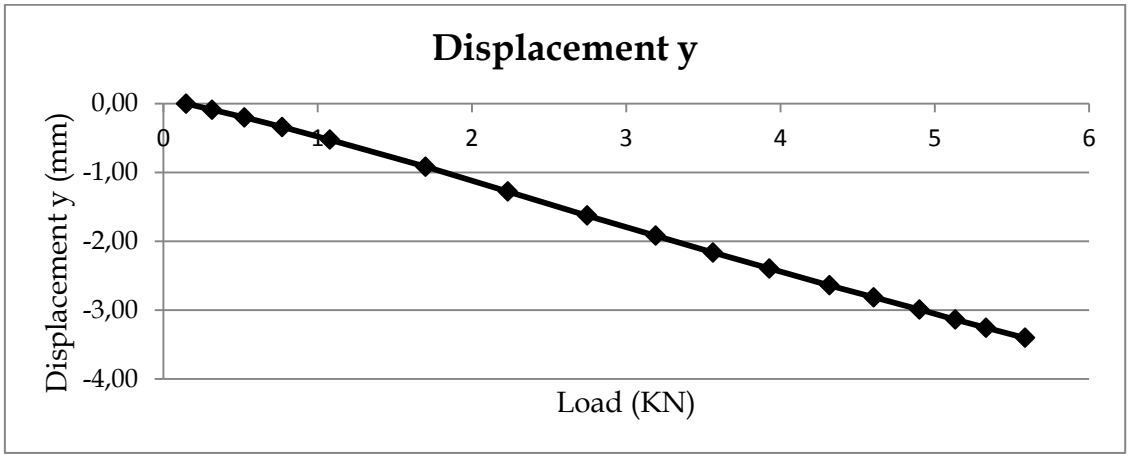
Displacement y
Displacement y (mm)
0,00
-1,00
-2,00
-3,00
-4,00
0
1
2
3
4
5
6
Load (KN)

4.2.2 Mid beam

Test 122

	Strain gauges	Aramis				
Load (KN)	Strain (%)	Strain (%)	Δ Lenght x (mm)	Δ Lenght y (mm)	Displ x (mm)	Displ y (mm)
0,13	0,0000	0,0000	0,00000	0,000	0,000	0,000
0,34	0,0011	0,0052	0,00068	0,002	0,011	-0,103
0,50	0,0021	0,0046	0,00049	0,006	0,023	-0,191
0,71	0,0034	0,0055	0,00074	0,010	0,036	-0,298
1,01	0,0051	-0,0038	-0,00025	0,016	0,061	-0,471
1,26	0,0066	0,0098	0,00070	0,021	0,083	-0,620
1,61	0,0087	0,0048	0,00045	0,029	0,116	-0,833
1,91	0,0105	0,0086	0,00039	0,035	0,148	-1,031
2,23	0,0126	0,0096	0,00048	0,043	0,181	-1,238
2,55	0,0148	0,0069	-0,00005	0,050	0,216	-1,451
2,85	0,0166	0,0171	0,00149	0,057	0,247	-1,641
3,10	0,0184	0,0085	0,00001	0,063	0,272	-1,798
3,35	0,0201	0,0222	0,00209	0,069	0,298	-1,960
3,59	0,0216	0,0218	0,00192	0,074	0,322	-2,108
3,90	0,0237	0,0173	0,00105	0,081	0,354	-2,299
4,13	0,0251	0,0217	0,00165	0,086	0,377	-2,439
4,40	0,0269	0,0290	0,00267	0,092	0,402	-2,597
4,74	0,0290	0,0262	0,00204	0,099	0,433	-2,793
4,93	0,0303	0,0335	0,00309	0,103	0,450	-2,906
5,32	0,0324	0,0349	0,00307	0,111	0,487	-3,132
5,48	0,0340	0,0368	0,00327	0,115	0,500	-3,222

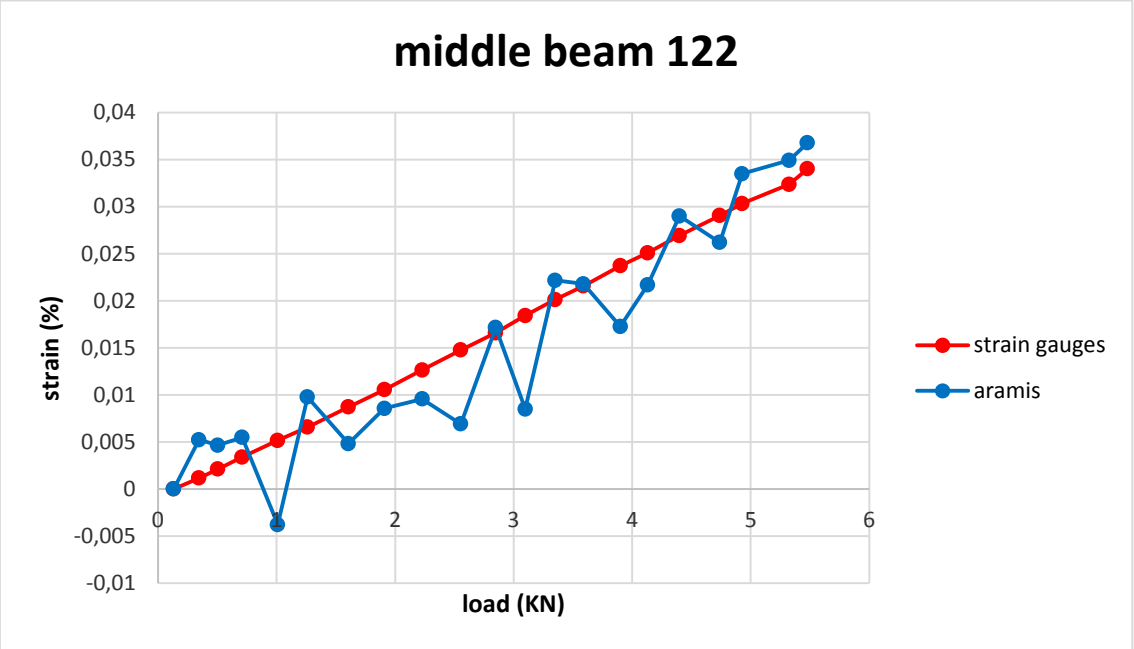

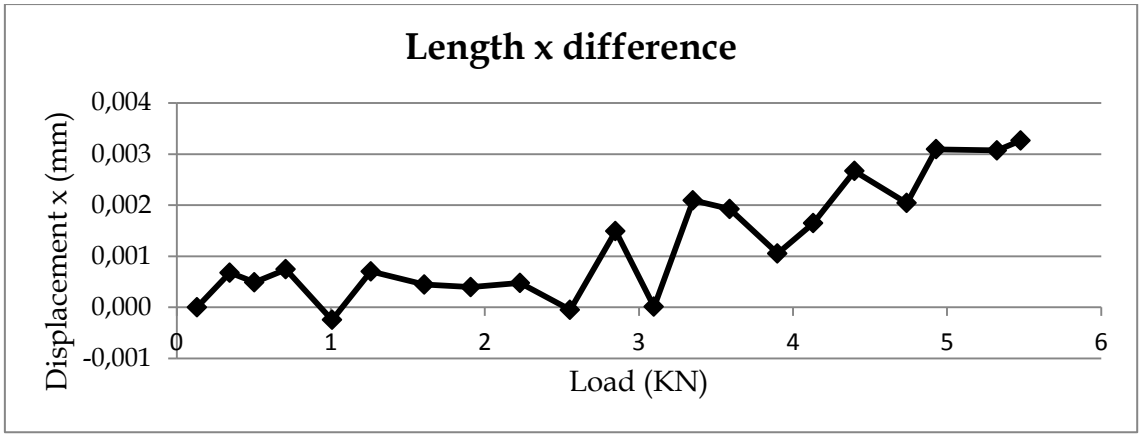
Length x difference
Displacement x (mm)
0,004
0,003
0,002
0,001
0,000
-0,001
0
1
2
3
4
5
6
Load (KN)

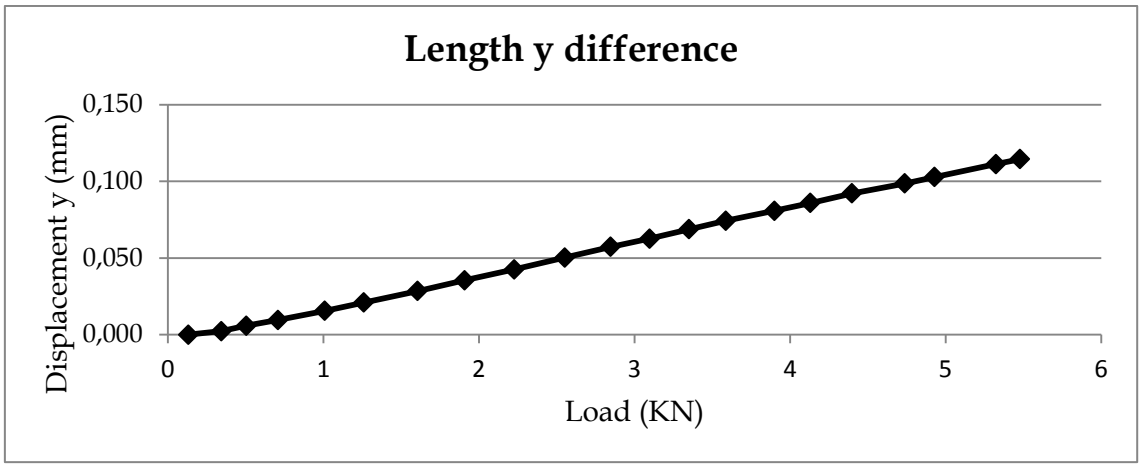
Length y difference
Displacement y (mm)
0,150
0,100
0,050
0,000
0
1
2
3
4
5
6
Load (KN)

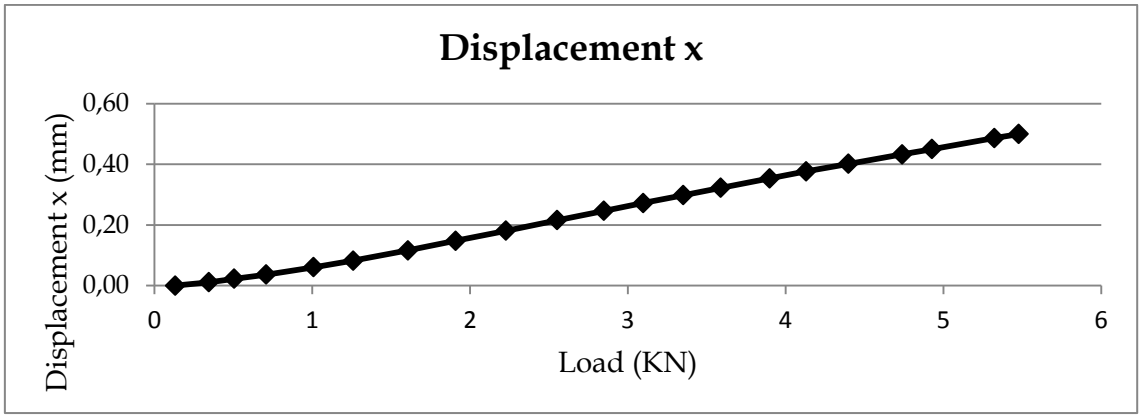
Displacement x
Displacement x (mm)
0,60
0,40
0,20
0,00
0
1
2
3
4
5
6
Load (KN)

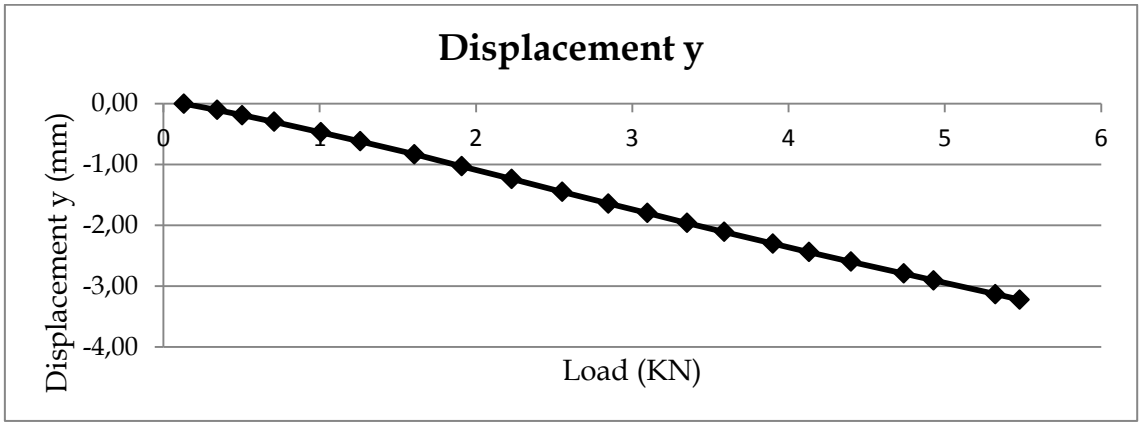
Displacement y
Displacement y (mm)
0,00
-1,00
-2,00
-3,00
-4,00
0
1
2
3
4
5
6
Load (KN)

Test 124

	Strain gauges	Aramis				
Load (KN)	Strain (%)	Strain (%)	Δ Lenght x (mm)	Δ Lenght y (mm)	Displ x (mm)	Displ y (mm)
0,14	0,0000	0,0000	0,0000	0,000	0,000	0,000
0,31	0,0009	0,0046	0,0015	0,002	0,006	-0,087
0,52	0,0022	0,0067	0,0028	0,002	0,016	-0,198
0,80	0,0038	0,0011	0,0012	0,010	0,036	-0,350
1,16	0,0059	-0,0020	0,0008	0,018	0,062	-0,563
1,49	0,0080	-0,0003	0,0010	0,023	0,089	-0,767
1,82	0,0101	0,0052	0,0015	0,031	0,117	-0,972
2,12	0,0121	0,0154	0,0026	0,038	0,145	-1,173
2,40	0,0136	0,0144	0,0025	0,044	0,172	-1,353
2,66	0,0155	0,0122	0,0007	0,048	0,197	-1,523
2,89	0,0170	0,0203	0,0030	0,056	0,216	-1,668
3,15	0,0187	0,0242	0,0034	0,059	0,240	-1,841
3,51	0,0210	0,0278	0,0037	0,068	0,272	-2,062
3,79	0,0229	0,0163	0,0025	0,075	0,297	-2,233
4,06	0,0247	0,0291	0,0038	0,081	0,320	-2,401
4,34	0,0266	0,0224	0,0027	0,087	0,344	-2,563
4,62	0,0285	0,0258	0,0027	0,091	0,367	-2,730
4,88	0,0300	0,0348	0,0042	0,099	0,386	-2,879
5,29	0,0322	0,0284	0,0027	0,106	0,420	-3,115
5,54	0,0338	0,0299	0,0036	0,110	0,439	-3,267

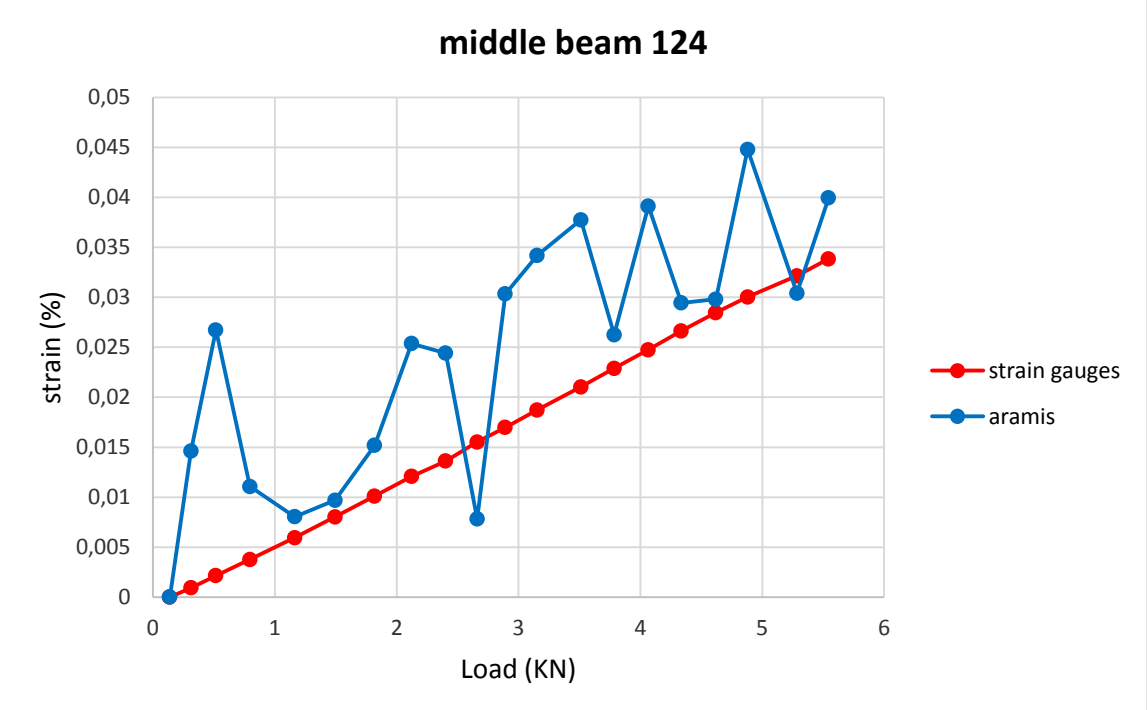

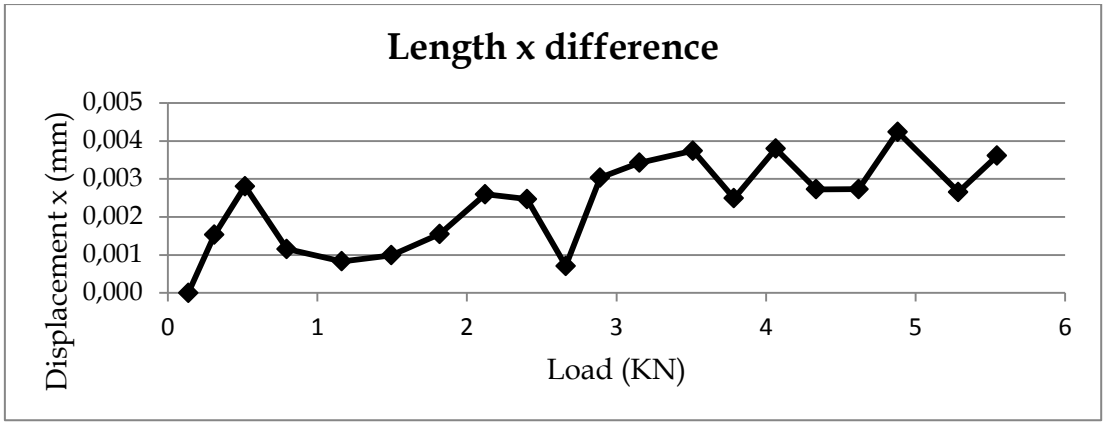
Length x difference
Displacement x (mm)
0,005
0,004
0,003
0,002
0,001
0,000
0
1
2
3
4
5
6
Load (KN)

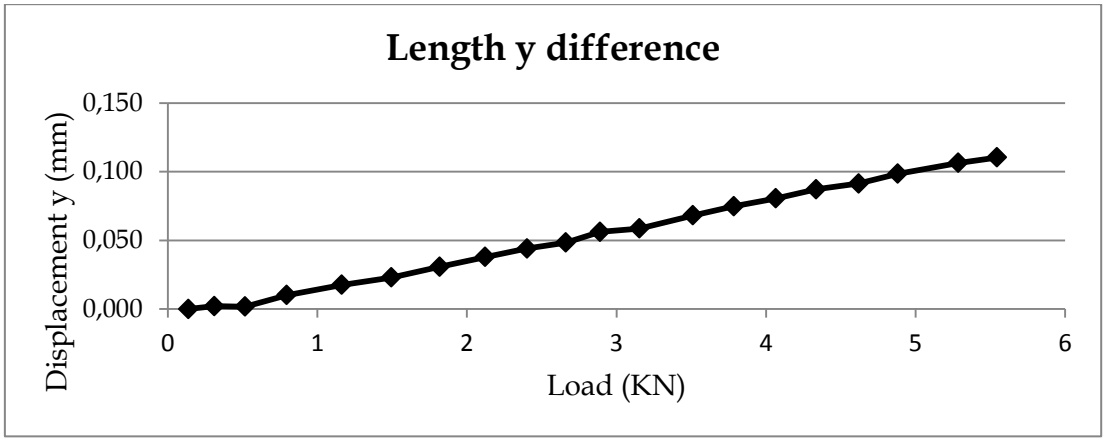
Length y difference
Displacement y (mm)
0,150
0,100
0,050
0,000
0
1
2
3
4
5
6
Load (KN)

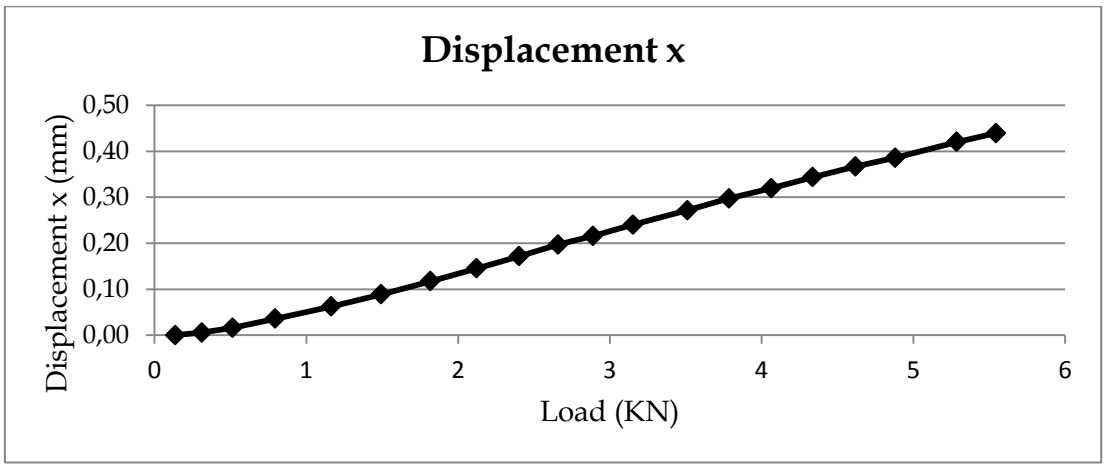
Displacement x
Displacement x (mm)
0,50
0,40
0,30
0,20
0,10
0,00
0
1
2
3
4
5
6
Load (KN)

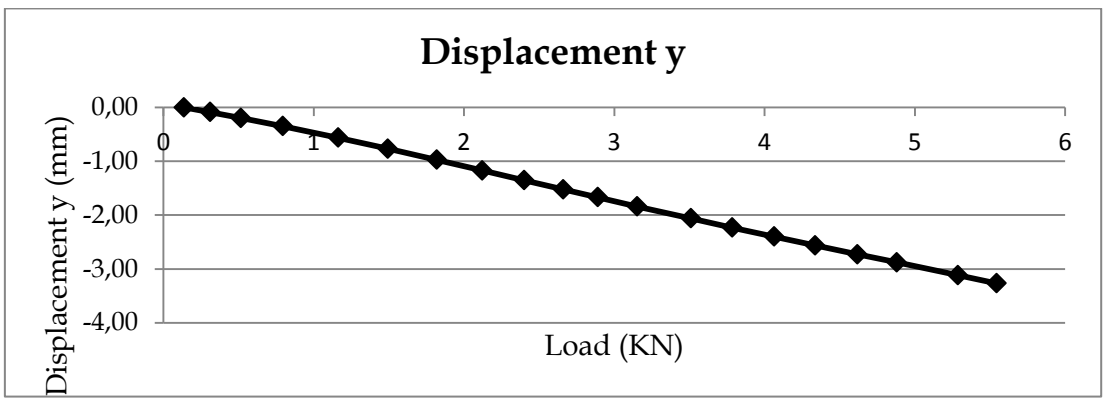
Displacement y
Displacement y (mm)
0,00
-1,00
-2,00
-3,00
-4,00
0
1
2
3
4
5
6
Load (KN)

4.2.3 Bottom beam

Test 107

	Strain gauges	Aramis				
Load (KN)	Strain (%)	Strain (%)	Δ Lenght x (mm)	Δ Lenght y (mm)	Displ x (mm)	Displ y (mm)
0,16	0,0000	0,0000	0,00000	0,0000	0,000	0,000
0,35	-0,0008	-0,0007	-0,00007	0,0030	-0,015	-0,090
0,56	-0,0017	0,0020	0,00010	0,0062	-0,032	-0,202
0,86	-0,0034	-0,0063	-0,00050	0,0112	-0,057	-0,370
1,30	-0,0059	-0,0059	-0,00053	0,0188	-0,096	-0,625
1,72	-0,0085	-0,0142	-0,00115	0,0262	-0,134	-0,888
2,08	-0,0109	-0,0113	-0,00101	0,0340	-0,167	-1,126
2,33	-0,0125	-0,0222	-0,00180	0,0384	-0,190	-1,293
2,60	-0,0143	-0,0169	-0,00148	0,0445	-0,214	-1,467
2,82	-0,0158	-0,0224	-0,00189	0,0487	-0,235	-1,611
3,01	-0,0170	-0,0187	-0,00167	0,0525	-0,251	-1,729
3,17	-0,0181	-0,0244	-0,00209	0,0557	-0,266	-1,836
3,34	-0,0194	-0,0238	-0,00208	0,0589	-0,281	-1,945
3,51	-0,0205	-0,0261	-0,00227	0,0622	-0,297	-2,054
3,69	-0,0218	-0,0244	-0,00219	0,0659	-0,313	-2,165
3,85	-0,0229	-0,0263	-0,00235	0,0696	-0,327	-2,263
3,99	-0,0240	-0,0335	-0,00287	0,0715	-0,340	-2,351
4,24	-0,0257	-0,0297	-0,00266	0,0766	-0,362	-2,500
4,47	-0,0274	-0,0319	-0,00284	0,0801	-0,383	-2,636
4,64	-0,0284	-0,0348	-0,00308	0,0832	-0,396	-2,734
4,92	-0,0307	-0,0372	-0,00330	0,0886	-0,423	-2,898
5,12	-0,0318	-0,0337	-0,00310	0,0926	-0,442	-3,014
5,34	-0,0334	-0,0343	-0,00318	0,0962	-0,462	-3,141

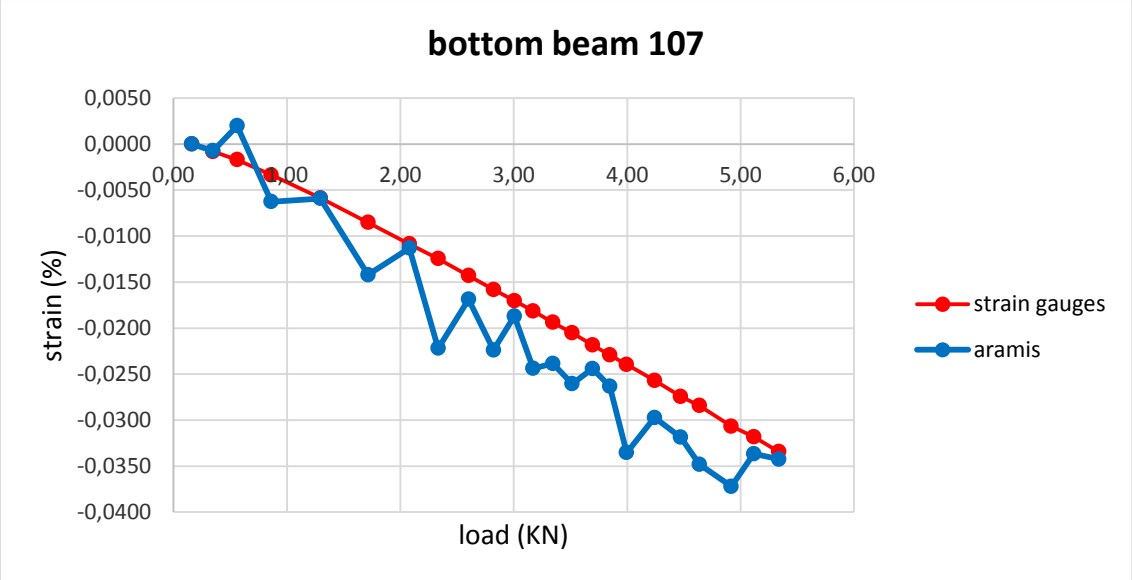

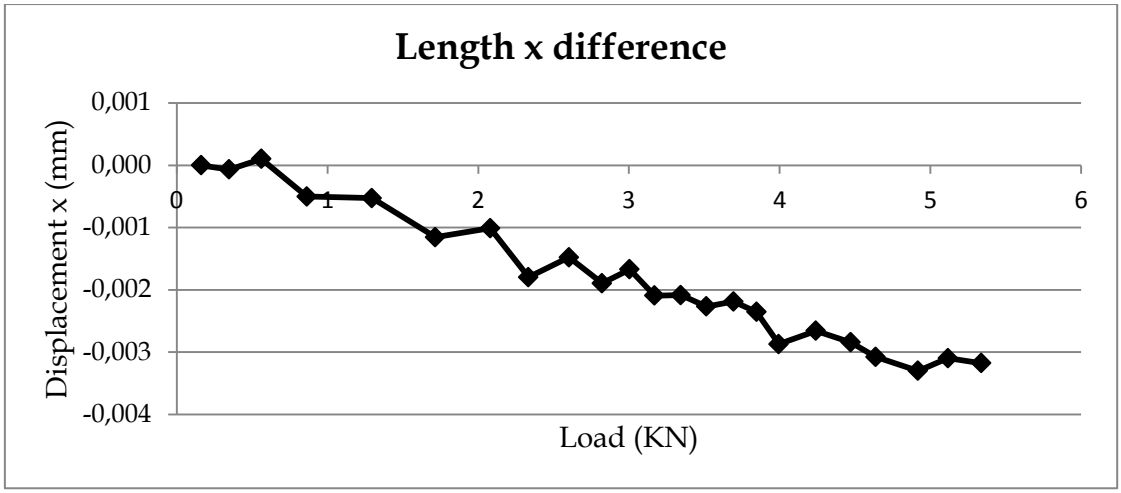
Length x difference
Displacement x (mm)
0,001
0,000
-0,001
-0,002
-0,003
-0,004
0
1
2
3
4
5
6
Load (KN)

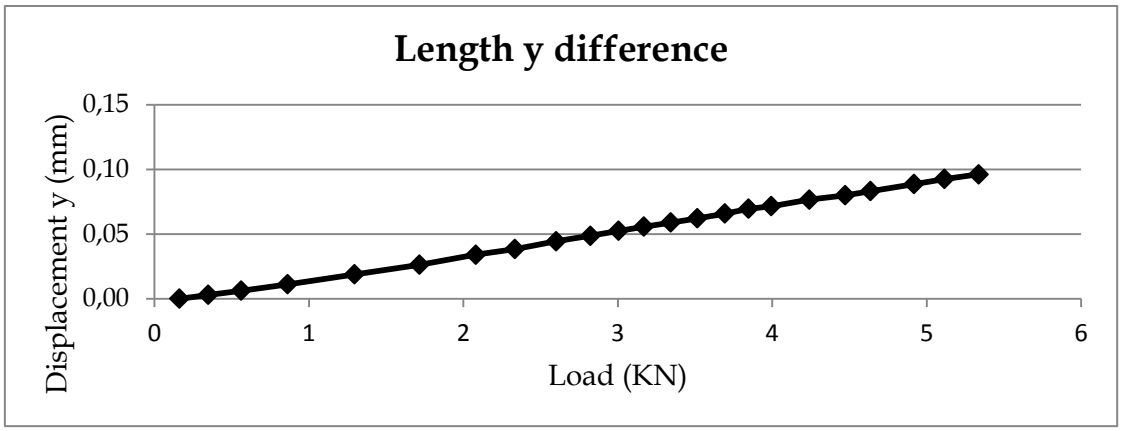
Length y difference
Displacement y (mm)
0,15
0,10
0,05
0,00
0
1
2
3
4
5
6
Load (KN)

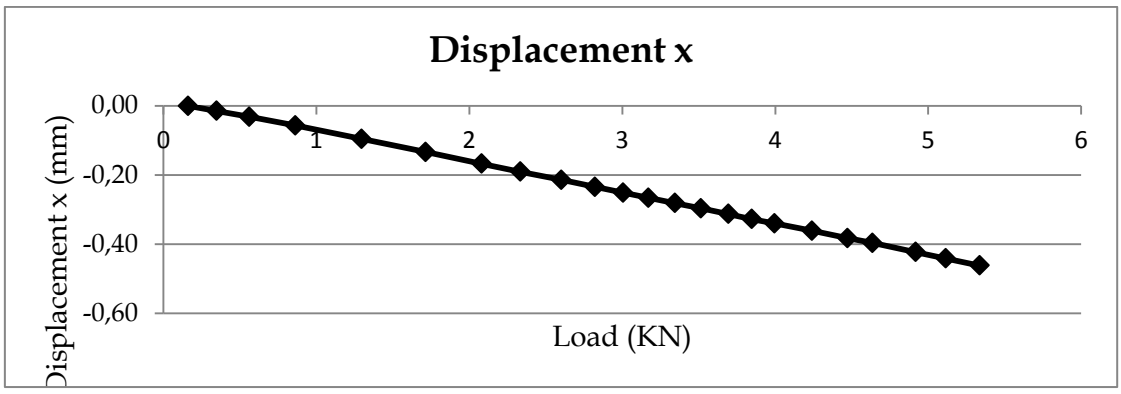
Displacement x
Displacement x (mm)
0,00
-0,20
-0,40
-0,60
0
1
2
3
4
5
6
Load (KN)

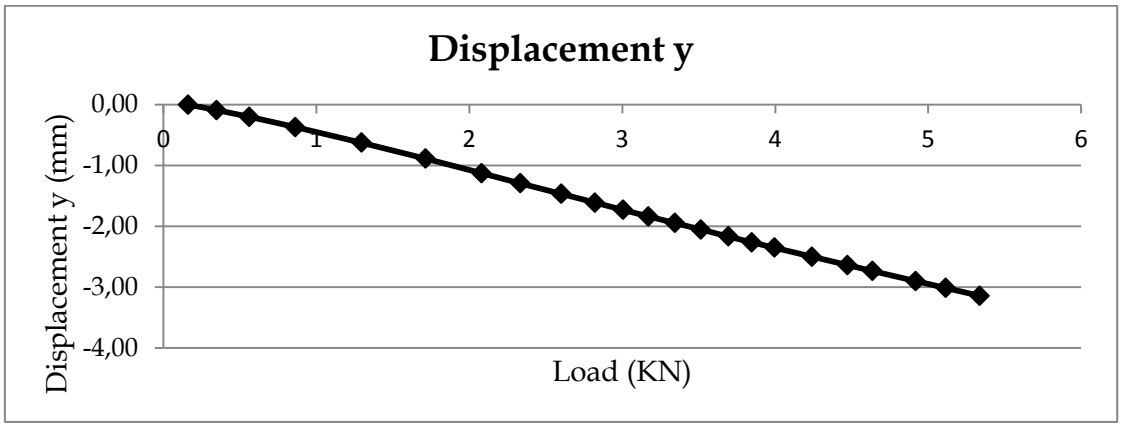
Displacement y
Displacement y (mm)
0,00
-1,00
-2,00
-3,00
-4,00
0
1
2
3
4
5
6
Load (KN)

Test 111

	Strain gauges	Aramis				
Load (KN)	Strain (%)	Strain (%)	Δ Lenght x (mm)	Δ Lenght y (mm)	Displ x (mm)	Displ y (mm)
0,15	0,0000	0,0000	0,00000	0,0000	0,000	0,000
0,43	-0,0014	0,0020	0,00010	0,0048	-0,023	-0,138
0,69	-0,0024	0,0020	0,00000	0,0096	-0,047	-0,276
1,16	-0,0051	-0,0101	-0,00144	0,0185	-0,089	-0,546
1,82	-0,0093	-0,0102	-0,00179	0,0332	-0,150	-0,955
2,31	-0,0126	-0,0138	-0,00242	0,0439	-0,195	-1,272
2,58	-0,0144	-0,0233	-0,00353	0,0497	-0,219	-1,445
2,94	-0,0168	-0,0284	-0,00427	0,0577	-0,253	-1,673
3,34	-0,0195	-0,0331	-0,00497	0,0662	-0,290	-1,927
3,56	-0,0211	-0,0281	-0,00459	0,0708	-0,309	-2,062
3,80	-0,0229	-0,0346	-0,00541	0,0761	-0,331	-2,207
4,21	-0,0255	-0,0384	-0,00605	0,0852	-0,369	-2,457
4,42	-0,0272	-0,0327	-0,00558	0,0891	-0,387	-2,582
4,64	-0,0285	-0,0305	-0,00549	0,0933	-0,407	-2,706
4,91	-0,0304	-0,0405	-0,00668	0,0988	-0,431	-2,862
5,13	-0,0322	-0,0401	-0,00680	0,1044	-0,452	-2,991
5,28	-0,0332	-0,0419	-0,00705	0,1065	-0,465	-3,077
5,46	-0,0346	-0,0513	-0,00812	0,1100	-0,480	-3,181

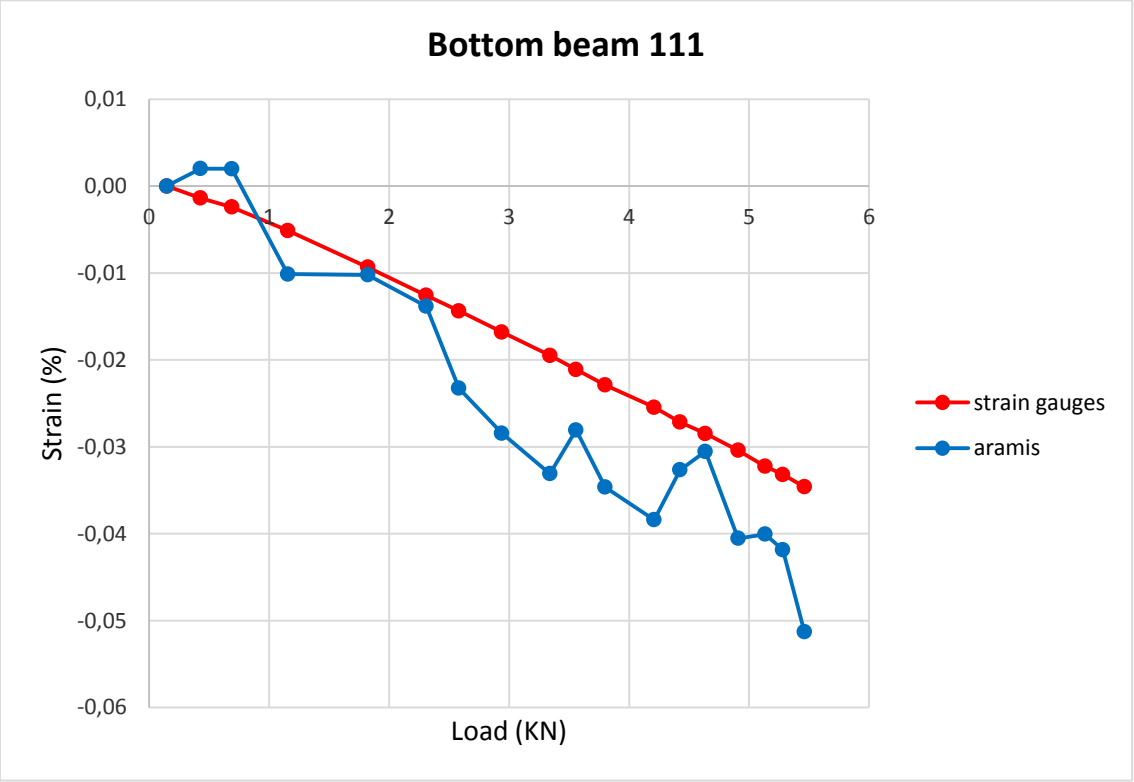

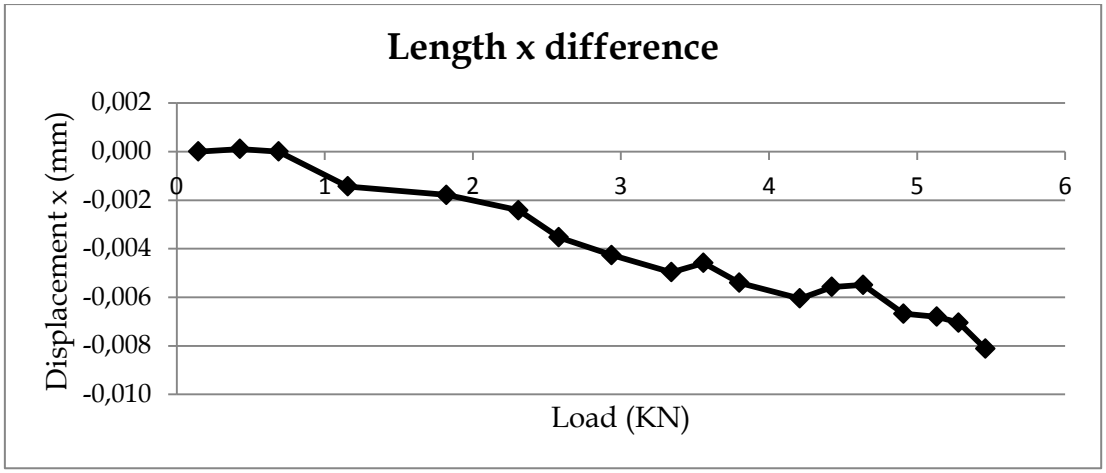
Length x difference
Displacement x (mm)
0,002
0,000
-0,002
-0,004
-0,006
-0,008
-0,010
0
1
2
3
4
5
6
Load (KN)

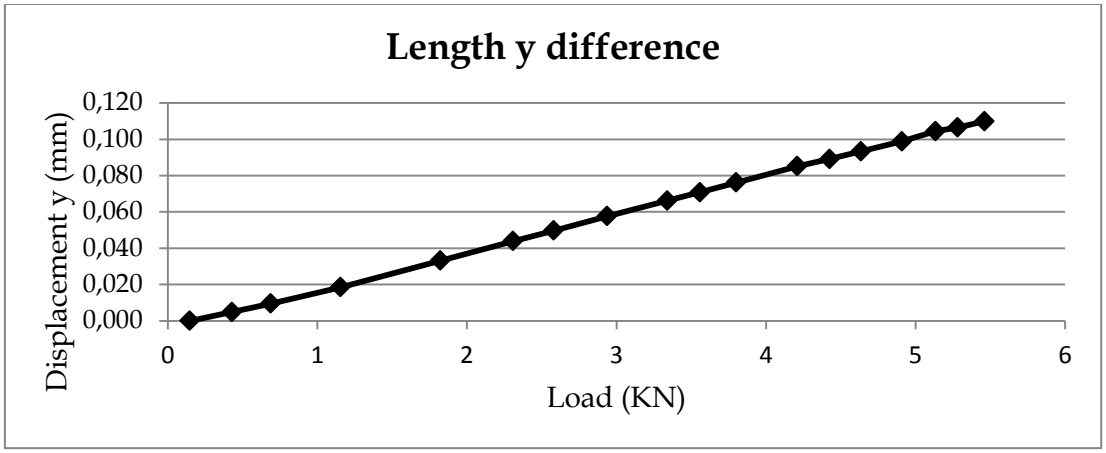
Length y difference
Displacement y (mm)
0,120
0,100
0,080
0,060
0,040
0,020
0,000
0
1
2
3
4
5
6
Load (KN)

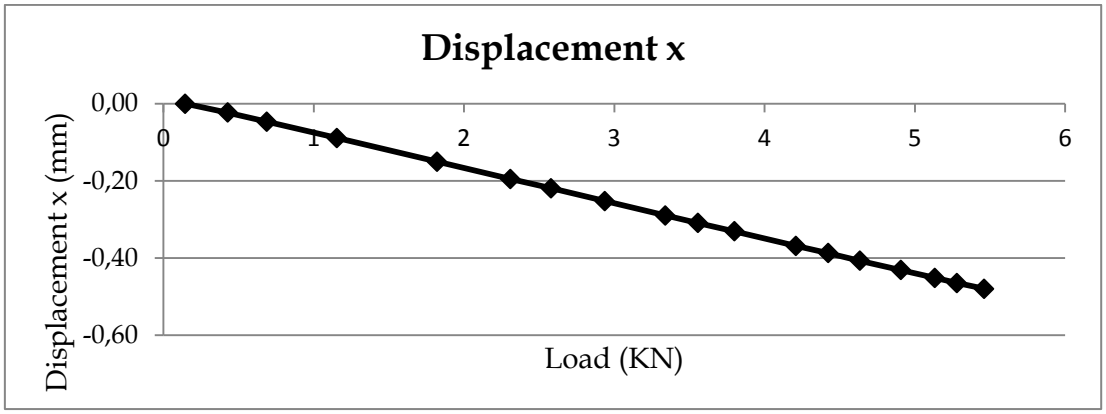
Displacement x
Displacement x (mm)
0,00
-0,20
-0,40
-0,60
0
1
2
3
4
5
6
Load (KN)

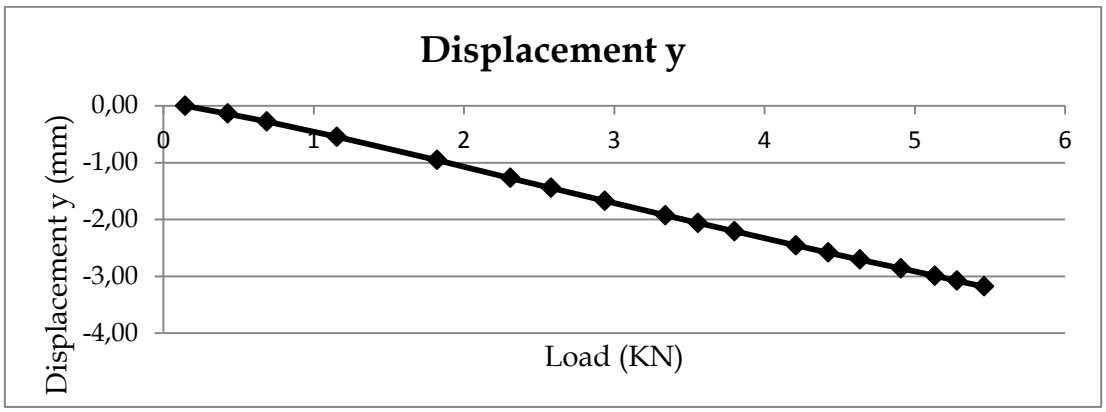
Displacement y
Displacement y (mm)
0,00
-1,00
-2,00
-3,00
-4,00
0
1
2
3
4
5
6
Load (KN)

4.2.4 Top joint

Test 109

	Strain gauges	Aramis				
Load (KN)	Strain (%)	Strain (%)	Δ Lenght x (mm)	Δ Lenght y (mm)	Displ x (mm)	Displ y (mm)
0,16	0,0000	0,000	0,0000	0,000	0,000	0,00
0,35	0,0003	-0,002	-0,0003	0,003	0,022	-0,06
0,56	0,0008	-0,014	-0,0018	0,007	0,049	-0,12
0,86	0,0013	-0,024	-0,0031	0,014	0,087	-0,23
1,30	0,0022	-0,051	-0,0064	0,023	0,153	-0,39
1,72	0,0031	-0,064	-0,0081	0,032	0,221	-0,55
2,08	0,0039	-0,072	-0,0093	0,041	0,287	-0,70
2,33	0,0043	-0,080	-0,0103	0,047	0,332	-0,80
2,60	0,0049	-0,084	-0,0109	0,053	0,380	-0,91
2,82	0,0054	-0,086	-0,0112	0,058	0,420	-1,00
3,01	0,0058	-0,094	-0,0122	0,062	0,452	-1,07
3,17	0,0061	-0,089	-0,0116	0,067	0,482	-1,14
3,34	0,0064	-0,090	-0,0119	0,070	0,511	-1,21
3,51	0,0068	-0,095	-0,0125	0,075	0,540	-1,27
3,69	0,0071	-0,093	-0,0123	0,078	0,571	-1,34
3,85	0,0074	-0,101	-0,0134	0,082	0,596	-1,40
3,99	0,0077	-0,101	-0,0134	0,085	0,620	-1,46
4,24	0,0081	-0,102	-0,0137	0,091	0,660	-1,55
4,47	0,0086	-0,106	-0,0141	0,095	0,697	-1,63
4,64	0,0090	-0,108	-0,0145	0,099	0,724	-1,69
4,92	0,0095	-0,106	-0,0144	0,105	0,767	-1,80
5,12	0,0099	-0,106	-0,0144	0,109	0,796	-1,87
5,34	0,0104	-0,107	-0,0147	0,114	0,830	-1,95

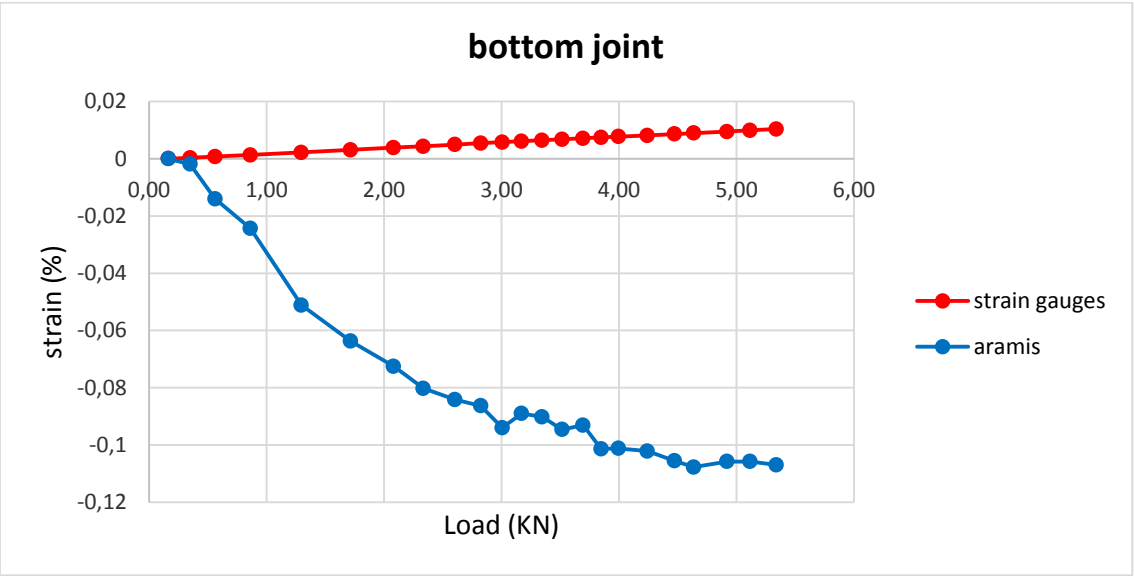

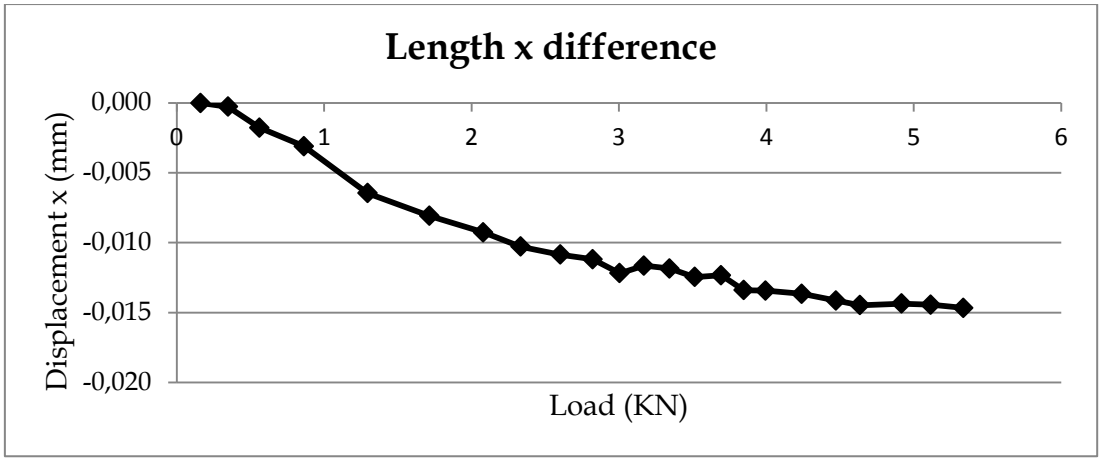
Length x difference
Displacement x (mm)
0,000
-0,005
-0,010
-0,015
-0,020
0
1
2
3
4
5
6
Load (KN)

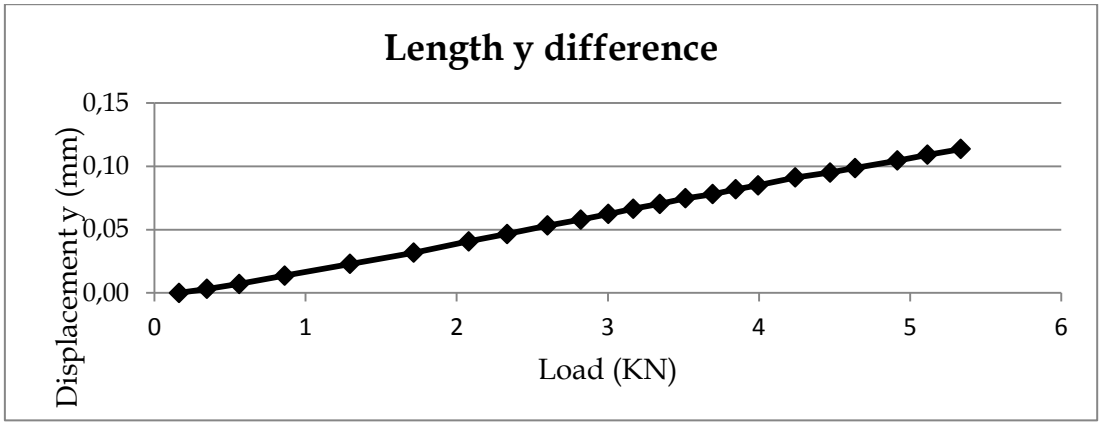
Length y difference
Displacement y (mm)
0,15
0,10
0,05
0,00
0
1
2
3
4
5
6
Load (KN)

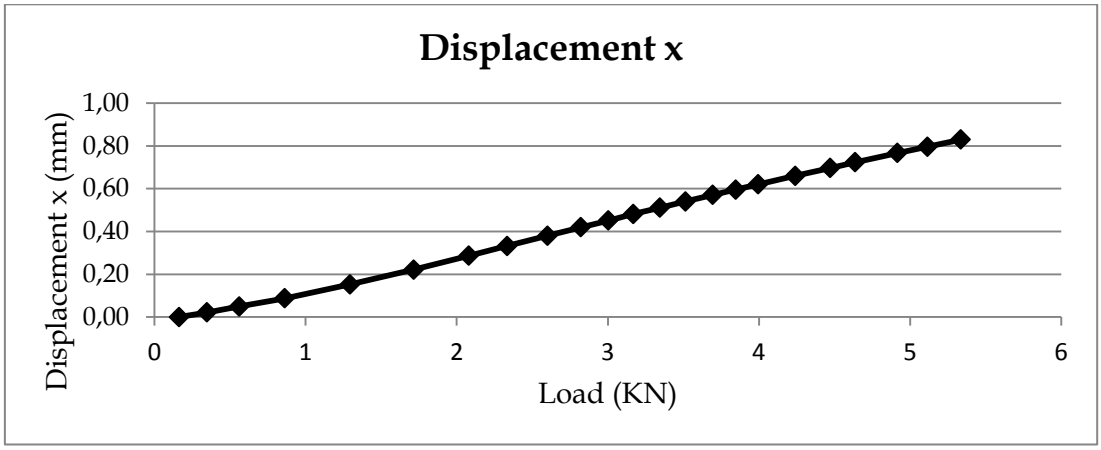
Displacement x
Displacement x (mm)
1,00
0,80
0,60
0,40
0,20
0,00
0
1
2
3
4
5
6
Load (KN)

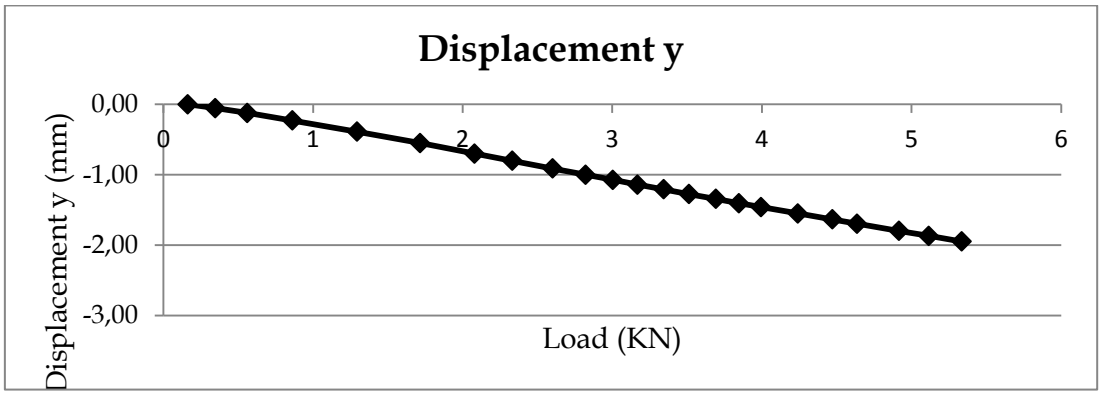
Displacement y
Displacement y (mm)
0,00
-1,00
-2,00
-3,00
0
1
2
3
4
5
6
Load (KN)

Test 110

	Strain gauges	Aramis				
Load (KN)	Strain (%)	Strain (%)	Δ Lenght x (mm)	Δ Lenght y (mm)	Displ x (mm)	Displ y (mm)
0,15	0,0000	0,0000	0,0000	0,000	0,000	0,000
0,37	0,0005	0,0010	-0,0006	0,001	0,001	0,000
0,54	0,0009	0,0025	-0,0016	0,003	0,029	-0,061
0,86	0,0014	0,0026	-0,0017	0,006	0,052	-0,113
1,24	0,0022	0,0033	-0,0023	0,012	0,096	-0,213
1,58	0,0028	0,0052	-0,0035	0,018	0,154	-0,342
1,90	0,0035	0,0056	-0,0039	0,025	0,207	-0,460
2,30	0,0043	0,0064	-0,0044	0,030	0,262	-0,577
2,75	0,0051	0,0063	-0,0046	0,039	0,335	-0,727
3,21	0,0061	0,0078	-0,0056	0,048	0,414	-0,893
3,60	0,0069	0,0085	-0,0062	0,056	0,493	-1,055
3,91	0,0074	0,0091	-0,0067	0,063	0,559	-1,197
4,15	0,0080	0,0094	-0,0070	0,069	0,611	-1,305
4,53	0,0088	0,0087	-0,0067	0,074	0,651	-1,391
4,83	0,0093	0,0084	-0,0066	0,080	0,709	-1,515
5,14	0,0100	0,0093	-0,0073	0,086	0,756	-1,617
5,33	0,0104	0,0099	-0,0078	0,091	0,802	-1,718
5,51	0,0107	0,0097	-0,0078	0,095	0,831	-1,782

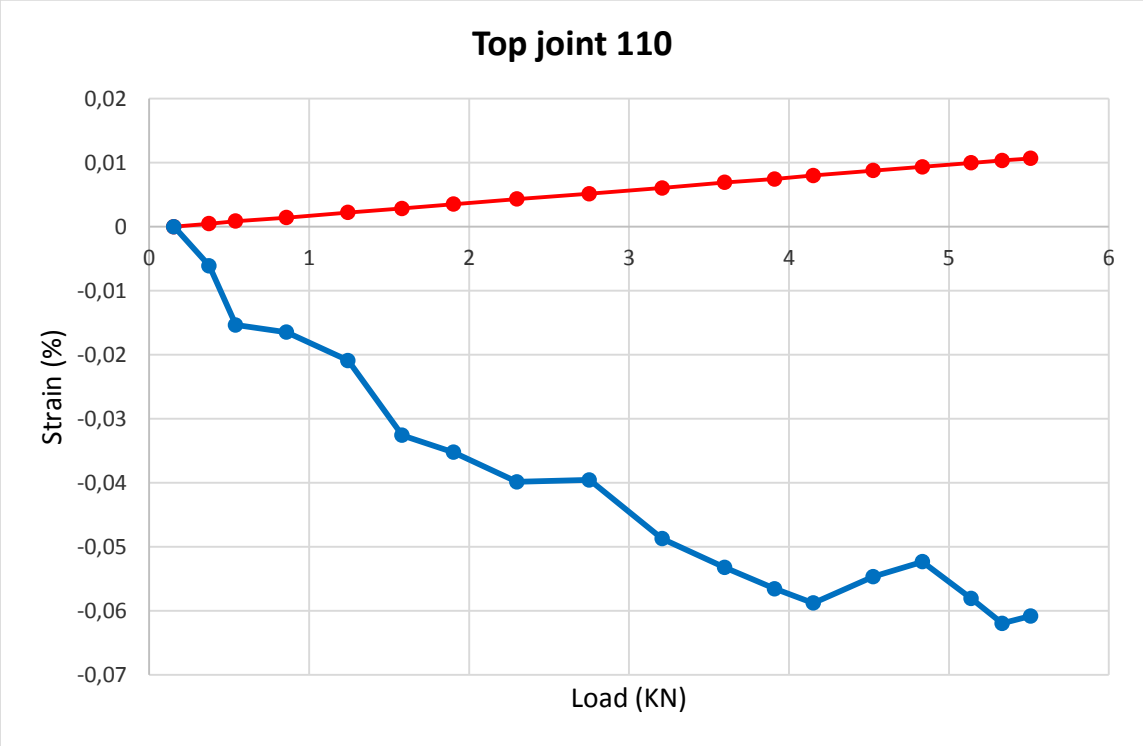

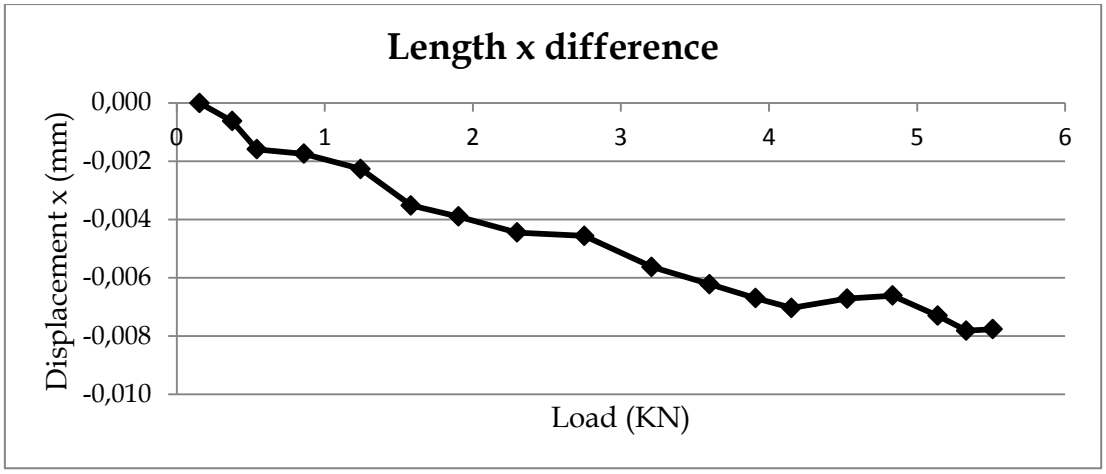
Length x difference
Displacement x (mm)
0,000
-0,002
-0,004
-0,006
-0,008
-0,010
0
1
2
3
4
5
6
Load (KN)

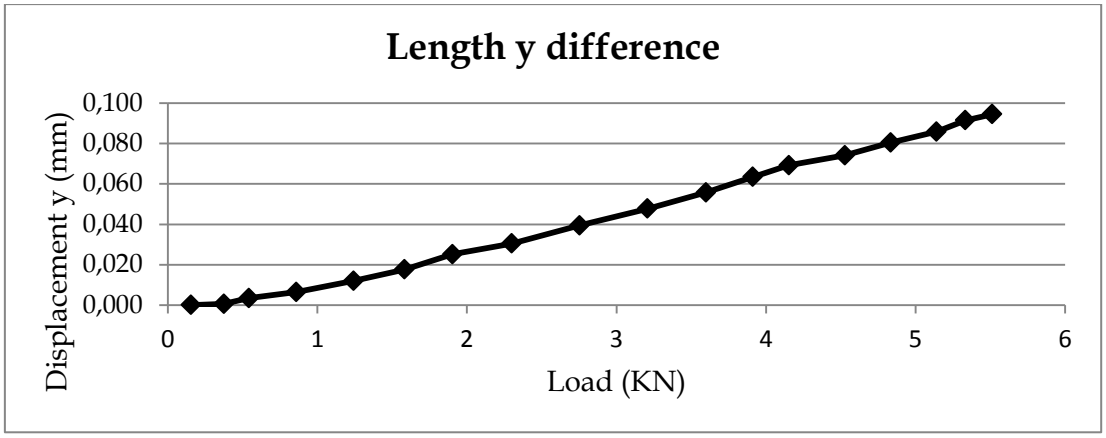
Length y difference
Displacement y (mm)
0,100
0,080
0,060
0,040
0,020
0,000
0
1
2
3
4
5
6
Load (KN)

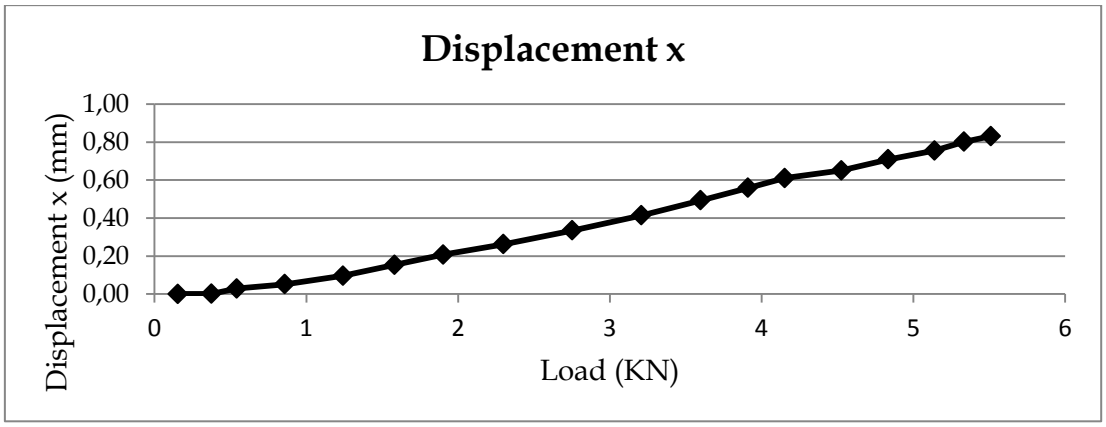
Displacement x
Displacement x (mm)
1,00
0,80
0,60
0,40
0,20
0,00
0
1
2
3
4
5
6
Load (KN)

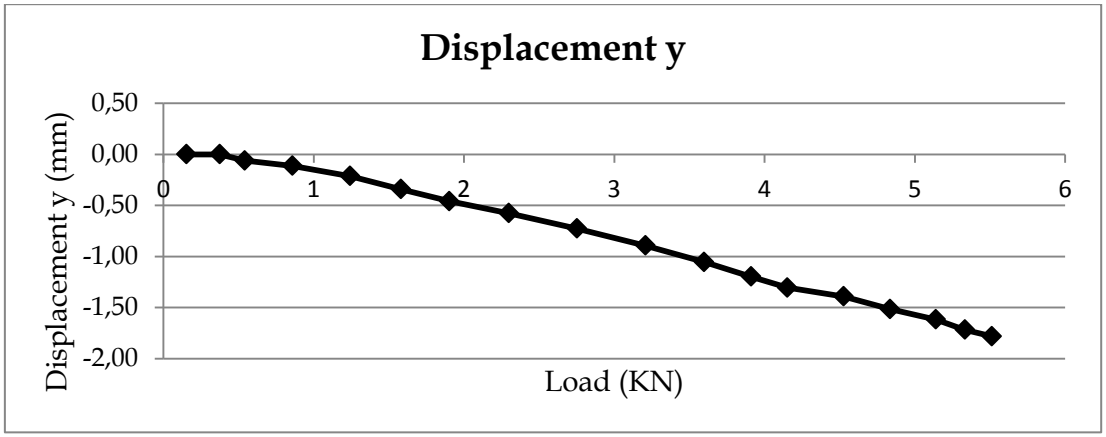
Displacement y
Displacement y (mm)
0,50
0,00
-0,50
-1,00
-1,50
-2,00
0
1
2
3
4
5
6
Load (KN)

4.2.5 Mid joint

Test 116

	Strain gauges	Aramis				
Load (KN)	Strain (%)	Strain (%)	Δ Lenght x (mm)	Δ Lenght y (mm)	Displ x (mm)	Displ y (mm)
0,14	0,0000	0,0000	0,00000	0,0000	0,000	0,000
0,33	0,0003	0,0033	0,00027	0,0027	0,007	-0,066
0,54	0,0006	0,0100	0,00086	0,0057	0,017	-0,141
0,93	0,0011	0,0085	0,00065	0,0116	0,040	-0,289
1,39	0,0018	-0,0002	-0,00029	0,0203	0,072	-0,479
1,75	0,0024	0,0055	0,00016	0,0256	0,100	-0,635
2,00	0,0030	-0,0128	-0,00161	0,0305	0,123	-0,749
2,39	0,0036	-0,0076	-0,00126	0,0386	0,153	-0,924
2,89	0,0046	-0,0107	-0,00170	0,0474	0,194	-1,149
3,34	0,0054	-0,0100	-0,00178	0,0559	0,230	-1,344
3,77	0,0061	-0,0111	-0,00763	0,0635	0,263	-1,533
4,21	0,0068	-0,0061	-0,00730	0,0709	0,295	-1,715
4,57	0,0074	-0,0100	-0,00780	0,0773	0,322	-1,859
4,84	0,0078	-0,0169	-0,00851	0,0807	0,342	-1,969
5,21	0,0082	-0,0100	-0,00802	0,0877	0,365	-2,112
5,60	0,0088	-0,0162	-0,00871	0,0935	0,393	-2,266

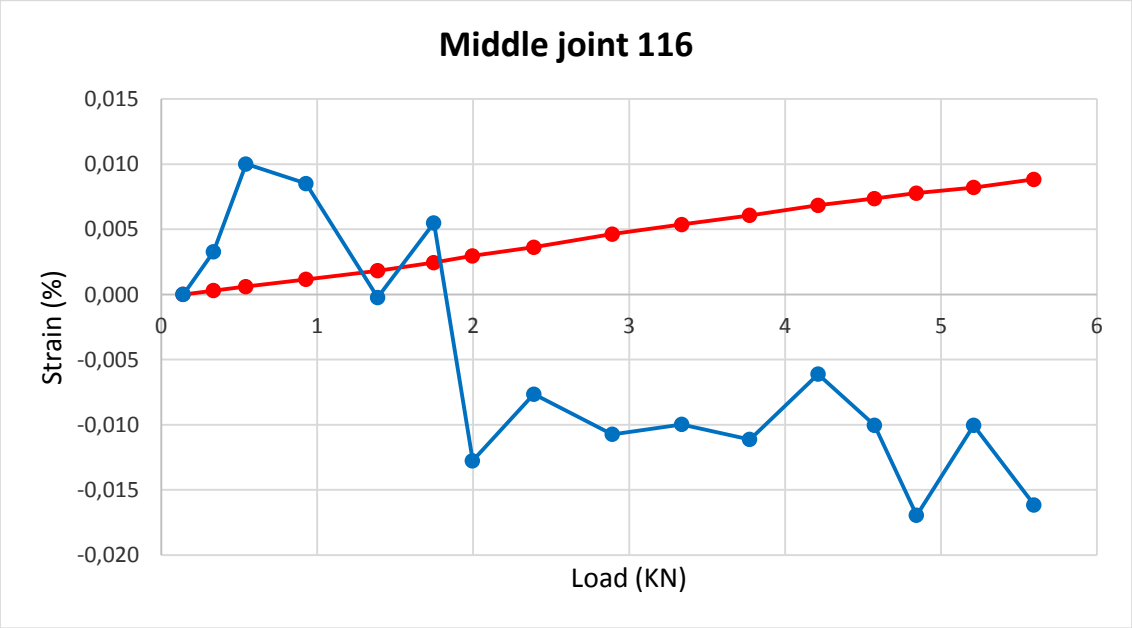

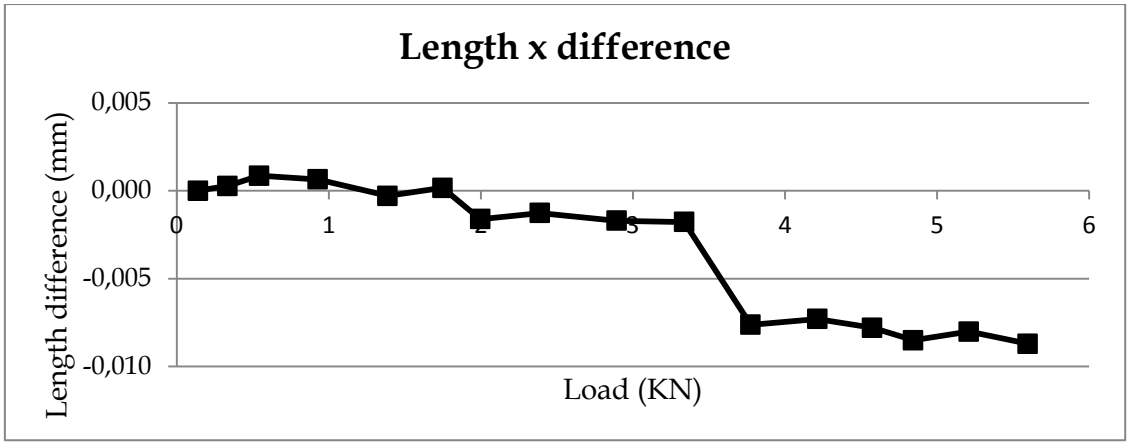
Length x difference
Length difference (mm)
0,005
0,000
-0,005
-0,010
0
1
2
3
4
5
6
Load (KN)

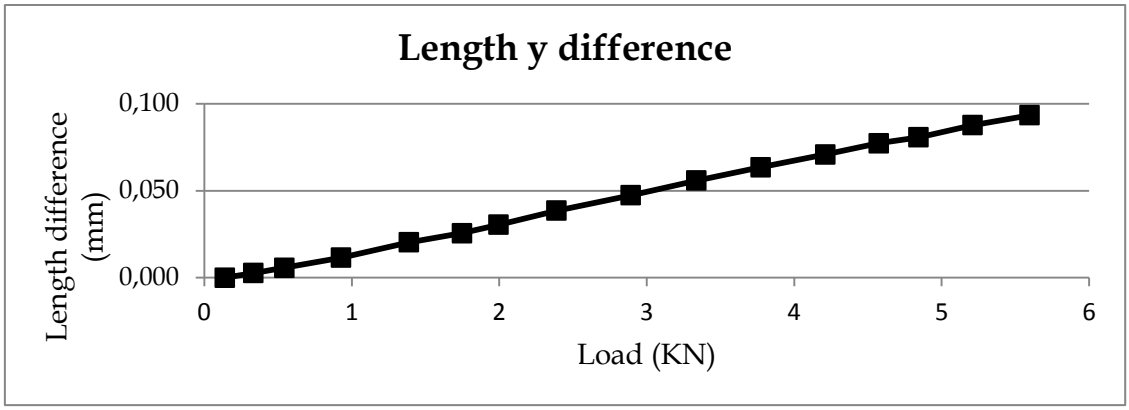
Length y difference
Length difference (mm)
0,100
0,050
0,000
0
1
2
3
4
5
6
Load (KN)

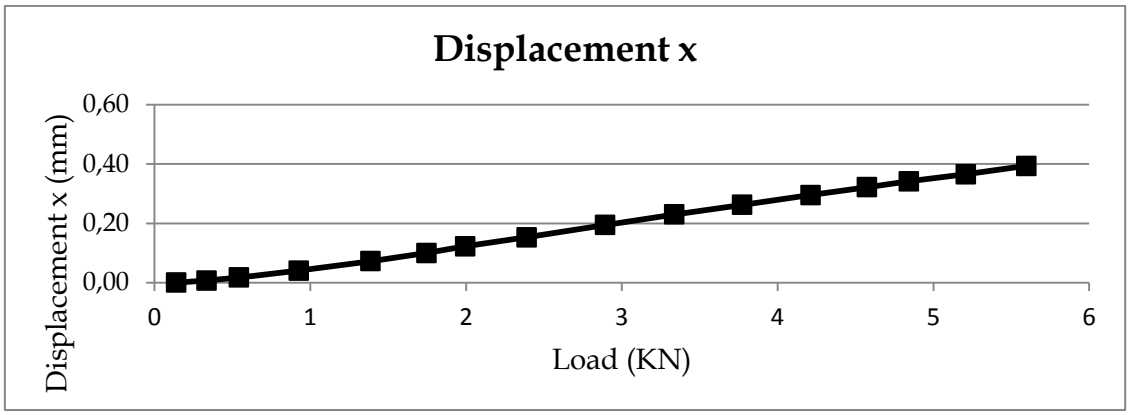
Displacement x
Displacement x (mm)
0,60
0,40
0,20
0,00
0
1
2
3
4
5
6
Load (KN)

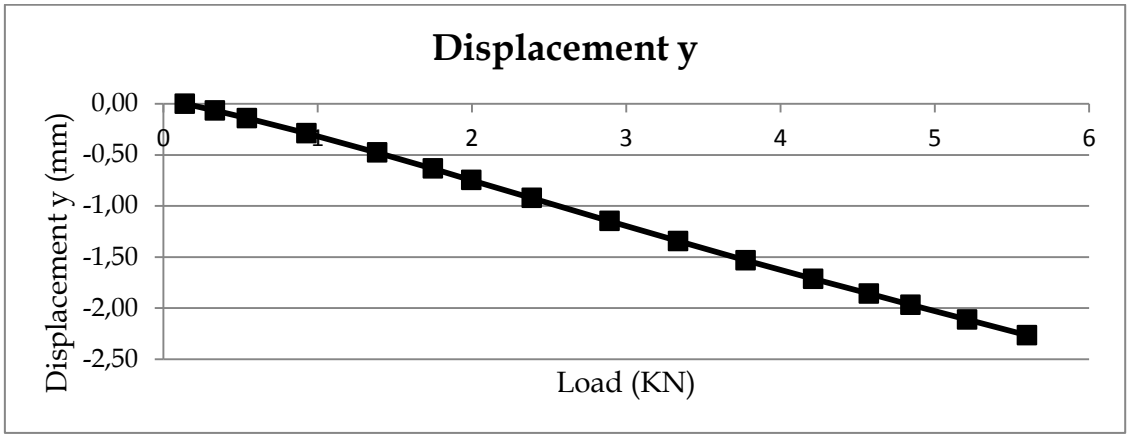
Displacement y
Displacement y (mm)
0,00
-0,50
-1,00
-1,50
-2,00
-2,50
0
1
2
3
4
5
6
Load (KN)

4.2.6 Bottom joint

Test 102

	Strain gauges	Aramis				
Load (KN)	Strain (%)	Strain (%)	Δ Lenght x (mm)	Δ Lenght y (mm)	Displ x (mm)	Displ y (mm)
0,22	0,0000	0,0000	0,0000	0,000	0,000	0,000
0,60	-0,0008	-0,0043	-0,0010	0,007	-0,025	-0,115
0,93	-0,0015	0,0011	-0,0004	0,014	-0,048	-0,226
1,46	-0,0030	-0,0023	-0,0008	0,025	-0,088	-0,418
1,73	-0,0037	-0,0013	-0,0007	0,030	-0,107	-0,516
1,95	-0,0043	-0,0051	-0,0012	0,035	-0,124	-0,607
2,14	-0,0048	-0,0013	-0,0008	0,039	-0,137	-0,679
2,46	-0,0056	-0,0105	-0,0018	0,046	-0,159	-0,805
2,74	-0,0064	-0,0081	-0,0016	0,053	-0,181	-0,915
2,99	-0,0070	-0,0107	-0,0019	0,058	-0,197	-1,012
3,29	-0,0079	-0,0078	-0,0016	0,064	-0,220	-1,126
3,49	-0,0084	-0,0100	-0,0019	0,069	-0,233	-1,200
3,72	-0,0089	-0,0109	-0,0020	0,073	-0,248	-1,286
4,06	-0,0097	-0,0134	-0,0023	0,081	-0,272	-1,414
4,47	-0,0107	-0,0081	-0,0018	0,088	-0,300	-1,559
4,72	-0,0115	-0,0128	-0,0024	0,094	-0,318	-1,649
5,02	-0,0123	-0,0184	-0,0030	0,099	-0,339	-1,755
5,24	-0,0129	-0,0041	-0,0015	0,105	-0,354	-1,832
5,39	-0,0133	-0,0101	-0,0022	0,107	-0,364	-1,883
5,50	-0,0135	-0,0101	-0,0022	0,109	-0,372	-1,925

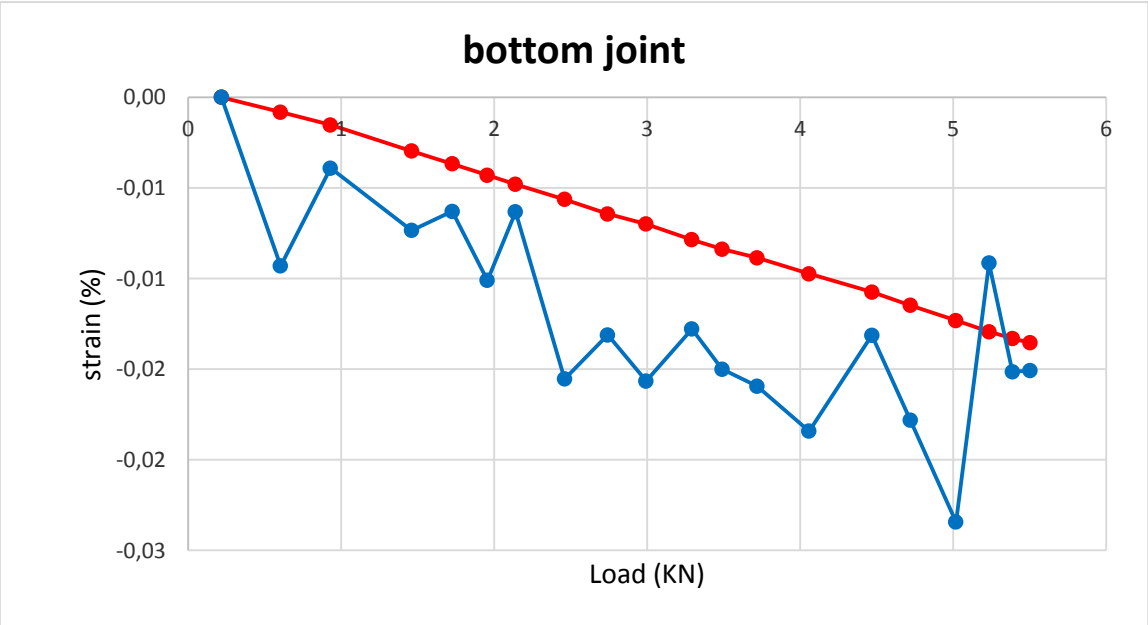

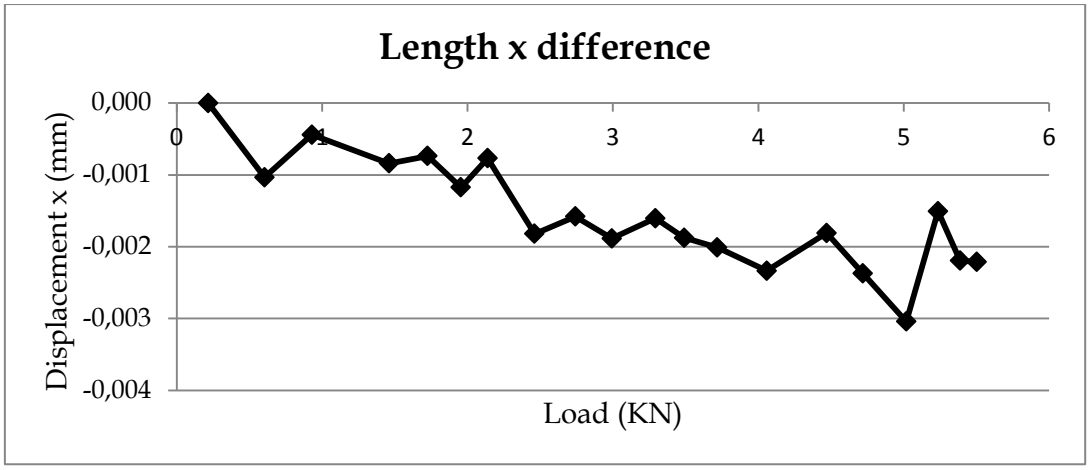
Length x difference
Displacement x (mm)
0,000
-0,001
-0,002
-0,003
-0,004
0
1
2
3
4
5
6
Load (KN)

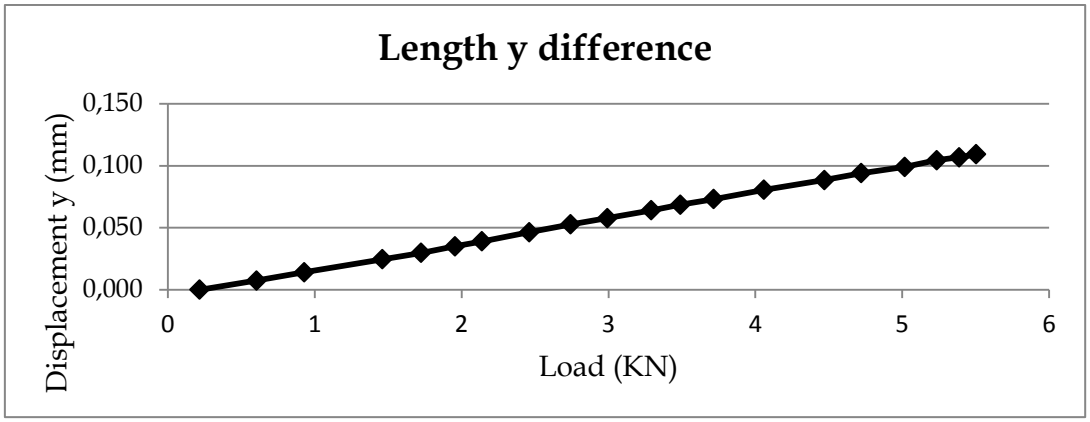
Length y difference
Displacement y (mm)
0,150
0,100
0,050
0,000
0
1
2
3
4
5
6
Load (KN)

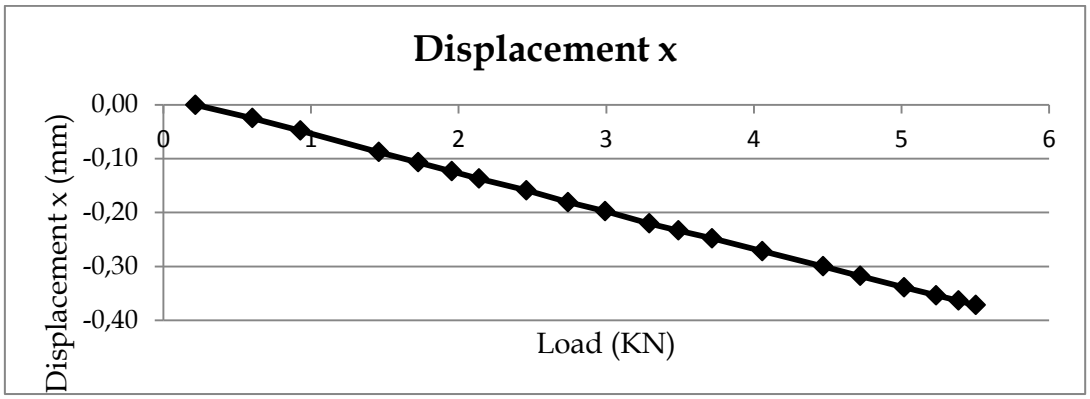
Displacement x
Displacement x (mm)
0,00
-0,10
-0,20
-0,30
-0,40
0
1
2
3
4
5
6
Load (KN)

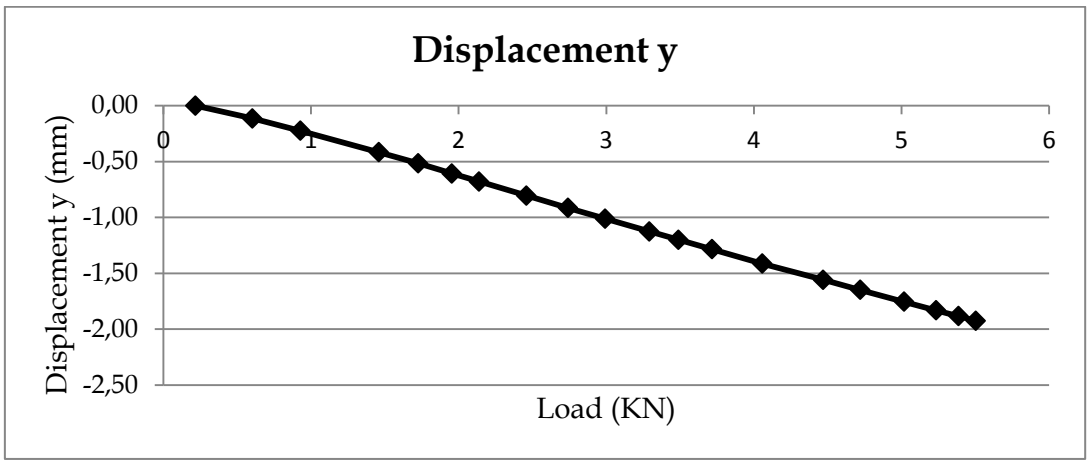
Displacement y
Displacement y (mm)
0,00
-0,50
-1,00
-1,50
-2,00
-2,50
0
1
2
3
4
5
6
Load (KN)

Test104

	Strain gauges	Aramis				
Load (KN)	Strain (%)	Strain (%)	Δ Lenght x (mm)	Δ Lenght y (mm)	Displ x (mm)	Displ y (mm)
0,20	0,0000	0,0000	0,0000	0,000	0,000	0,000
0,30	-0,0003	-0,0055	-0,0005	0,001	-0,006	-0,028
0,56	-0,0008	-0,0052	-0,0005	0,005	-0,025	-0,109
0,76	-0,0011	-0,0041	-0,0004	0,007	-0,039	-0,171
1,14	-0,0021	-0,0125	-0,0011	0,014	-0,066	-0,299
1,57	-0,0031	-0,0172	-0,0016	0,021	-0,097	-0,448
1,80	-0,0038	-0,0121	-0,0011	0,024	-0,115	-0,538
2,03	-0,0044	-0,0162	-0,0015	0,029	-0,131	-0,618
2,25	-0,0050	-0,0136	-0,0013	0,032	-0,146	-0,701
2,41	-0,0054	-0,0155	-0,0015	0,036	-0,157	-0,760
2,63	-0,0059	-0,0214	-0,0020	0,040	-0,172	-0,844
2,91	-0,0067	-0,0193	-0,0018	0,044	-0,192	-0,947
3,15	-0,0073	-0,0263	-0,0025	0,049	-0,209	-1,035
3,39	-0,0079	-0,0243	-0,0023	0,052	-0,225	-1,121
3,73	-0,0089	-0,0228	-0,0022	0,059	-0,250	-1,243
3,96	-0,0095	-0,0220	-0,0022	0,062	-0,267	-1,323
4,18	-0,0101	-0,0358	-0,0034	0,065	-0,281	-1,399
4,40	-0,0108	-0,0300	-0,0029	0,069	-0,296	-1,474
4,62	-0,0113	-0,0340	-0,0033	0,072	-0,310	-1,549
4,87	-0,0121	-0,0362	-0,0035	0,077	-0,328	-1,634
5,18	-0,0129	-0,0413	-0,0043	0,081	-0,346	-1,729
5,37	-0,0136	-0,0418	-0,0041	0,085	-0,363	-1,801

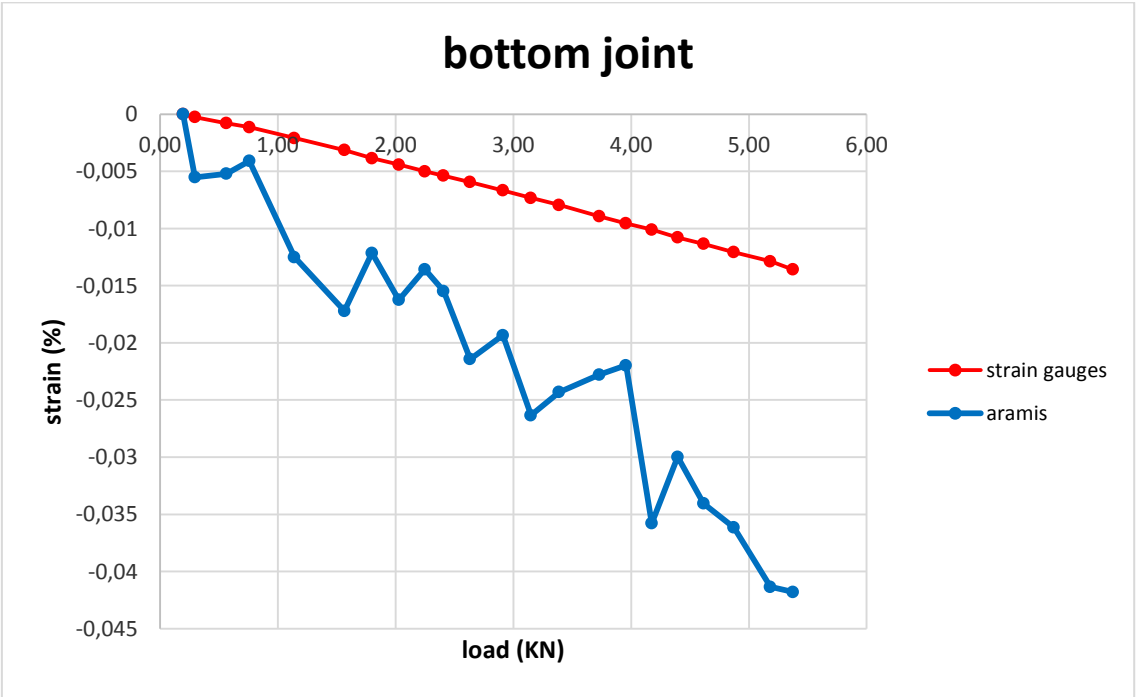

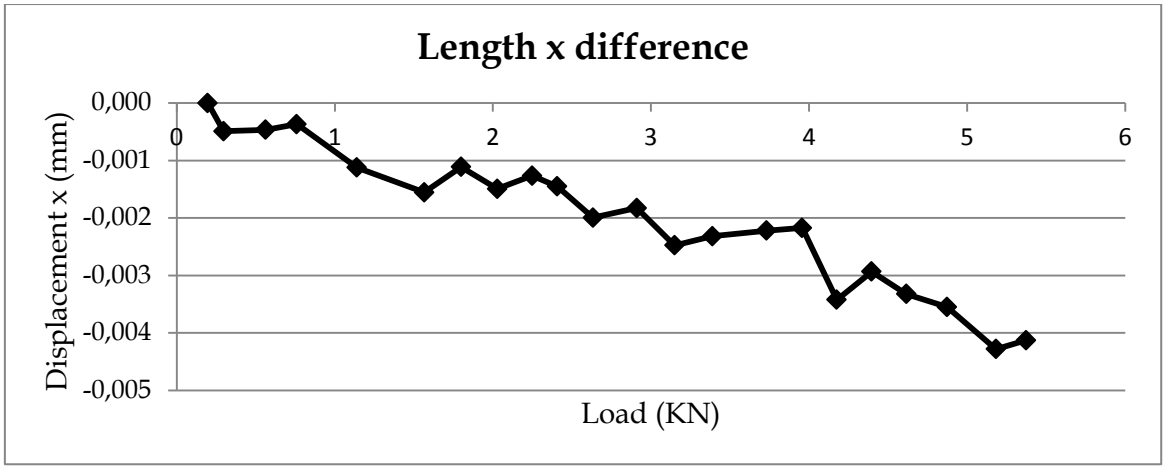
Length x difference
Displacement x (mm)
0,000
-0,001
-0,002
-0,003
-0,004
-0,005
0
1
2
3
4
5
6
Load (KN)

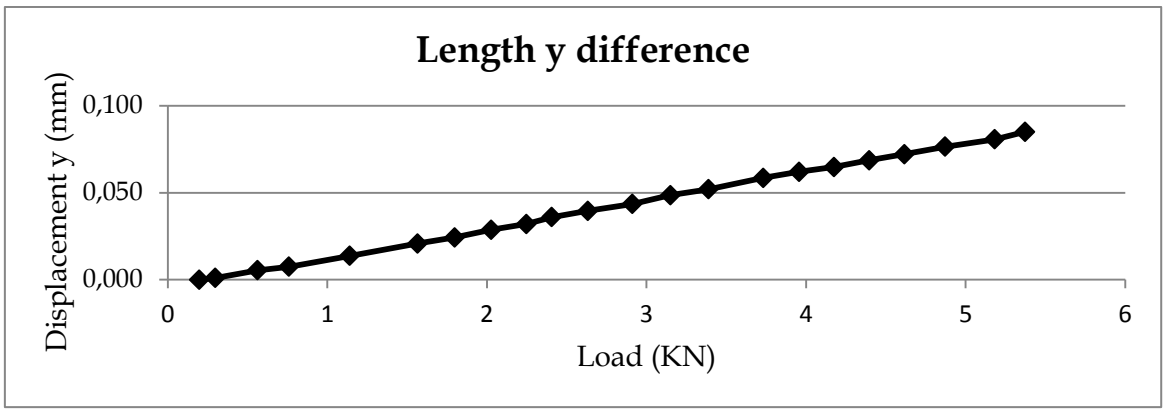
Length y difference
Displacement y (mm)
0,100
0,050
0,000
0
1
2
3
4
5
6
Load (KN)

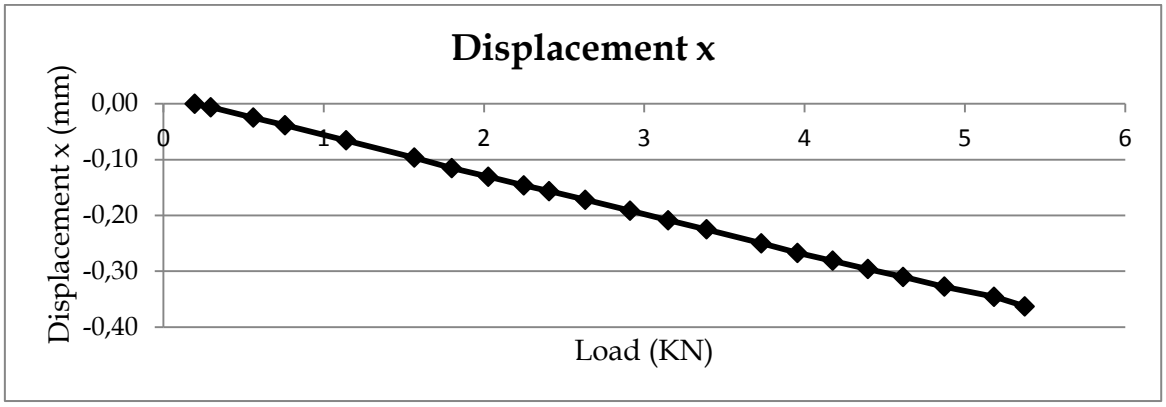
Displacement x
Displacement x (mm)
0,00
-0,10
-0,20
-0,30
-0,40
0
1
2
3
4
5
6
Load (KN)

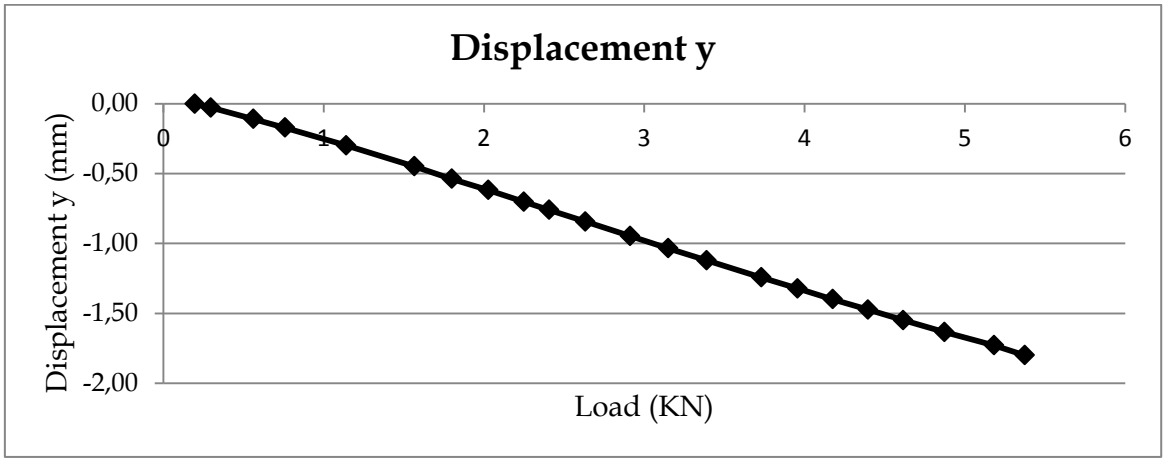
Displacement y
Displacement y (mm)
0,00
-0,50
-1,00
-1,50
-2,00
0
1
2
3
4
5
6
Load (KN)

4.3 Considerations

Graphs presented in this chapter show the comparison between Aramis and strain gauges results in the damaged situation, which means with the presence of the crack. All the test in the damaged condition were carried out loading the beam up to 5,57 KN which coincides with the 70% of the yield strength. All the photos were taken positioning the camera really close to the beam, in order to evaluate only one of the analyzed areas.

Relatively to strain comparison in different parts of the model, in the beam part of the structure strain analyzed were up to 0,035% and a quite good comparison was obtained, in particular in the compressed part (bottom beam), meanwhile some tests on the tense part were not comparable. In fact some tests presented strain-load graphs with Aramis trend completely different from the ones obtained from strain gauges. This consideration is even more present in the joint part, where strain values were really low (not up to 0,013%): here a not reliable comparison were found in many tests.

Chapter 5

Results comparison

This chapter presents a strain comparison between the two analyzed states, damaged and undamaged, in order to understand if the presence of the crack brings variation on the pattern and for this reason if it is possible to realize the presence of an hidden crack.

The first part presents a comparison between strain of the undamaged and damaged condition for the beam part of the structure obtained with Aramis, with strain gauges and with Abaqus. In the second part the joint area is considered and, due to not enough reliable result from digital image correlation, are presented strain comparison provided with strain gauges and with Abaqus. Strain comparison obtained from Aramis considered test 18, test 25 and test 32 for the undamaged values, while test 103, test 111 and test 122 have been used for the damaged condition.

5.1 Beam part

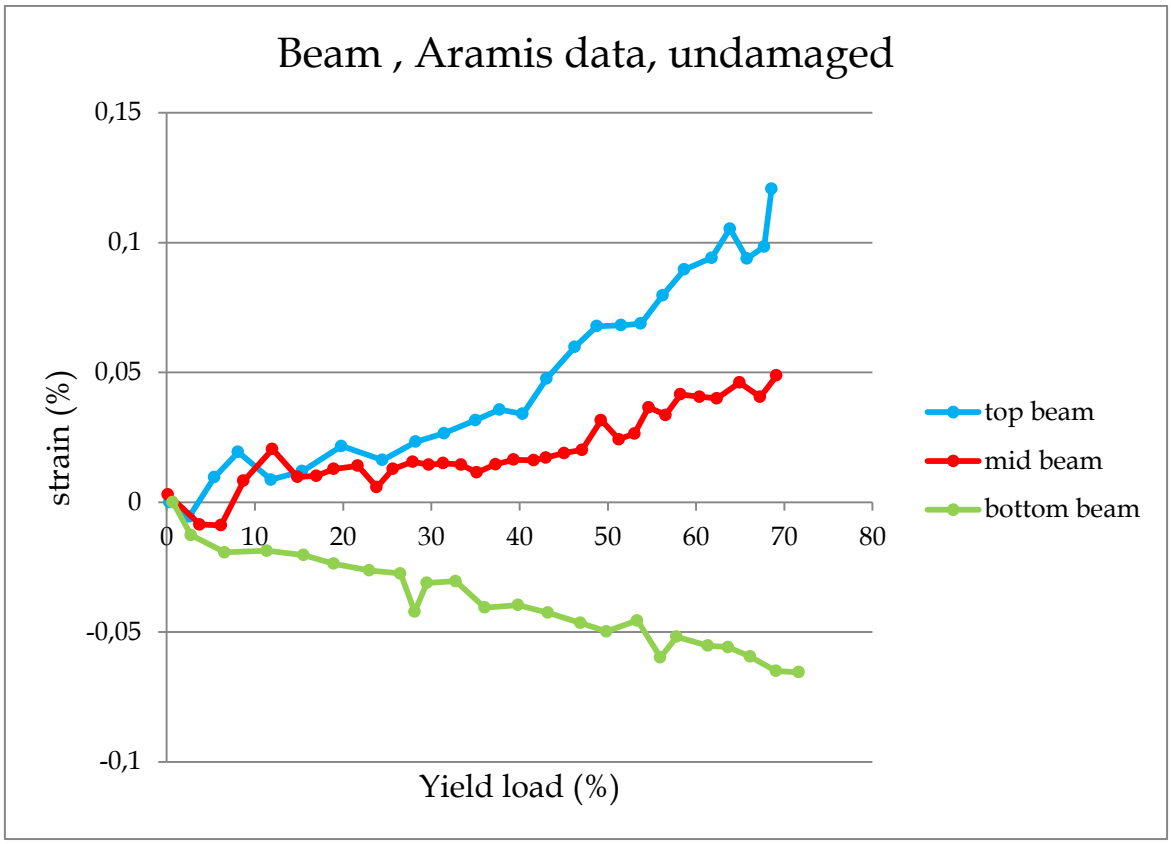
Beam , Aramis data, undamaged
0,15
0,1
0,05
0
-0,05
-0,1
strain (%)
0
10
20
30
40
50
60
70
80
Yield load (%)
top beam
mid beam
bottom beam

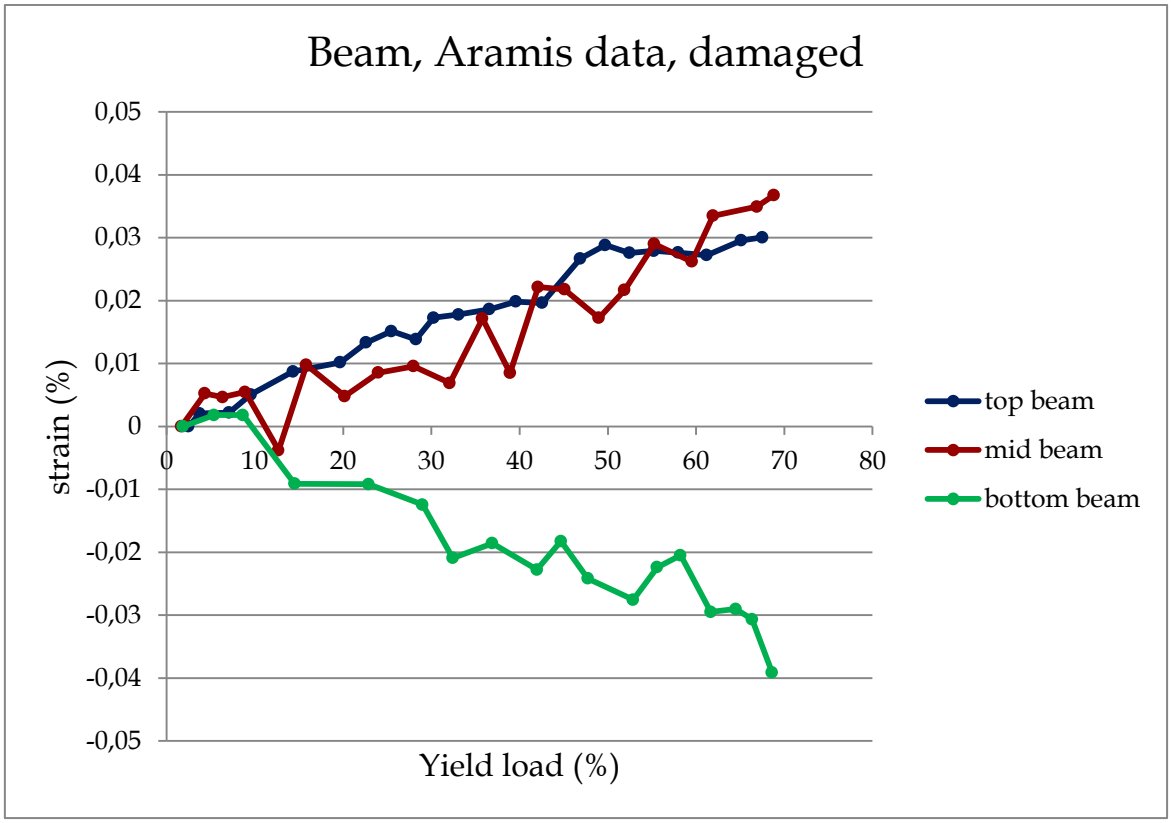
Beam, Aramis data, damaged
0,05
0,04
0,03
0,02
0,01
0
-0,01
-0,02
-0,03
-0,04
-0,05
strain (%)
0
10
20
30
40
50
60
70
80
Yield load (%)
top beam
mid beam
bottom beam

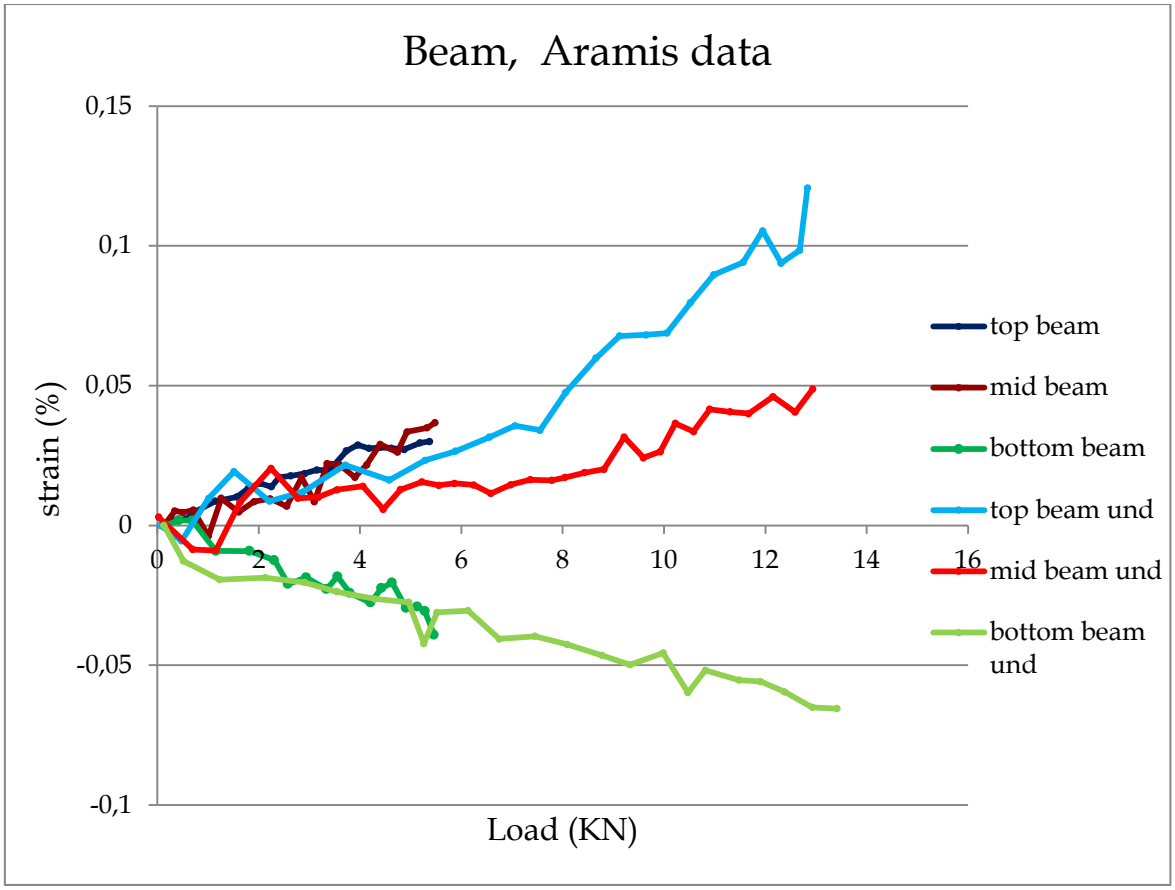
Beam, Aramis data
0,15
0,1
0,05
0
-0,05
-0,1
strain (%)
0
2
4
6
8
10
12
14
16
Load (KN)
top beam
mid beam
bottom beam
top beam und
mid beam und
bottom beam und

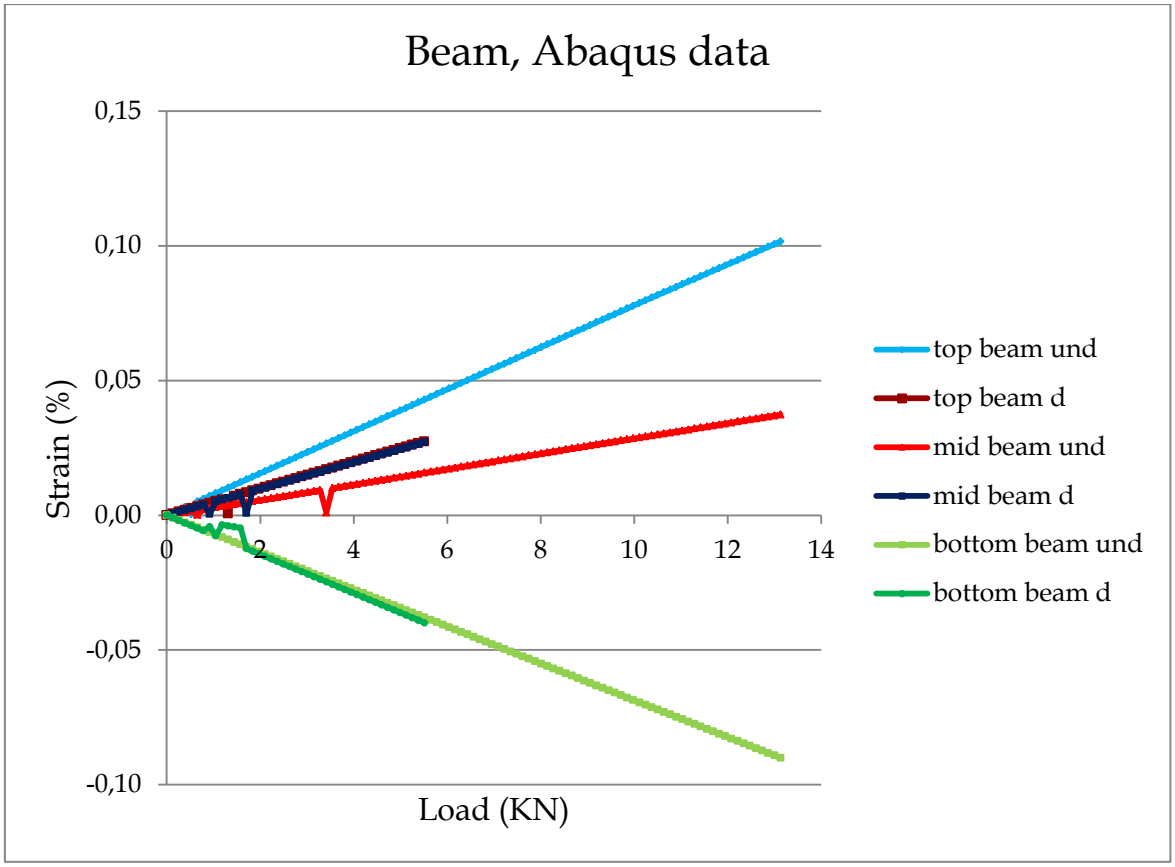
Beam, Abaqus data
0,15
0,10
0,05
0,00
-0,05
-0,10
Strain (%)
0
2
4
6
8
10
12
14
Load (KN)
top beam und
top beam d
mid beam und
mid beam d
bottom beam und
bottom beam d

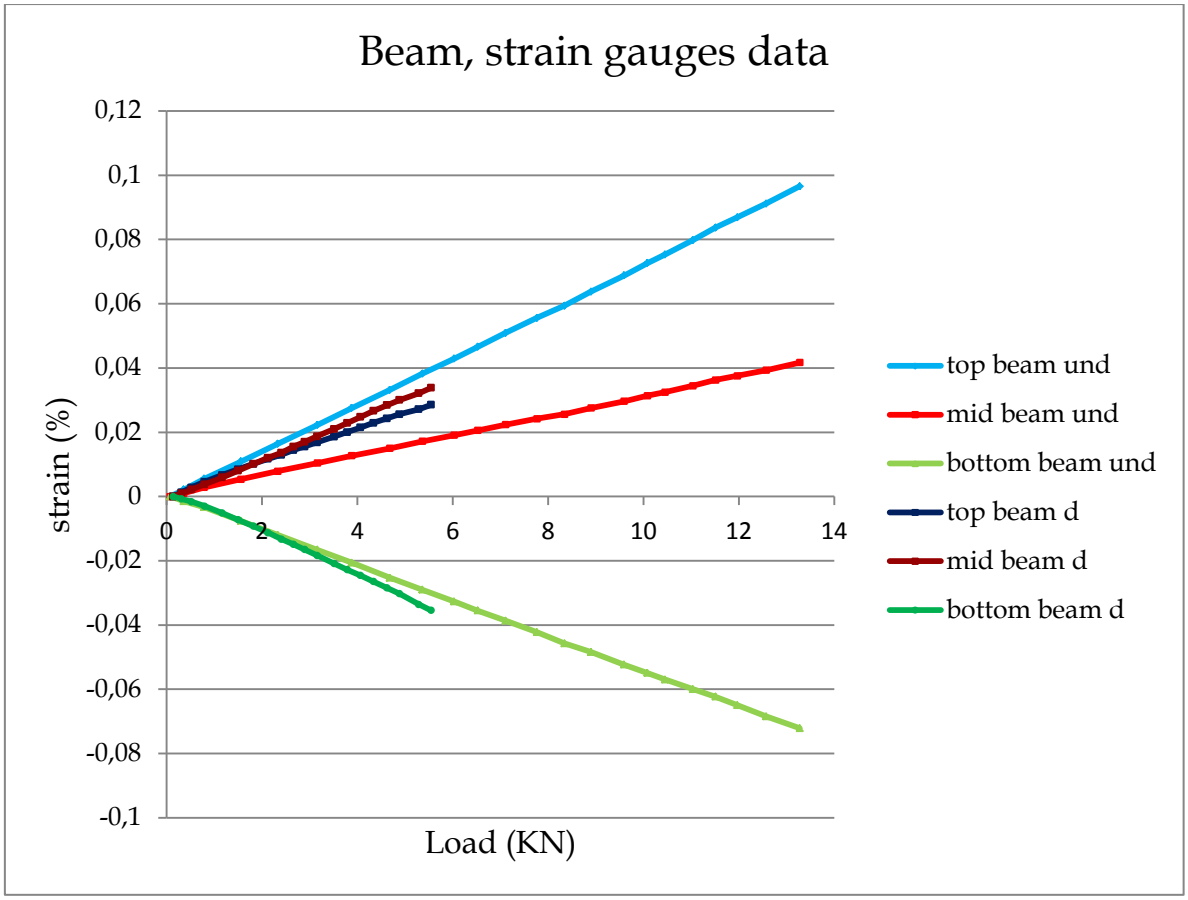

5.2 Joint part

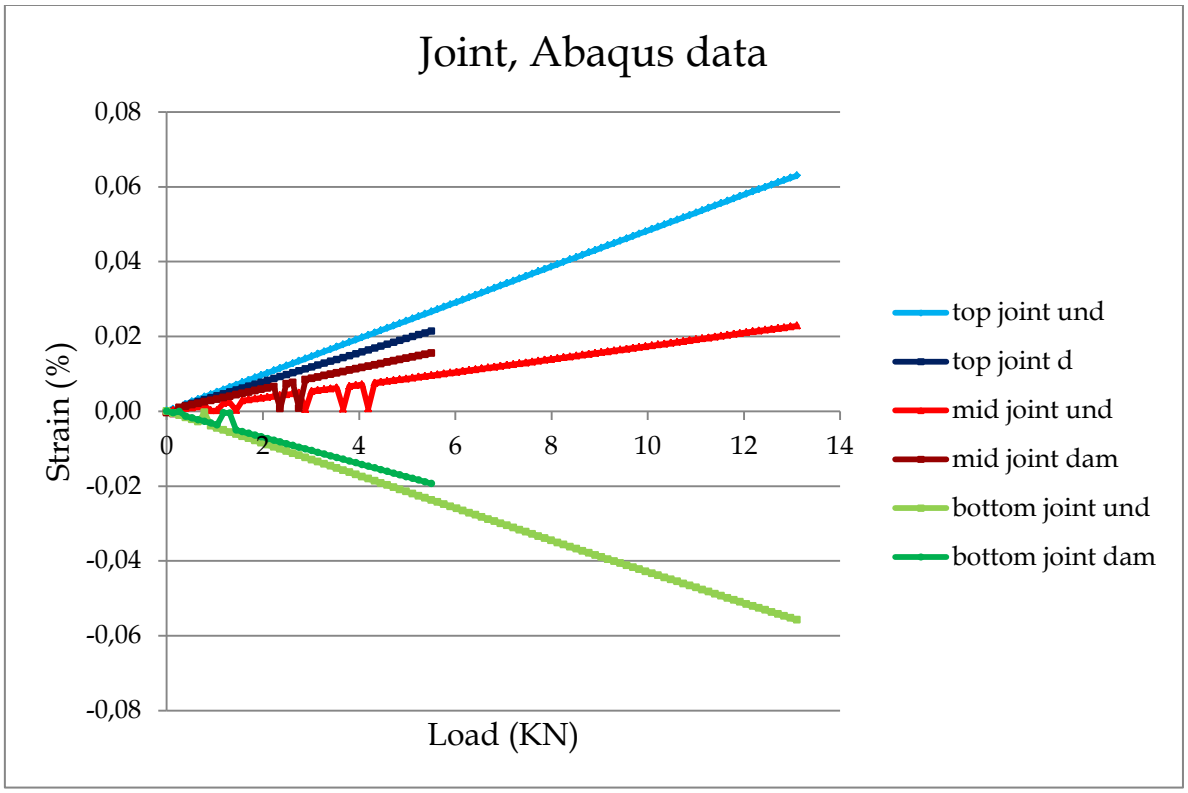

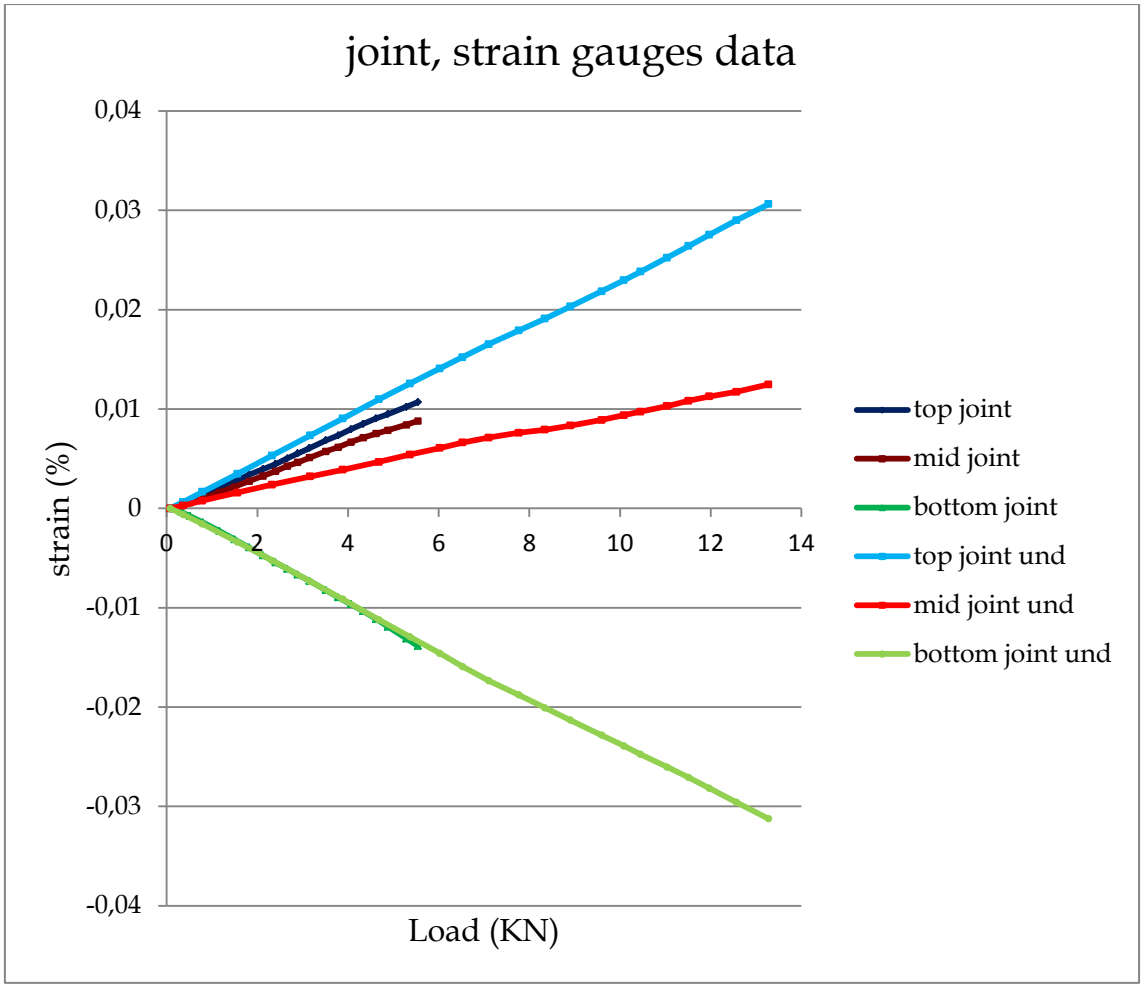
joint, strain gauges data
0,04
0,03
0,02
0,01
0
-0,01
-0,02
-0,03
-0,04
strain (%)
0
2
4
6
8
10
12
14
Load (KN)
top joint
mid joint
bottom joint
top joint und
mid joint und
bottom joint und

Chapter 6

Conclusions

The previous chapters presented a comparison between results provided from Aramis, from strain gauges and from a finite element model. Two main conclusions are presented in this chapter: the first one is about the comparison of the structure strains in undamaged and damaged condition, in order to evaluate the possibility to understand the presence of a crack hidden by plates in a steel structure, while the second one concerns the reliability of digital image correlation as structural health monitoring method.

Regarding the identification of a hidden crack using digital image correlation as structural health monitoring, graphs reported in the previous chapter show that it is possible, but depends from the strain values considered. In fact can be observed as the pattern changes from undamaged to damaged condition. Due to the presence of the crack, the variation of strain in the beam part is not linear from the bottom to the top of the structure, because the crack causes the higher part is not working as in the previous condition. In this way, as it is also confirmed by the finite element method model, from the bottom of the beam to the top there is an increase in strain values that suddenly stops and starts to decrease. This is the reason why in the damaged condition the strain presents almost the same values in the mid and top analyzed areas, differently from the situation without crack were values are distinct. The bottom part of the beam, that is in the other side of the structure compared to the crack, does not present a variation in the strain trend. The same speech could be done for the joint part looking at the graphs obtained with strain gauges and Abaqus, but this result

could not be obtained with Aramis because the strain values were really low and carried tests did not give correct results.

Regarding the Aramis reliability as structural health monitoring method, the evaluation has to be provide in order of the strain values considered. In this work good results were obtained until strain of 0,10%, with almost all the test providing expected values once the set up (spray pattern, camera distance from the beam, set up of the camera) was correctly fixed. Below strain values of 0,10% was still possible to obtain reliable results, but just until values of 0,035% and with an high attention to set up details: have to be stated that also doing this some of the tests failed providing results quite far from the expected. Generally better results were found in the compressed part, but under the strain level of 0,035% just few tests gave good results. Must be considered, as showed in chapters three and four, that the trend of the strain were really dependent by the length x difference trend. In fact, despite the software was able to get perfectly linear trend of displacement in both direction, the length x difference presented undulations in the graph. In this way, can be affirmed that digital image correlation is a really good structural health monitoring if used for checking displacements.

Appendices

ARAMIS GUIDE

An easy guide about how to upload pictures from image series into the ARAMIS system and all the steps needed to create a project will be explained in the following:

1. Run CodeMeter: we have to choose the right license to get into the system because there is just 1 full license (to create projects) and 4 half-licenses (to do calculations). To run the CodeMeter, we have to choose the program on the taskbar.

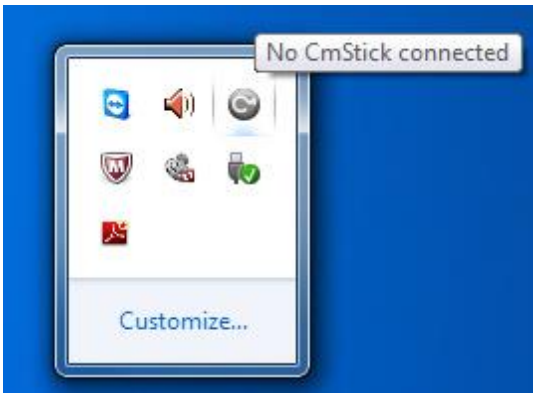

2. Choose the full license to create a project.

· Click on WebAdmin.

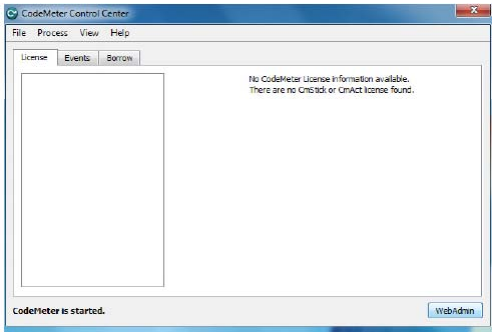

·Select 172.16.0.78 IP, then click “up” and finally “apply”:

3. Run ARAMIS system.

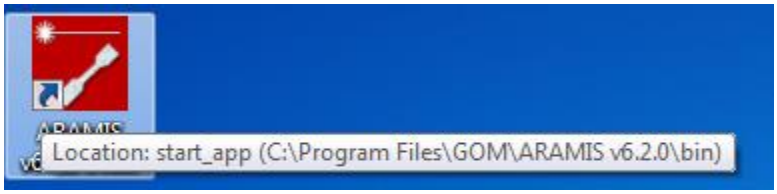

4. Create a project:

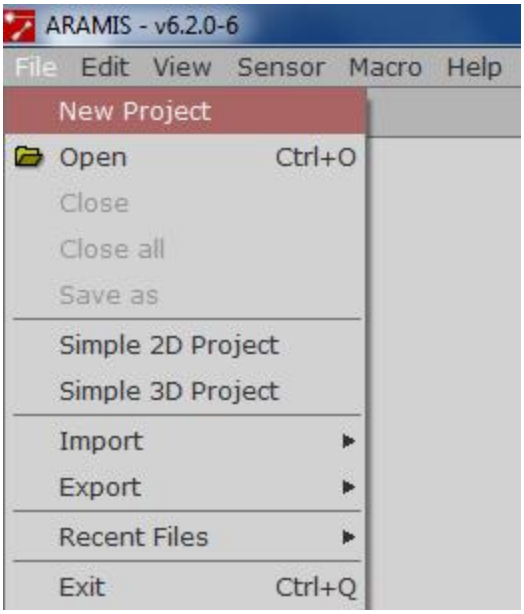

5. Set the parameters: they can be changed later, so the best we can do is select the folder where we want to save the project and click next in all the following windows:

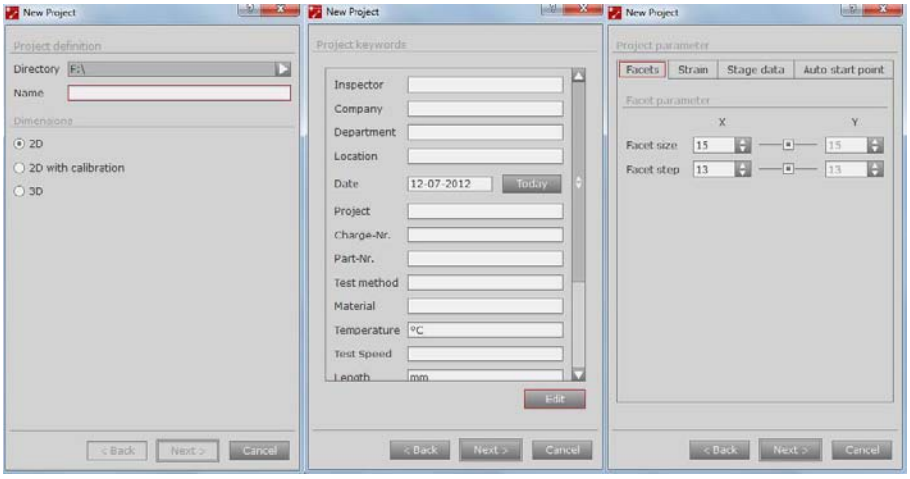

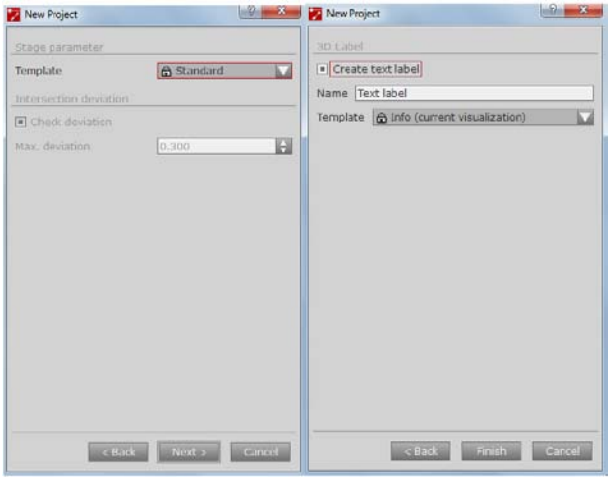

6. Attach the photos to the project: “From image series” has to be choosen, if the photos were taken with a camera and we want to compute them with ARAMIS.

·If photos are taken with an external camera:

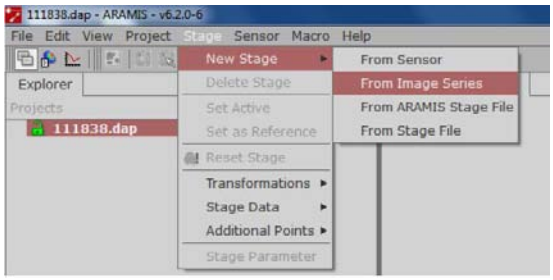

·Now is time to select the first photo of the series, all the photos have to be correlative:

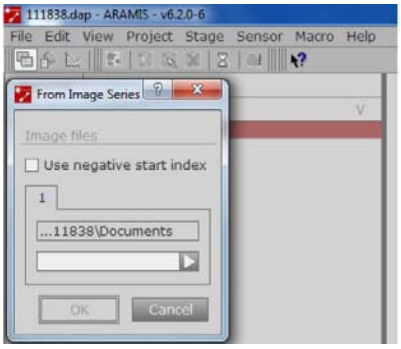

·We will be asked about if we want to convert the photos. "Yes" has to be clicked.

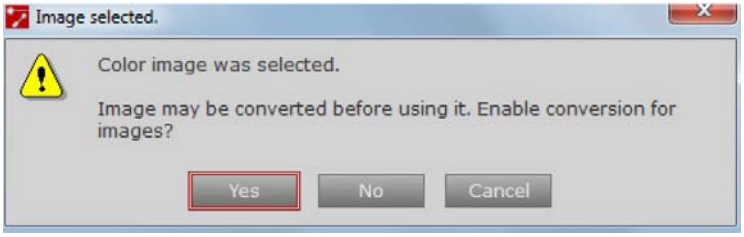

·Then, "OK" has to be clicked.

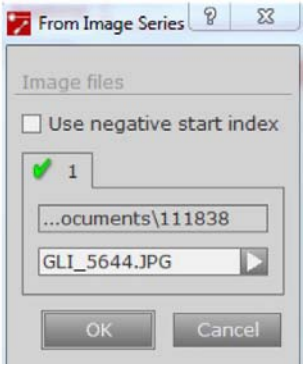

·Finally, "USE ALL" has to be clicked.

7. Define the mask.

8. Add the start point.

9. Click compute.

10. Once the computation is finished, the program has to be closed.

11. The step 2 has to be repeated but now choosing the other IP.

12. Go to the folder where the project is and run it.

References

ARAMIS 6.1 [Computer software]. Braunschweig, Germany, Mittelweg.

Filippo Lorenzoni(2013) "Integrated methodologies based on Structural health monitoring for the Protection of cutural heritage buildings."

NKRemote 2.7 [computer software]

Chiang, C., Shih, M., Chen, W., and Yu, C. (2011) "Displacement measurements of highway bridges using digital image correlation methods." Proc. SPIE, 8321(1), 83211G.

Jauregui, D. V., White, K. R., Woodward, P. E., and Leitch, K. R. (2003). "Noncontact photogrammetric measurement of vertical bridge deflection."

Lee, J. J., and Shinozuka, M. (2006a). "A vision-based system for remote sensing of bridge displacement."

Jan Winkler, G.Fisher and C. Georgakis (2014). "Measurement of local deformations in steel monostrands using digital image correlation".

Luis Santiago Perez (2012) "Determination of localized strains and global deformations using video system".

Simon Stafford [Nikon Manual] Magic Lantern guides.

Jan Winkler, G.Fisher and C. Georgakis (2012), "Localized bending fatigue behavior of high-strength steel monostrands."

Jan Winkler, G.Fisher and C. Georgakis (2012), "Monitoring of localized deformations in high-strength steel cables."

Busca, G., Cigada, A., Mazzoleni, P., Zappa, E., and Franzi, M. (2012). "Cameras as displacement sensors to get the dynamic motion of a bridge: Performance evaluation against traditional approaches." Proc., 6th Int. Conf. on Bridge Maintenance, Safety and Management, Taylor & Francis, LondonJ.J.Lee, M.

Shinozuka (2006), "Real-time displacement measurement of a flexible bridge using digital image correlation."
Brad Pease, "Aramis users' manual – Quick guide to setup, calibration, and data collection and analysis."
Bales, F. B. (1985). "Close-range photogrammetry for bridge measurement."